

AFFDL-TR-77-87

**DEMONSTRATION OF ACOUSTIC EMISSION  
SYSTEM FOR DAMAGE MONITORING OF  
FULL SCALE METALLIC AIRCRAFT STRUCTURES  
DURING FATIGUE TESTING**

*GRUMMAN AEROSPACE CORPORATION  
QUALITY CONTROL – ADVANCED DEVELOPMENT  
DEPT. 851 – PLANT 10  
BETHPAGE, NEW YORK 11714*

SEPTEMBER 1977

TECHNICAL REPORT AFFDL-TR-77-87  
Final Report for Period August 1976 – July 1977

Approved for public release; distribution unlimited.

AIR FORCE FLIGHT DYNAMICS LABORATORY  
AIR FORCE WRIGHT AERONAUTICAL LABORATORIES  
AIR FORCE SYSTEMS COMMAND  
WRIGHT-PATTERSON AIR FORCE BASE, OHIO 45433

20070921514

NOTICE

*When Government drawings, specifications, or other data are used for any purpose other than in connection with a definitely related Government procurement operation, the United States Government thereby incurs no responsibility nor any obligation whatsoever; and the fact that the government may have formulated, furnished, or in any way supplied the said drawings, specifications, or other data, is not to be regarded by implication or otherwise as in any manner licensing the holder or any other person or corporation, or conveying any rights or permission to manufacture, use, or sell any patented invention that may in any way be related thereto.*

This report has been reviewed by the Information Office (IO) and is releasable to the National Technical Information Service (NTIS). At NTIS, it will be available to the general public, including foreign nations.

This technical report has been reviewed and is approved for publication.



Signature

Name FREDERICK E. HUSSONG

Project Engineer/Scientist

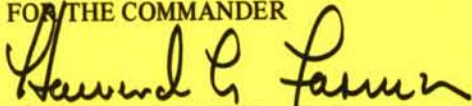


Signature

Name SANFORD LUSTIG

Supervisor Chief, Structures Test Branch

FOR THE COMMANDER



HOWARD L. FARMER, Colonel, USAF  
Chief, Structural Mechanics Division

*Copies of this report should not be returned unless return is required by security considerations, contractual obligations, or notice on a specific document.*

# UNCLASSIFIED

SECURITY CLASSIFICATION OF THIS PAGE (When Data Entered)

REPORT DOCUMENTATION PAGE		READ INSTRUCTIONS BEFORE COMPLETING FORM
1. REPORT NUMBER AFFDL-TR-77-87	2. GOVT ACCESSION NO.	3. RECIPIENT'S CATALOG NUMBER
4. TITLE (and Subtitle) Demonstration of acoustic Emission System for damages monitoring of full scale metallic aircraft structures during fatigue testing.		5. TYPE OF REPORT & PERIOD COVERED Final, Aug. 1976-July 1977
		6. PERFORMING ORG. REPORT NUMBER
7. AUTHOR(s) A.D. Hencken C.R. Horak		8. CONTRACT OR GRANT NUMBER(s) F33615-76-C-3073
9. PERFORMING ORGANIZATION NAME AND ADDRESS Grumman Aerospace Corporation Pl. 10 - Dept. 851 Bethpage, N.Y. 11714		10. PROGRAM ELEMENT, PROJECT, TASK AREA & WORK UNIT NUMBERS 62201F 1347-04-23
11. CONTROLLING OFFICE NAME AND ADDRESS Air Force Flight Dynamics Laboratory Wright Patterson Air Force Base Dayton, Ohio		12. REPORT DATE September 1977
		13. NUMBER OF PAGES
14. MONITORING AGENCY NAME & ADDRESS (if different from Controlling Office)		15. SECURITY CLASS. (of this report)  UNCLASSIFIED
		15a. DECLASSIFICATION/DOWNGRADING SCHEDULE
16. DISTRIBUTION STATEMENT (of this Report) Approved for Public Release; Distribution Unlimited.		
17. DISTRIBUTION STATEMENT (of the abstract entered in Block 20, if different from Report)		
18. SUPPLEMENTARY NOTES		
19. KEY WORDS (Continue on reverse side if necessary and identify by block number) Acoustic Emission, Fatigue Test, Extraneous Noise Discrimination, Coincidence Time, Slave Sensors		
20. ABSTRACT (Continue on reverse side if necessary and identify by block number) This report describes the acoustic emission monitoring work performed on a full scale metallic aircraft wing carry through structure of the swing wing bomber type. The structure was monitored during fatigue testing with a Grumman developed system. The program was designed to prove the feasibility of using a real time acoustic emission monitoring system to detect and locate crack propagation in a full scale complex airframe structure during fatigue cycling. (Over)		

DD FORM 1 JAN 73 1473

EDITION OF 1 NOV 65 IS OBSOLETE  
S/N 0102-014-6601

## UNCLASSIFIED

SECURITY CLASSIFICATION OF THIS PAGE (When Data Entered)



**UNCLASSIFIED**

SECURITY CLASSIFICATION OF THIS PAGE(When Data Entered)

20. ABSTRACT (Cont)

The report includes a description of the Acoustic Emission System operation and the concepts of noise discrimination used on fatigue tests. The installation and monitoring techniques used on the fatigue test are described. The test results, the problems associated with monitoring the complex structure, the conclusions, and system monitoring recommendations are also discussed in this report.

**UNCLASSIFIED**

SECURITY CLASSIFICATION OF THIS PAGE(When Data Entered)

## PREFACE

This report covers work performed under Contract F33615-76-C-3073 (62201F 1347-04-23), "Demonstration of Acoustic Emission System for Damage, Monitoring of Full Scale Metallic Aircraft Structures During Fatigue Testing". The fatigue test article monitored is a wing carry-through structure patterned after the B-1 Bomber Aircraft. The structure was designed and built by the General Dynamics Corporation as part of an Advanced Development Program (ADP) entitled Advanced Metallic Air Vehicle Structures (AMAVS). Period covered was from August 1976 through July 1977.

The work was performed under the direction of the Air Force Flight Dynamics Laboratory, Wright-Patterson Air Force Base, Dayton, Ohio, with Mr. Frederick E. Hussong (AFFDL/FBT) as Project Engineer. The work was performed at Wright-Patterson Air Force Base by personnel from the Quality Control Laboratory, Department 851, Plant 10, Grumman Aerospace Corporation, Bethpage, N.Y. 11714, with Richard F. Chance as the Program Manager and Charles R. Horak and Alan D. Hencken as the Project Engineers.

## CONTENTS

<u>Section</u>		<u>Page</u>
I.	Introduction . . . . .	1
II.	System Operation . . . . .	2
III.	Second Half of Second Life Fatigue Test . . . . .	14
IV.	Third Fatigue Life . . . . .	23
V.	Fourth Fatigue Life . . . . .	49
VI.	Static Test . . . . .	63
VII.	Conclusions . . . . .	67
VIII.	Recommendations . . . . .	69
	Glossary of Terms . . . . .	73

## ILLUSTRATIONS

<u>Figure</u>		<u>Page</u>
1	Basic AE System Operation . . . . .	3
2	Discrimination Concepts . . . . .	5
3	Grumman AE System Block Diagram . . . . .	7
4	Grumman AE System Operation . . . . .	8
5	Output Data Format . . . . .	10
6	Two-dimensional Location vs One-dimensional Signal Source Location . . . . .	11
7	Signal Source Location Format . . . . .	12
8	Sensor Configuration and Areas Monitored during AMVAS Fatigue Test . . . . .	15
9	Areas Monitored (Second Half-Second Life) . . . . .	16
10	FS 992 Outboard Bulkhead . . . . .	17
11	FS 992 Outboard Bulkhead (Second Life) . . . . .	18
12	FS 992 Outboard Bulkhead (Second Life) . . . . .	19
13	FS 992 Outboard Bulkhead (Second Life) . . . . .	20
14	FS 992 Outboard Bulkhead . . . . .	21
15	Bottom Cover . . . . .	24
16	Left Upper Longeron . . . . .	24
17	FS 992 Bulkhead . . . . .	25
18	FS 932 Bulkhead . . . . .	26
19	XF84 Outboard Intermediate Rib . . . . .	27
20	Areas Monitored (Third Life) . . . . .	28
21	Bottom Cover (Third Life) . . . . .	29
22	Bottom Cover (Third Life) . . . . .	30
23	Bottom Cover . . . . .	31
24	Bottom Cover (Third Life) . . . . .	32
25	Bottom Cover (Third Life) . . . . .	33
26	Bottom Cover (Third Life) . . . . .	34
27	Left Upper Longeron (Third Life) . . . . .	35
28	Left Upper Longeron (Third Life) . . . . .	36
29	FS 992 Outboard Bulkhead (Third Life) . . . . .	37
30	FS 992 Outboard Bulkhead (Third Life) . . . . .	38

## ILLUSTRATIONS (Cont)

<u>Figure</u>		<u>Page</u>
31	FS 992 Outboard Bulkhead (Third Life) . . . . .	38
32	FS 992 Outboard Bulkhead (Third Life) . . . . .	39
33	FS 992 Outboard Bulkhead (Third Life) . . . . .	40
34	FS 992 Bulkhead . . . . .	41
35	FS 932 Bulkhead (Third Life). . . . .	42
36	FS 932 Bulkhead (Third Life). . . . .	43
37	FS 932 Bulkhead . . . . .	44
38	FS 932 Bulkhead (Third Life). . . . .	45
39	FS 932 Bulkhead (Third Life). . . . .	46
40	FS 932 Bulkhead (Third Life). . . . .	47
41	FS 932 Bulkhead (Fourth Life) . . . . .	50
42	FS 932 Bulkhead (Fourth Life) . . . . .	51
43	FS 932 Bulkhead (Fourth Life) . . . . .	52
44	FS 932 Bulkhead . . . . .	53
45	FS 932 Bulkhead (Fourth Life) . . . . .	54
46	Areas Monitored - Lower Wing Pivot (Fourth Life) . . . . .	55
47	Wing Pivot (Bottom) Left (Fourth Life) . . . . .	56
48	Wing Pivot (Bottom) Left (Fourth Life) . . . . .	57
49	FS 992 Inboard Bulkhead (Fourth Life) . . . . .	58
50	FS 992 Inboard Bulkhead (Fourth Life) . . . . .	59
51	FS 992 Inboard Bulkhead (Fourth Life) . . . . .	60
52	FS 992 Bulkhead . . . . .	61
53	AMAVS Static Test System Block Diagram . . . . .	64
54	AMAVS Static Test . . . . .	65
55	AMAVS Static Test . . . . .	66
56	Area Designation for Proposed AE Monitoring System . . . . .	71
57	Proposed AE Monitoring System . . . . .	72



## SUMMARY

The Grumman-developed Acoustic Emission Monitoring System was used to monitor the AMAVS Fatigue Test for damages during the second half of the second fatigue life, and the entire third and fourth fatigue lives. All of the areas monitored for acoustic emission were on the left half of the AMAVS test structure. Two of six independent areas were monitored simultaneously on a time-sharing basis with the other four areas. Acoustic emission activity was detected but not located on the FS 992 outboard bulkhead during the second half of the second fatigue life. Crack propagation was detected and located on the bottom cover (induced flaw) and the bottom of the FS 932 bulkheads during the third life. The crack propagation in these two areas was detected by AE monitoring prior to detection by any other inspection techniques. Crack propagation on the bottom cover and FS 932 bulkheads was confirmed by conventional inspection methods. Acoustic emission activity was also detected and located on the FS 992 left outboard bulkhead during the third life fatigue testing. The area detected was under a cover plate which was inaccessible for inspection.

During the fourth fatigue life an existing propagating crack on the lower wing pivot was monitored. The AE events associated with crack elongation were detected and located. Acoustic emission activity was generated on the top half of the FS 932 bulkhead and the FS 992 inboard bulkhead, during the fourth fatigue life. These two areas could not be inspected because of inaccessibility.

A thorough examination should be made of the top half of the FS 932 and the FS 992 inboard and outboard bulkheads when the test structure is dismantled to confirm areas of AE activity.

Induced flaws on the FS 932 bulkhead, the FS 992 outboard bulkheads, and the bottom cover propagated extremely slowly during the fourth life. These slow crack propagations were not detectable by acoustic emission because of the high extraneous noise background of the AMAVS.

Seven areas on the AMAVS were monitored for AE activity during the static test to failure. A comparison of the seven areas was made for the greatest amount of AE activity. The area of failure (lower forward longeron) was located between the two monitored areas with the most activity.

## Section I

### INTRODUCTION\*

The objective of the program was to demonstrate a means of detecting and locating propagating structural cracks using a real time acoustic emission monitoring system during the fatigue testing of a full scale complex aircraft structure. Information gathered during this study will be used to determine system requirements and techniques necessary to completely monitor large primary structures for noting the onset of fatigue cracking.

The development of acoustic emission monitoring as an effective nondestructive evaluation technique during fatigue testing has been severely hampered by extraneous noise signals originating from test fixture apparatus, pumps, jacks, and loading points. The extraneous noise signals create false signal source locations within the monitored area and interfere with AE event signals from propagating flaws. Consequently, little practical acoustic emission analysis has been accomplished on airframe elements or components undergoing high noise fatigue testing.

The Grumman system was designed to detect acoustic emission event signals in a background of extraneous noise signals of all levels, and locate crack initiation sites. The system utilizes wave form conditioning and spatial and wave form discrimination to identify and reject extraneous noise signal data. The size of the cracks detected are a function of the severity of the extraneous noise signals, i.e., acoustic emission event signals are detected during the time periods between extraneous noise signals. The structure which was monitored is a wing carry-through structure patterned after the B-1 Bomber Aircraft, and is shown in Fig. 9. The structure built by the General Dynamics Corporation as part of an Advanced Development Program is entitled, "Advanced Metallic Air Vehicle Structure" (AMAVS).

- - - - -

\*It is necessary to understand the "Glossary of Terms" prior to reading this report.



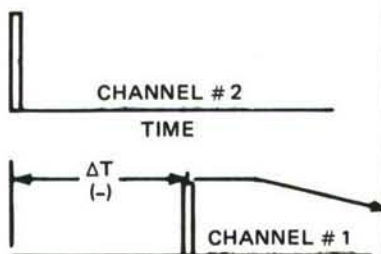
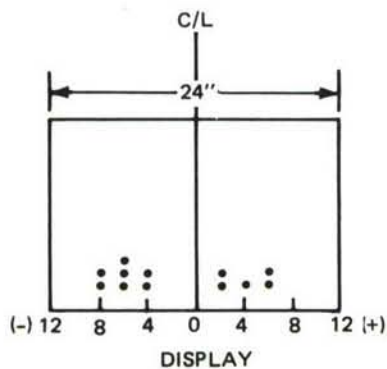
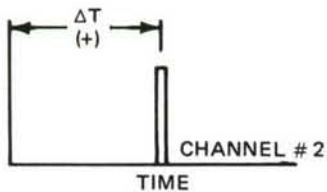
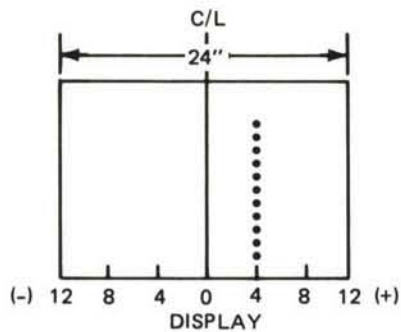
## Section II

### SYSTEM OPERATION

For illustration purposes, Fig. 1a shows AE one-dimensional area monitoring, utilizing a single line between two sensors. After calibration, a signal source at "X" would be detected and located as being on the line between the sensors at the intersection of the hyperbola on which it lies. This location is based on the basic definition of a hyperbola, wherein the difference of distances of any point on the hyperbola from the foci (sensors) is a constant. Thus, for constant velocity, the microsecond difference in signal source arrival time at the sensor locations is also a constant for all locations on the same hyperbola.

The acoustic emission system indicates where the signal-source hyperbola crosses the sensor baseline. Actual source location is then accomplished by manual extrapolation. The locations are referenced to the centerline distance which is designated as "0" between the sensors. The locations are indicated in inches from "0" to each sensor (one half of the distance between sensors) with a polarity sign of (+) or (-). Signals detected by Channel #1 before Channel #2 (Fig. 1a) are (+) positive. Signals detected in the reverse order are (-) negative. A pulse is generated when a signal is detected by a sensor.  $\Delta t$  time later a second pulse is generated by a second sensor. The resulting  $\Delta T$ , with a polarity sign (Fig. 1a), is transferred to the computer for source location calculation. The hyperbolic location of the detected signal, on the line between the sensors, with a polarity sign, is printed on paper tape by the digital printer. A repetitious signal source at X (Fig. 1a) would print out a series of (+) 004.0 locations on paper tape and accumulate signal sources at (+)4 inches from "0" on a histogram display, as shown.

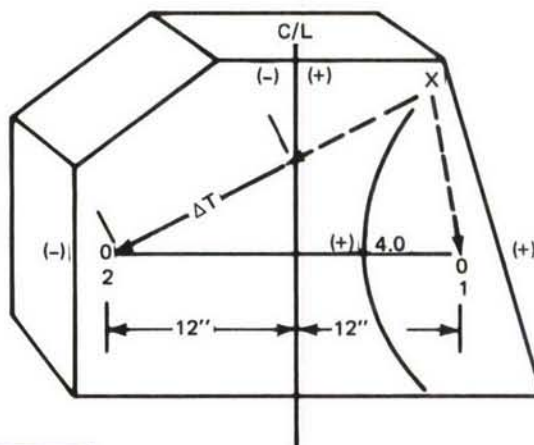
Figure 1b shows the same area monitored in Fig. 1a with the introduction of extraneous noise sources at "A" and "B" as would be experienced with fatigue testing. Extraneous noise sources generate false  $\Delta T$  data and mask AE event signals because the same signal source is not detected by both sensors. An example is shown in Fig. 1b. When extraneous noise signal "B" is first detected by sensor 2 and AE event signal X is first detected by sensor 1,  $\Delta T$  data is generated. This resultant  $\Delta T$  data is false because different sources are detected by sensors 1 and 2. AE event signal X cannot be detected by sensor 2 because it has been actuated by extraneous noise signal "B" and remains inoperative until the previous  $\Delta T$  data is processed and the system reset some milliseconds later. The false  $\Delta T$  data indicates an erroneous signal source location at (-)008.2 which does not exist. With



(+) 002.1  
 (-) 007.4  
 (-) 007.2  
 (+) 004.1  
 (-) 005.0  
 (+) 005.2  
 (+) 002.0  
 (-) 004.1  
 (-) 007.0  
 (-) 008.2

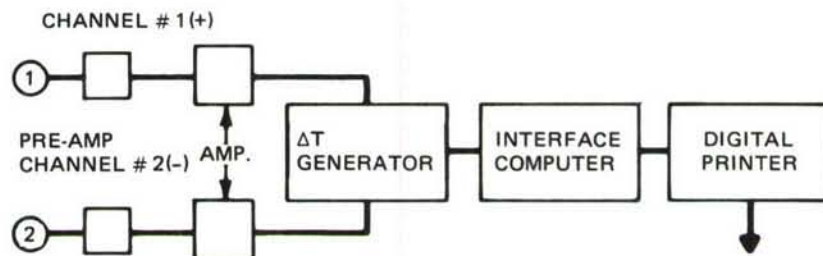
PRINTER TAPE

A.

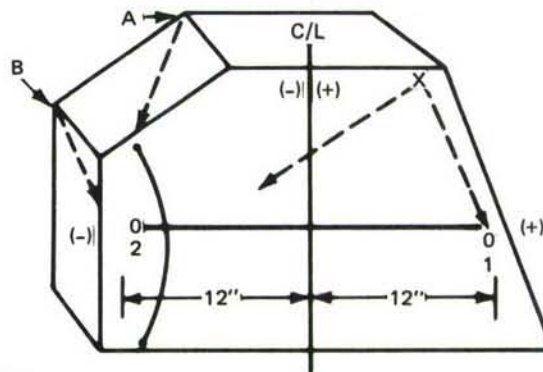


(+) 004.1  
 (+) 004.0  
 (+) 004.0  
 (+) 004.1  
 (+) 004.1

PRINTER TAPE



B.



**SYMBOLS**

X - VALID AE SOURCE

A&B - INTERMITTENT EXTRANEUS NOISE SIGNAL SOURCE

Fig. 1 Basic AE System Operation



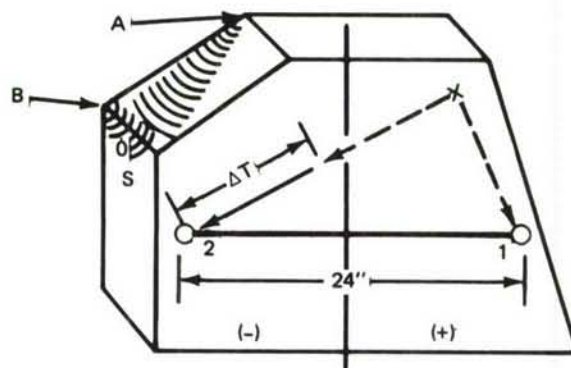
multiple extraneous noise signal sources present, the output is flooded with erroneous signal source locations, making AE event signal detection virtually impossible. Figure 2 illustrates the extraneous noise discrimination concepts used by Grumman to eliminate the signal interference problem described in Fig. 1b.

The Slave-Sensor concept of spatial discrimination (Fig. 2a) imposes a requirement that both locating sensors 1 and 2 must receive a signal before a signal is received by slave sensor "S" for acceptable  $\Delta T$  data. Intermittent extraneous noise signals from "A" and "B" are detected by sensor "S" before detection by sensors 1 and 2. The resultant  $\Delta T$  data generated by sensors 1 and 2 is rejected as erroneous because it has been caused by "A" or "B" or has interfered with the valid AE event signal at "X". Acceptable  $\Delta T$  data is generated during time periods when signals from acceptable locations such as "X" are detected by sensors 1 and 2 prior to detection of any signals at sensor "S". This concept effectively eliminates interference and erroneous  $\Delta T$  data generated by extraneous noise signal sources originating from outside the AE area of surveillance.

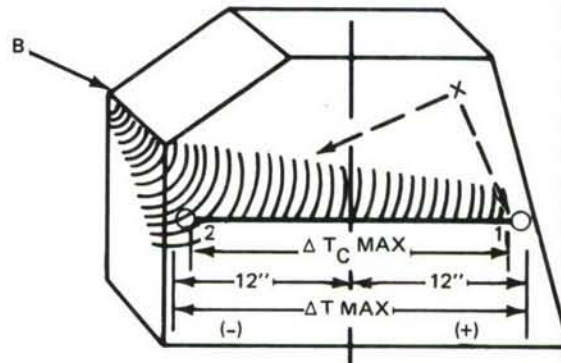
Coincidence Time-Spatial discrimination is shown in Fig. 2b. An extraneous noise signal source at "B" would cause  $\Delta T_{MAX}$  to be generated.  $\Delta T_{MAX}$  is the maximum time required for a signal source beyond the extremities of the two locating sensors to be detected by each. An extraneous noise signal source at "B" would indicate a signal source location at (-)12 inches, which is erroneous. This condition not only creates false  $\Delta T$  data but also interferes with the detection of valid AE event signals shown at "X". This problem is overcome by imposing a "Coincidence Time",  $\Delta T_{C MAX}$ , on sensors 1 and 2.  $\Delta T_{C MAX}$  is preset a few microseconds less than  $\Delta T_{MAX}$  which rejects all  $\Delta T_{MAX}$  data caused by "B".

Figure 2c shows the concept of Wave Form Discrimination, which eliminates interference from extraneous noise signals originating within the surveillance area. This type of interference with AE event signal detection cannot be eliminated by the spatial discrimination concepts of Fig. 2a and 2b, but requires examination of the signal generating the  $\Delta T$  data. During initial fatigue cycling, the extraneous noise signals are evaluated for certain characteristics. As a result of the evaluation, several variable conditions relating to signal wave form are preset as a requirement for all signals which cause  $\Delta T$  data to be generated. In a fashion similar to a filter or gate, signals not meeting the wave form requirement cause the resulting  $\Delta T$  data to be rejected.

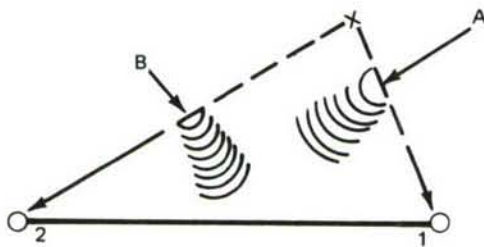
The AE system is calibrated by taking attenuation and velocity measurements with a pulsed sensor as a simulated AE source. Based on previous experience, the system sensitivity should be such as to detect AE event signal sources of several hundred microvolts amplitude



A. SLAVE SENSOR - SPATIAL DISCRIMINATION



B. COINCIDENCE TIME - SPATIAL DISCRIMINATION



C. WAVE FORM DISCRIMINATION

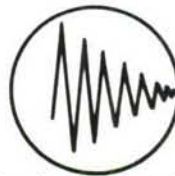
**SYMBOLS**  
 X - VALID AE SOURCE  
 A & B INTERMITTENT EXTRANEIOUS  
 NOISE SIGNAL SOURCE

WAVE FORM A & B



- REJECT  $\Delta T$  DATA

WAVE FORM X



- ACCEPT  $\Delta T$  DATA

Fig. 2 Discrimination Concepts



at the maximum sensor spacing. Attenuation measurements are made with the pulsed sensor in a fixed position on the area to be monitored.

Another sensor connected to a system input channel is placed on the area at a distance, for example, of 36 inches from the pulsed sensor. The overall system gain is set at 80 dB and the pulsed sensor amplitude adjusted such that the detected amplified signal is 1.0 volt peak at the output. (Nominal threshold detection level is +0.5 volt.) The sensor connected to the system input channel is then moved 12 inches closer to the pulsed sensor and the detected amplified signal is measured again. (System gain and pulse amplitude remain fixed as for first measurement.) This procedure is repeated for several directions from the pulsed sensor at different distances to determine the maximum attenuation per foot. If the amplified signal attenuation was 0.5 volt peak per foot, this means an attenuation of 50 microvolts per foot for an AE event signal (Gain  $10^4$  - 80dB). For a 1.0 volt peak amplified output signal at 24 inches, a 200 microvolt AE event signal can be detected. At a distance of 36 inches, a 250 microvolt AE event signal can be detected. All sensors used to monitor the area are tested for the required sensitivity using the same pulsed sensor and amplitude as used to determine the signal attenuation. Sensitivity adjustments are made as required by amplifier gain.

Acoustic velocity in the monitored area is determined with a pulsed sensor at a specific location between two locating sensors. With the locating sensor spacing and pulsed sensor location as input information, an AE system computer program is used to calculate the velocity when the pulsed sensor is activated. A number of velocity measurements are made with various orientations in the area to determine the average area velocity. Typical velocities in common metals are between 100,000 and 200,000 inches per second.

The Grumman AE system utilizes piezoelectric type sensors with maximum sensitivity at a resonant frequency of 280-320 kHz. Tuned preamplifiers operate at a frequency of 300 kHz (+/- 50 kHz) with a fixed gain of 46 dB. Filters with a bandpass of 100-400 kHz are used with 60 dB variable gain amplifiers. The amplified signals are processed for  $\Delta T$  data information, discrimination functions, and computer source location calculation.

Figure 3 is a block diagram of the two independent one-dimensional Grumman AE systems used to monitor the AMAVS fatigue tests. The basic system operation is explained as follows, with reference to Fig. 4 (System #1). The operation of System #1 and 2 is identical. The first locating channel #1 or #2 to detect a signal generates an event pulse (A) which determines the polarity of the location and starts the signal range time pulse (B). The  $\Delta T$  data is determined and transferred to the computer interface when the second locating channel detects the signal and an event pulse is generated (C). If, by the end of the signal

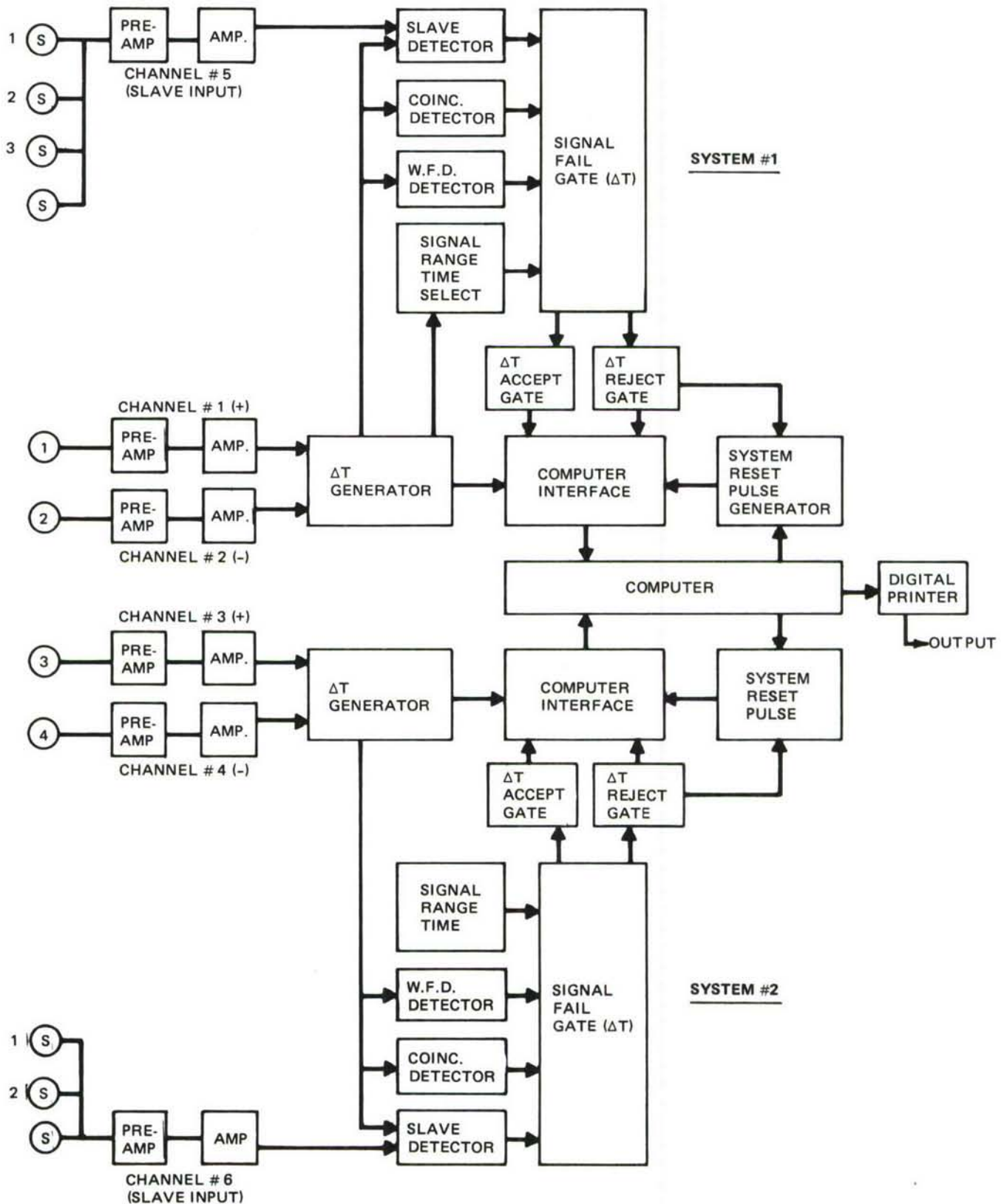
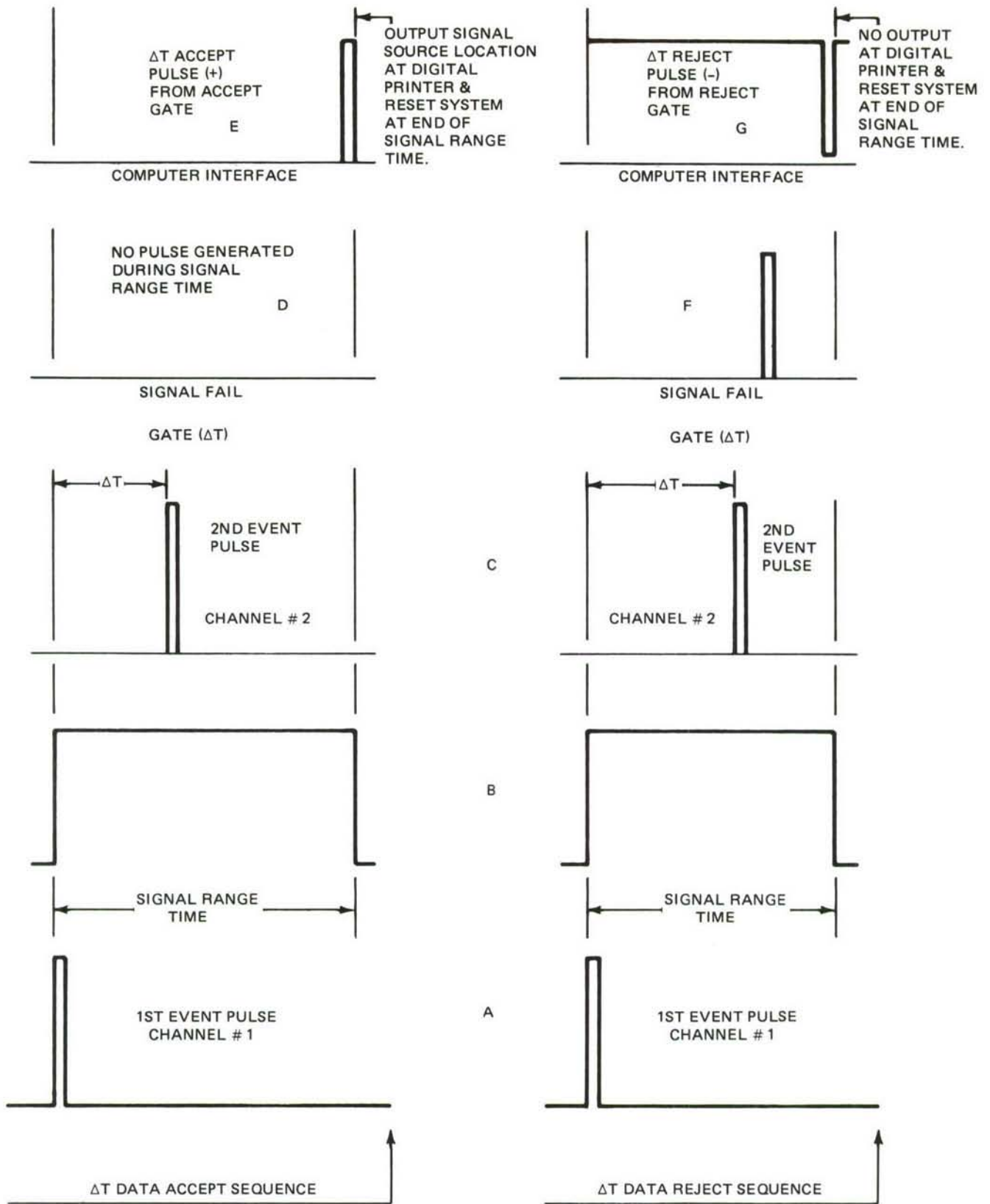


Fig. 3 Grumman AE System Block Diagram





2293-004

Fig. 4 Grumman AE System Operation

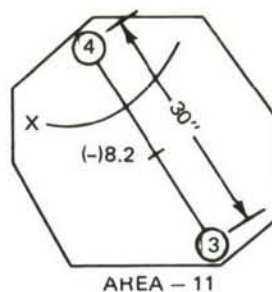
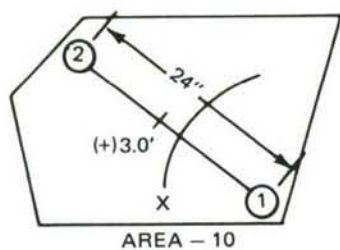
range time, the signal fail gate ( $\Delta t$ ) does not generate a pulse (D), (no pulse received from the "slave sensor", "coincidence time", or "wave form discrimination" detectors), a  $\Delta T$  data accept pulse (E) is generated by the  $\Delta T$  accept gate. This pulse will output the signal source location on the digital printer tape and reset the system for additional  $\Delta T$  data. If, however, by the end of the signal range time, a pulse (F) is generated from the signal fail gate  $\Delta T$  (pulse received from one or more of the discrimination detectors) a  $\Delta T$  reject pulse (G) is generated. This pulse will reject the  $\Delta T$  data in the computer interface and reset the system. No signal source location will appear at the digital printer output.

Figure 5 shows the output data format of two independent areas being monitored simultaneously in a one-dimensional mode. The signal source locations are calculated by the computer and printed together with the time of output by the digital line printer. The output rate of the printer is twenty lines per second, and data in excess of this rate is stored in a computer memory buffer for subsequent output.

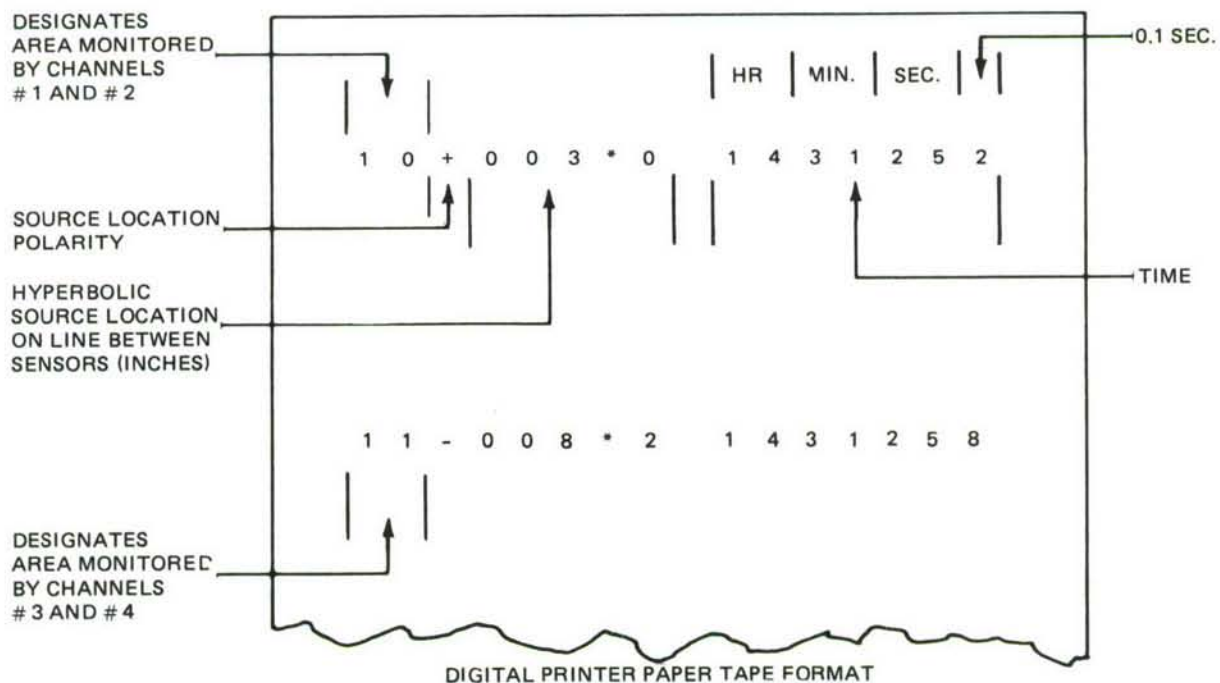
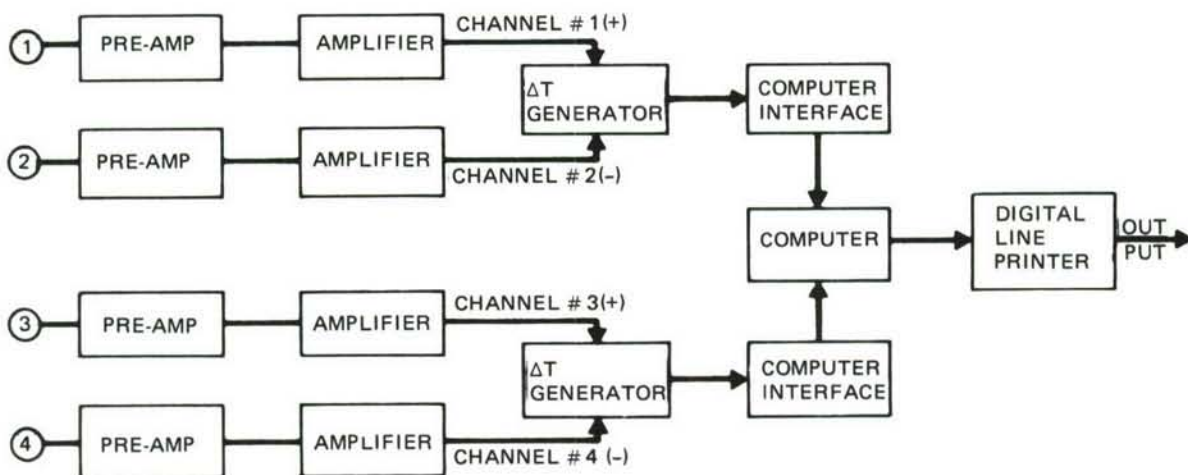
Multiple single axis, one-dimensional, signal source location, as shown in Fig. 6b, was selected to monitor the AMAVS fatigue tests over the two-dimensional X-Y axis capability of the monitoring system shown in Fig. 6a. The single dimension sensor arrangement was more flexible on the irregular geometries (holes and cover plates) and provided greater coverage of the areas compared to the two-dimensional sensor arrangement of Fig. 6a. Single dimension monitoring provides greater sensitivity than two-dimensional monitoring because signals are required at only two sensors instead of four. Figure 6a shows that a signal source at "X" could actuate three sensors but not four, because of spatial attenuation. This data would be lost with the two-dimensional arrangement but would be retained with multiple single dimension monitoring, as shown in Fig. 6b.

Figure 6b also illustrates how signal sources were located during the AMAVS test. A signal source, such as "X", was located hyperbolically with respect to two axes (2-5 and 1-5). The intersection of the two hyperbolas determined the location of the signal source by manual extrapolation.

Figure 7 shows the source location data format used to record the results of the AMAVS fatigue test. The data shown is that which would have been obtained from the example of Fig. 6b. With all the sensors connected, a signal source at "X" would appear as shown in Fig. 7a detected by the closest (+) & (-) sensor pair, all other axes being locked out. Each dot represents a single source location of "multiple signals". To determine the location of "X" in area "A", it is necessary to detect the signal source on two single axes, as shown



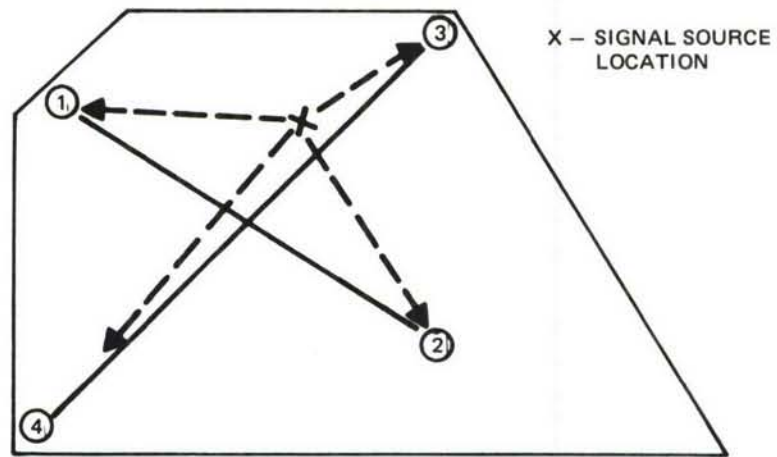
X - SIGNAL SOURCE LOCATION



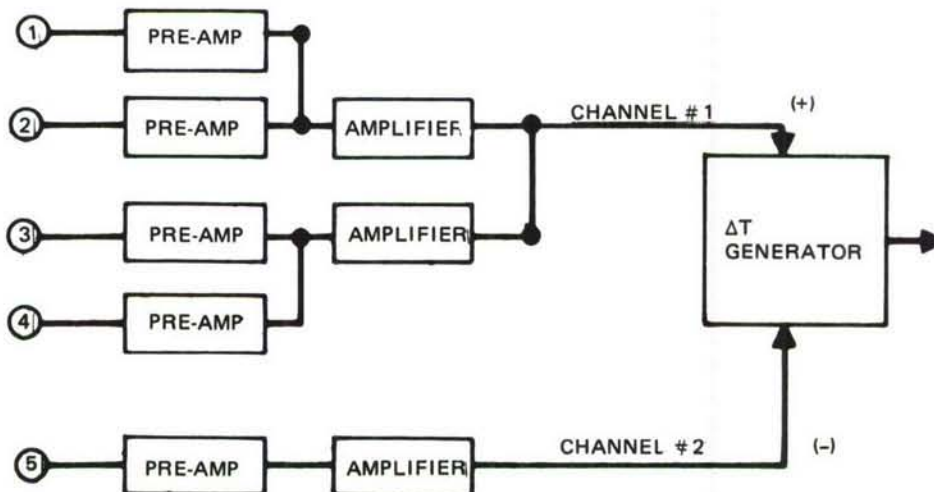
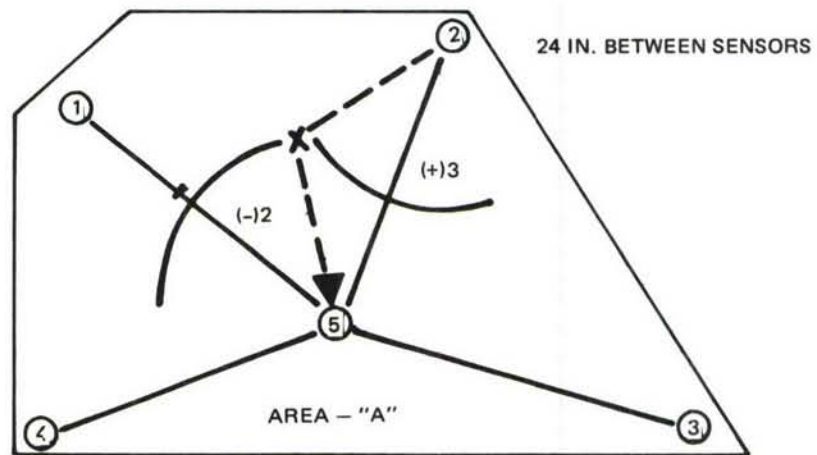
2293-005

Fig. 5 Output Data Format

A.



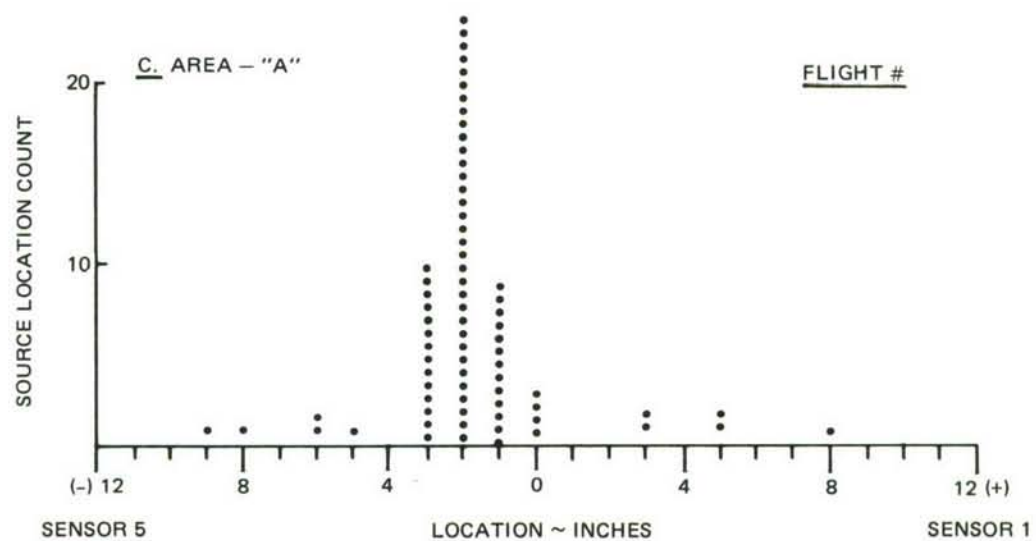
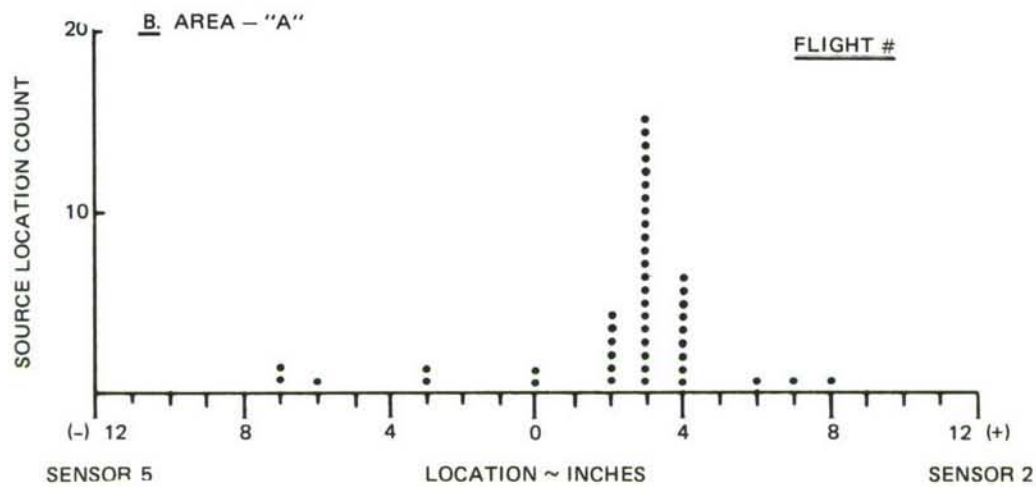
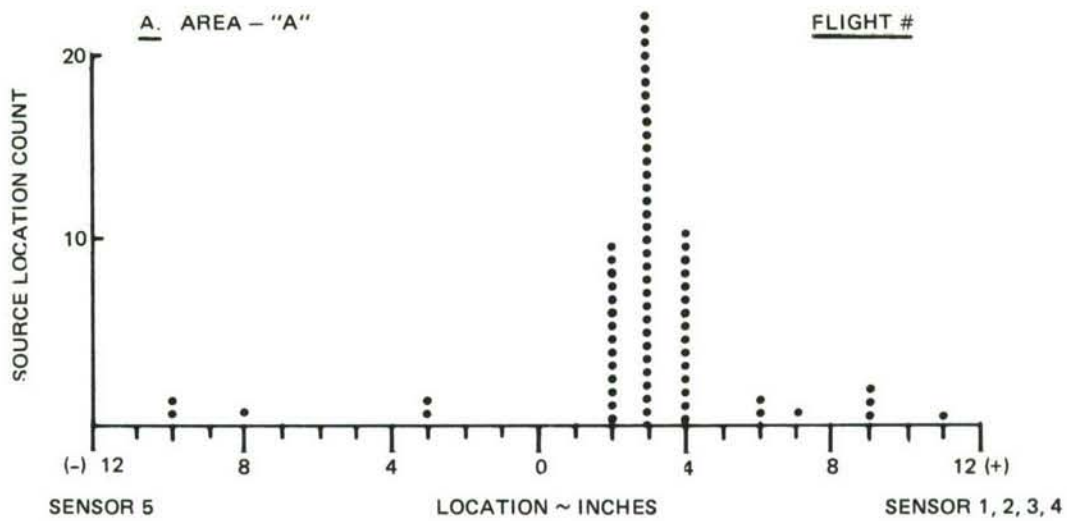
B.



2293-006

**Fig. 6 Two-Dimensional Location vs One-Dimensional Signal Source Location**





2293-007

**Fig. 7 Signal Source Location Format**

in Fig. 7b and 7c. Figure 7b shows a hyperbolic signal source location between sensors 2 and 5 at (+) 3 inches. Figure 7c shows a hyperbolic signal source location between sensors 1 and 5 at (-) 2 inches. The intersection of these two hyperbolas is the signal source location "X".

Each signal source location data format used to record the results of the AMAVS fatigue test indicates the area and the flight numbers during which it was monitored.

### Section III

#### AMAVS FATIGUE TEST – ACOUSTIC EMISSION MONITORING – SECOND HALF OF THE SECOND LIFETIME

Grumman-developed Acoustic Emission equipment was installed after the completion of one and one-half lifetimes of fatigue testing. Each lifetime was comprised of 1280 flights (25 minutes each flight). Acoustic Emission equipment and sensors were installed during the inspection period after one and one-half lifetimes.

#### INSTALLATION

The sensor locations and the areas of the AMAVS monitored for acoustic emission are shown in Fig. 8. The monitored areas are referenced to the AMAVS in Fig. 9. Twenty piezoelectric sensors and preamplifiers were used to monitor the selected areas. The sensors were attached to the structure using a fast setting contact cement. Any of the sensors could be used as either a locating sensor or a slave sensor, depending upon extraneous noise interferences occurring during fatigue testing. In each area, velocity and attenuation measurements were made to calibrate the system before the start of fatigue testing, as described in Section II, "System Operation".

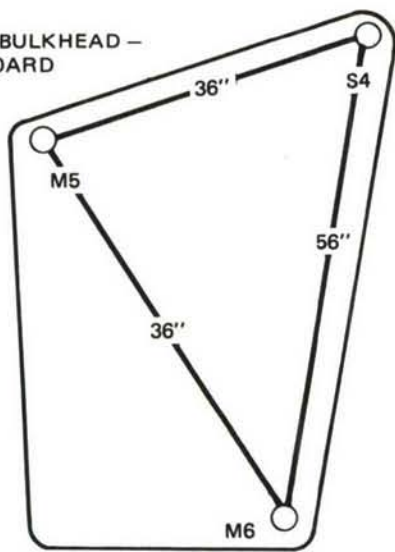
#### FATIGUE TEST MONITORING

The six areas were monitored utilizing the extraneous noise discrimination techniques of Spatial (including master-slave and coincidence) and Wave Form discrimination. Figure 10 shows a histogram display of false signal source locations generated by extraneous noise with the discrimination functions turned off for 15 seconds during flight #801 on the FS 992 outboard bulkhead. If the discrimination functions were left off for the duration of the entire flight (approximately 25 minutes) there would be about 6500 false signal source locations generated, making it impossible to detect AE event signals. It was observed that approximately 50% of the false signal source locations, caused by extraneous noise signals, were eliminated with "Wave Form" discrimination. The test could not have been monitored without all of the discrimination functions in operation. With the discrimination functions on, approximately 98% of the extraneous noise signals were eliminated.

The extraneous noise interference in each monitored area was different from the other areas. Each area had to be considered as an individual test with specific slave sensors,

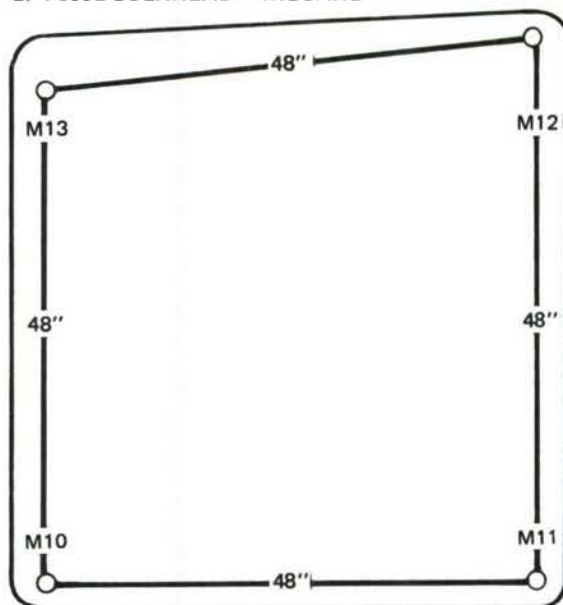


A) FS992 BULKHEAD – OUTBOARD



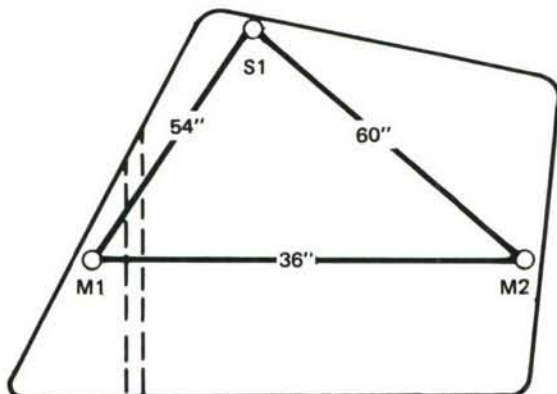
10 NICKEL STEEL

B) FS992 BULKHEAD – INBOARD



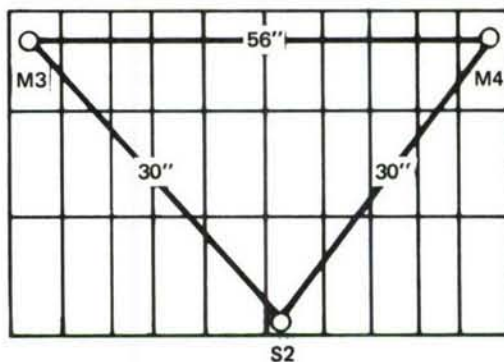
6A1 4V TITANIUM

C) FS932 BULKHEAD



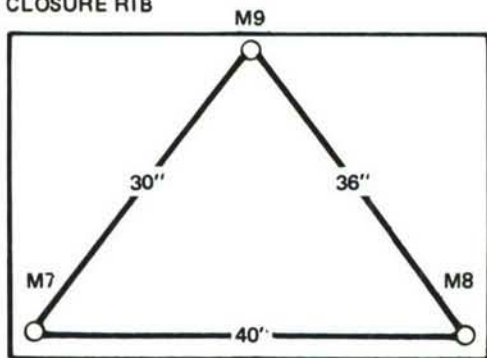
6A1 4V TITANIUM

D) BOTTOM COVER



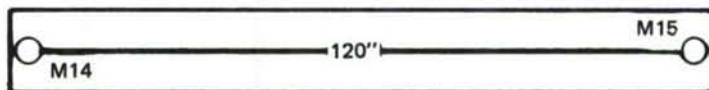
10 NICKEL STEEL

E) CLOSURE RIB



6A1 4V TITANIUM

F) LONGERON – LEFT UPPER



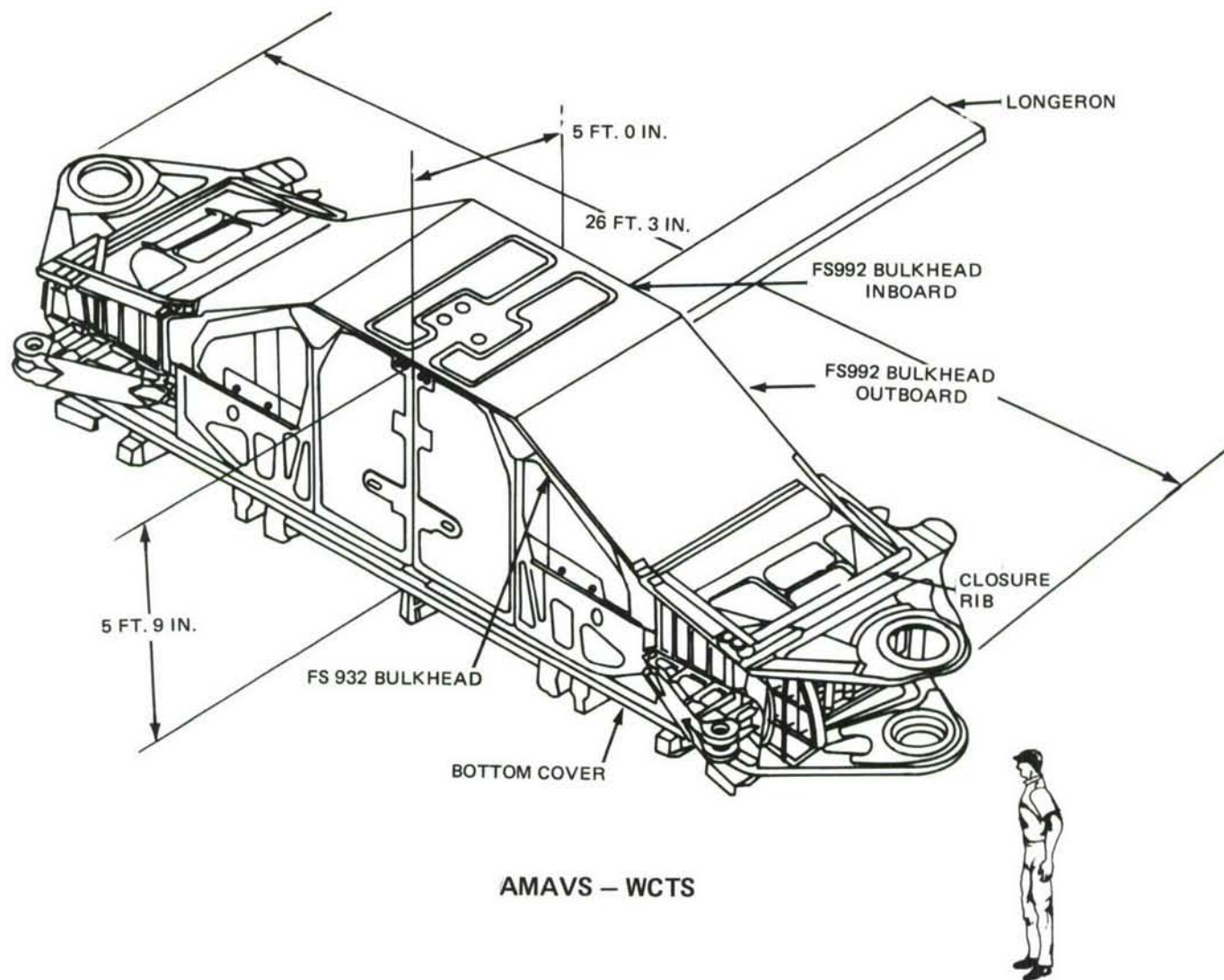
7050 ALUMINUM

2293-008

**Fig. 8 Sensor Configuration and Areas Monitored During AMVAS Fatigue Test – Second Half – Second Life**

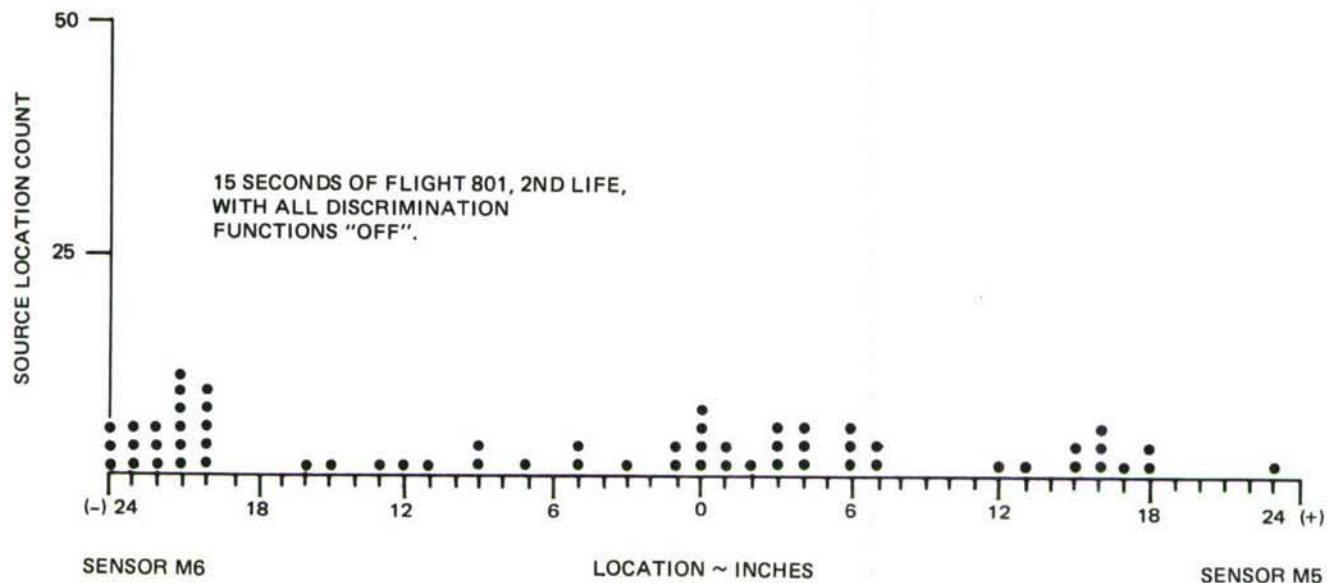
coincidence time settings and wave form settings to minimize extraneous noise interference in that area. Specified locating sensors from other areas were used as slave sensors in the areas being monitored.

Remotely operated pulsed test sensors were installed on the test structure to simulate AE event signals. The test sensors were used to calibrate the system's sensitivity under operating conditions to ensure the ability to detect AE event signals occurring between extraneous noise signals.



2293-009

Fig. 9 Areas Monitored (Second Half – Second Life)



2293-010W

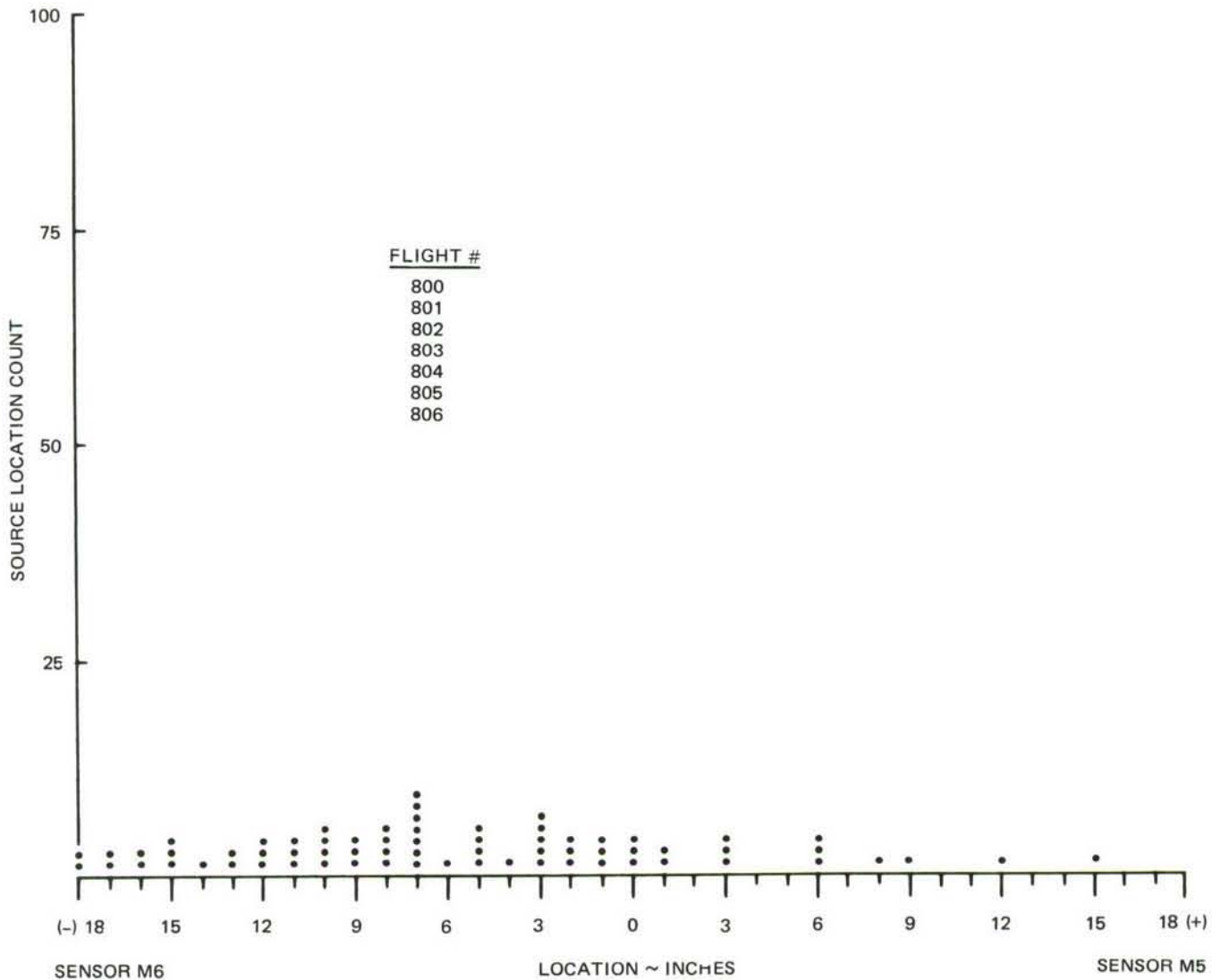
Fig. 10 FS 992 Outboard Bulkhead

## TEST RESULTS

The system was operated at 300 kHz with tuned preamplifiers, an overall system gain of 90dB and a threshold detection level of 0.5 volt DC. Wave form and spatial discrimination was used for reduction of extraneous noise interference. The extraneous noise interference generated by the fatigue apparatus and structure allowed approximately 50% of cycling time for detection of AE events between the extraneous noise signals. The FS 992 outboard bulkhead was the only area of the six monitored which showed indications of crack initiation and propagation. Figure 11 shows a histogram of the AE activity on the FS 992 outboard bulkhead during flights 800 through 806. There is no significant activity at that point during this 3-hour period. Figure 12 shows a buildup of AE events at a signal source location of -9 to -11 between locating sensors M6 and M5 from flights 1050 to 1061. Figure 13 shows an increasing number of the same signal source locations between locating sensors M6 and M5 as the test progressed.

The AE events generated at signal source locations (-)9 and (-)11 continued through flight 1280, the end of the second fatigue life. The shaded area shown in Fig. 14 between hyperbolas (-) 9 and (-) 11 indicates the area of concern on the FS 992 outboard bulkhead. However, after completion of the second fatigue life, an inspection revealed an 8 to 10-inch crack at the location between hyperbolas (+) 7 and +(10) of Fig. 14. The acoustic emission system detected the crack propagation in the 992 outboard bulkhead (Fig. 12 and 13), but the location was inverted 180° because of an incorrect polarity sign (negative half of sensor axis instead of positive).



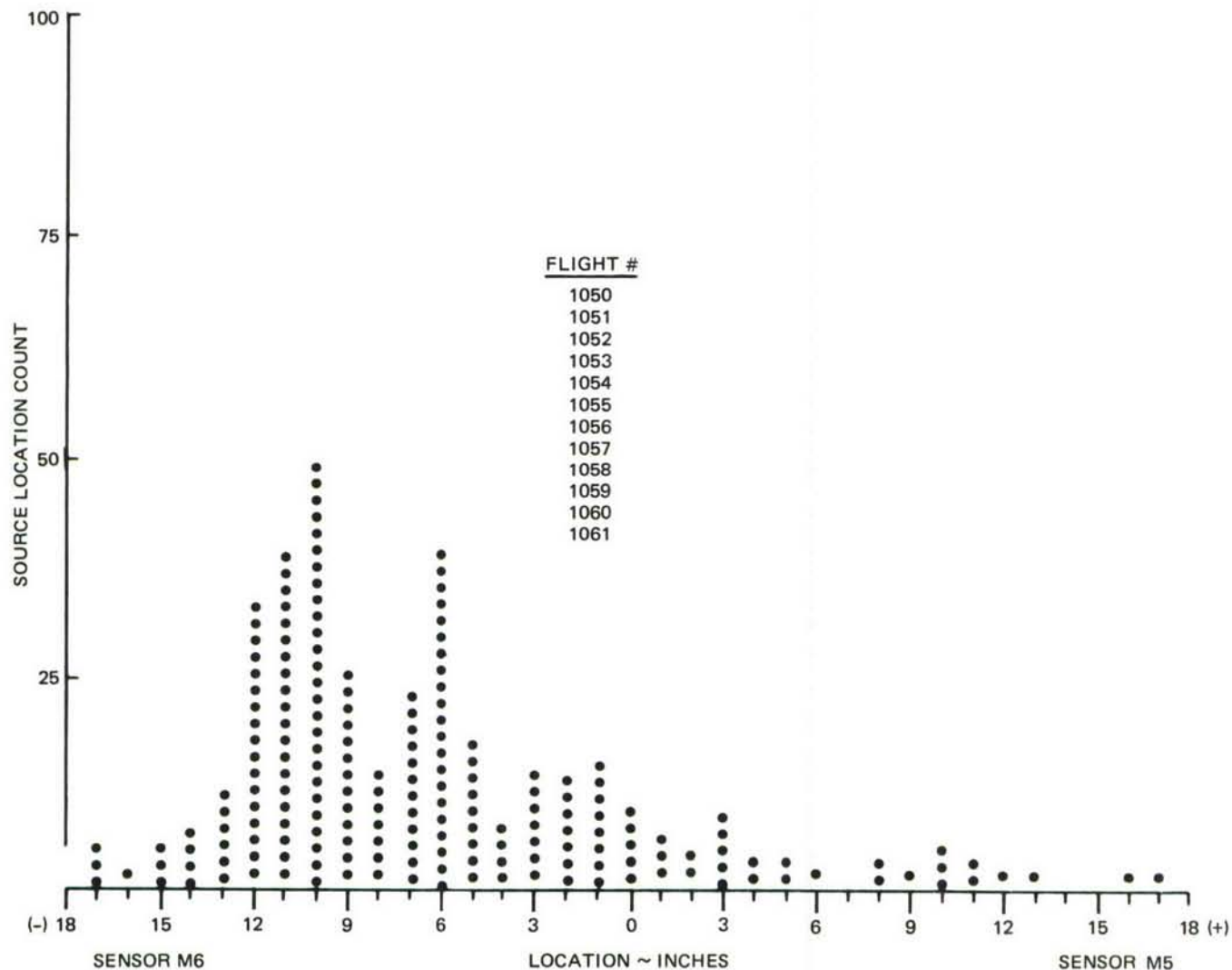


2293-011

**Fig. 11 FS 992 Outboard Bulkhead (Second Life)**

## TEST RESULTS ANALYSIS

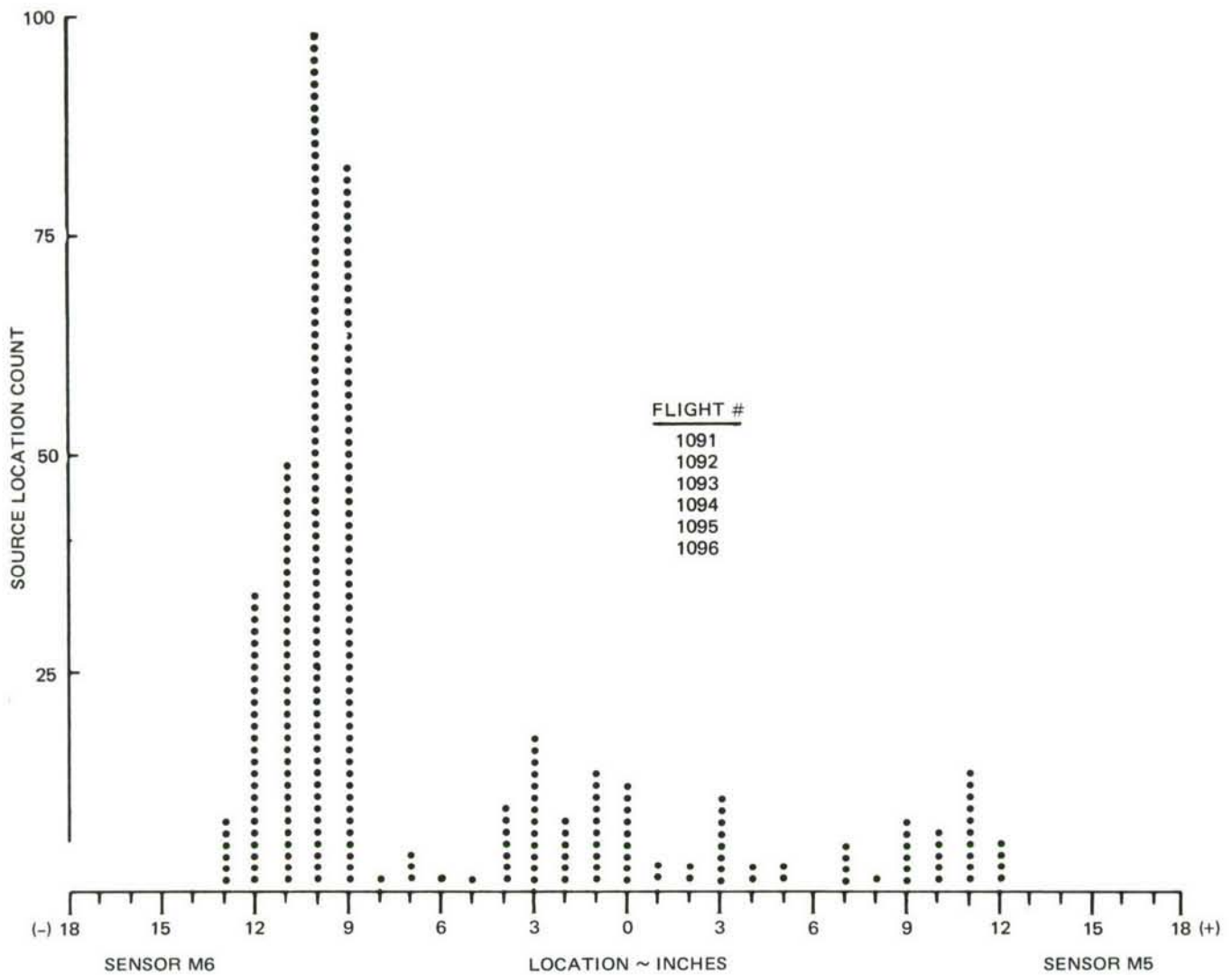
An investigation was conducted to determine the cause of the 180° error in the crack location on the FS 992 outboard bulkhead. It is believed that cyclic extraneous noise interference introduced at the loading point below sensor M6 (Fig. 14) interacted with the acoustic emission event signals and caused the error in the following manner. Without interference, the crack would be located as follows (Fig. 14): sensors M5 would be actuated first by the AE event signal which would register a (+) polarity; at  $\Delta T$  time later, sensor M6 would be actuated to determine the signal source location on the positive half of the axis between the sensors. This location is shown in the hyperbolic area between (+)7 and (+)10.



2293-012W

Fig. 12 FS 992 Outboard Bulkhead (Second Life)

Without placing a slave sensor at the loading point, repetitious, unrejected extraneous noise was introduced into the area. Sensor M6 was actuated first, registering a (-) polarity. At  $\Delta T$  time later, an AE event signal from the cracked area received at sensor M5 would determine a signal source location on the negative half of the axis between the sensors. Based on the location of the loading point, multiple erroneous signal source locations would be located in the shaded area between hyperbolas (-)9 and (-)11, as indicated by fatigue test data results.

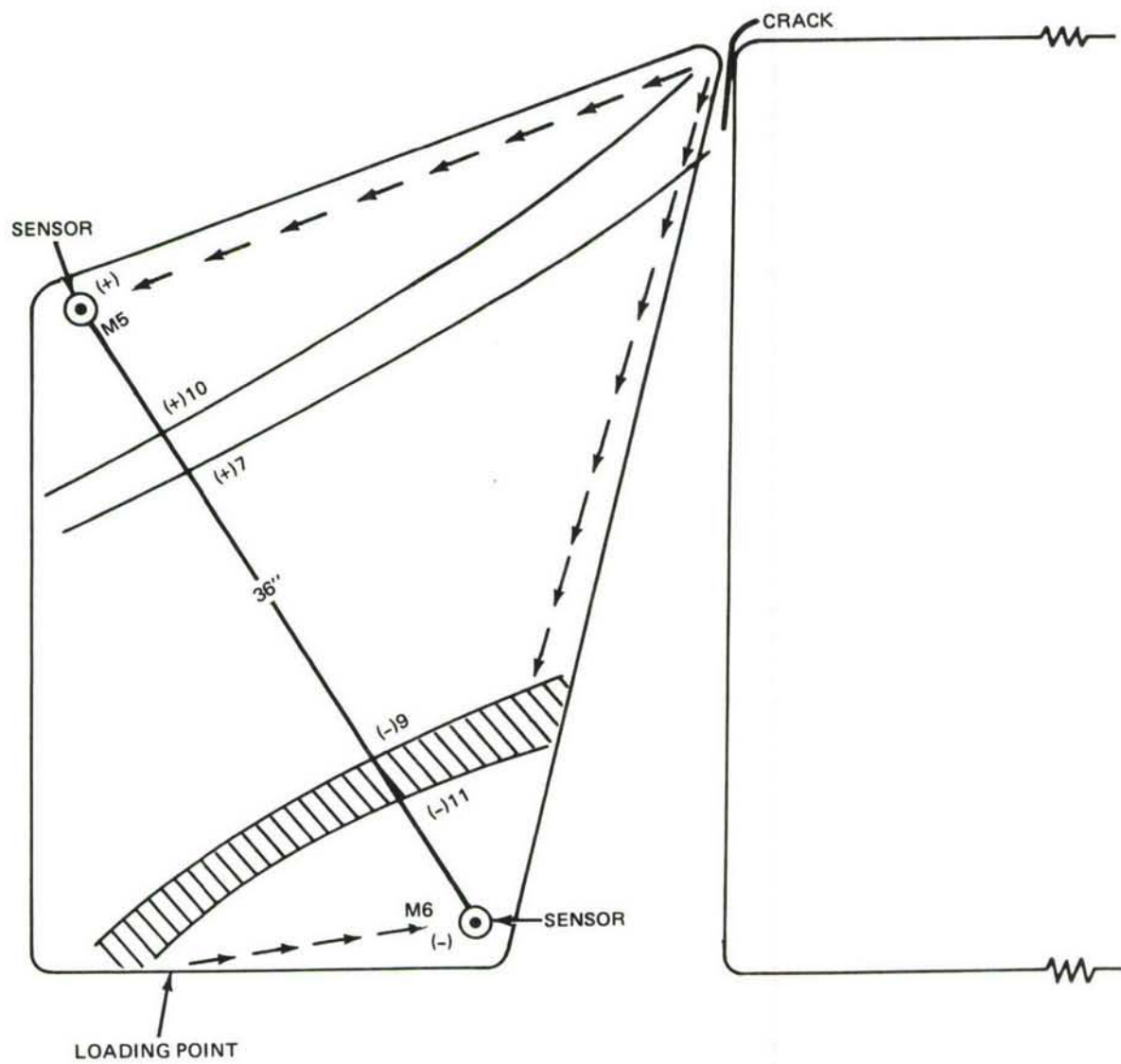


2293-013W

Fig. 13 FS 992 Outboard Bulkhead (Second Life)

The erroneous crack location experienced demonstrates the complexity of detecting acoustic emission signals during fatigue cycling because of extraneous noise interference. It was possible to detect acoustic emission activity on the FS 992 outboard bulkhead despite unrejected extraneous noise interference, only because of the cyclic nature of the noise interference. If the extraneous noise had been random in nature, it would not have been possible to detect any acoustic emission activity on the bulkhead without rejection of the extraneous noise interference by the system hardware. Unrejected random extraneous noises would interfere with AE event signals, generating a multitude of random erroneous signal source locations, and masking AE event signals, as explained in System Operation, Section II.





2293-014

Fig. 14 FS 992 Outboard Bulkhead

## Section IV

### AMAVS FATIGUE TEST - ACOUSTIC EMISSION MONITORING - THIRD FATIGUE LIFE

#### INSTALLATION CHANGES

Based on the results obtained during acoustic emission monitoring of the second half of the second fatigue life test, the following changes were made prior to monitoring the third fatigue life.

Twelve additional locating sensors and four preamplifiers were added to the areas being monitored to provide increased sensitivity. The geometry of the sensor placement was changed to provide more reliable coverage of all the areas monitored. The locating sensors were placed in geometric configurations such that the multi-sensor axes could be monitored as described in Section II, System Operation. The sensor arrangements and the six areas monitored are shown in Fig. 15 through 19. The areas monitored referenced to the AMAVS are shown in Fig. 20.

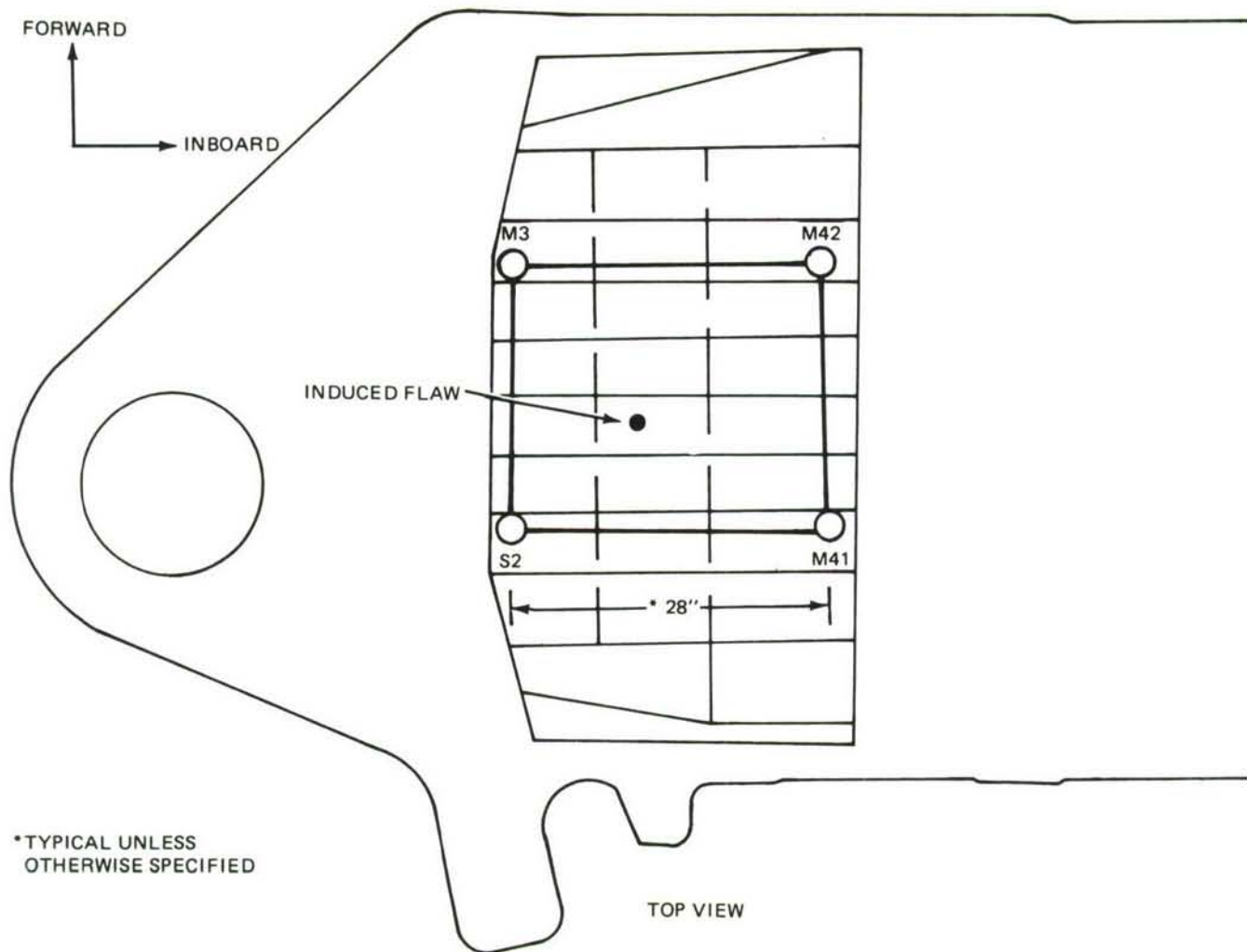
Two additional slave sensors and one preamplifier were added in the vicinity of four independent loading points on the AMAVS. The four slave sensors used previously were re-located to eliminate more of the extraneous noise interference generated at loading points common to the monitored areas.

Acoustic emission sensors were removed from the closure rib and were installed to monitor the XF84 Outboard Intermediate Rib, as shown in Fig. 19.

As part of the third lifetime test program, induced flaws approximately 0.150 in. long were added to the FS 932 bulkhead, the FS 992 outboard bulkhead, and the bottom cover, as shown in Fig. 18, 17 and 15.

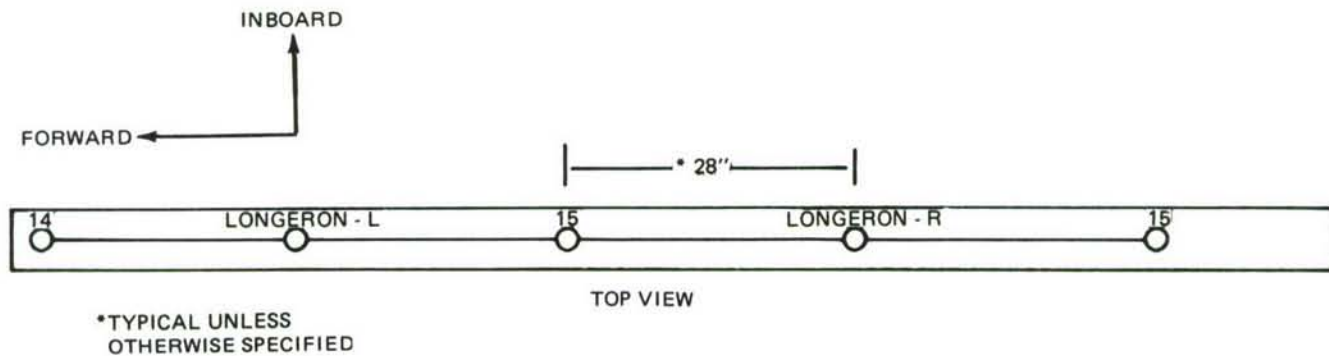
#### TEST RESULTS

There was no significant acoustic emission activity on the XF84 Outboard Intermediate Rib or the FS 992 inboard bulkhead during monitoring of the third fatigue life (1280 flights). Inspection at the end of three lifetimes showed that cracking had not occurred on either the XF84 Outboard Intermediate Rib or the 992 inboard bulkheads. These bulkheads had not been previously flawed.



2293-015

Fig. 15 Bottom Cover



2293-016

Fig. 16 Left Upper Longerons



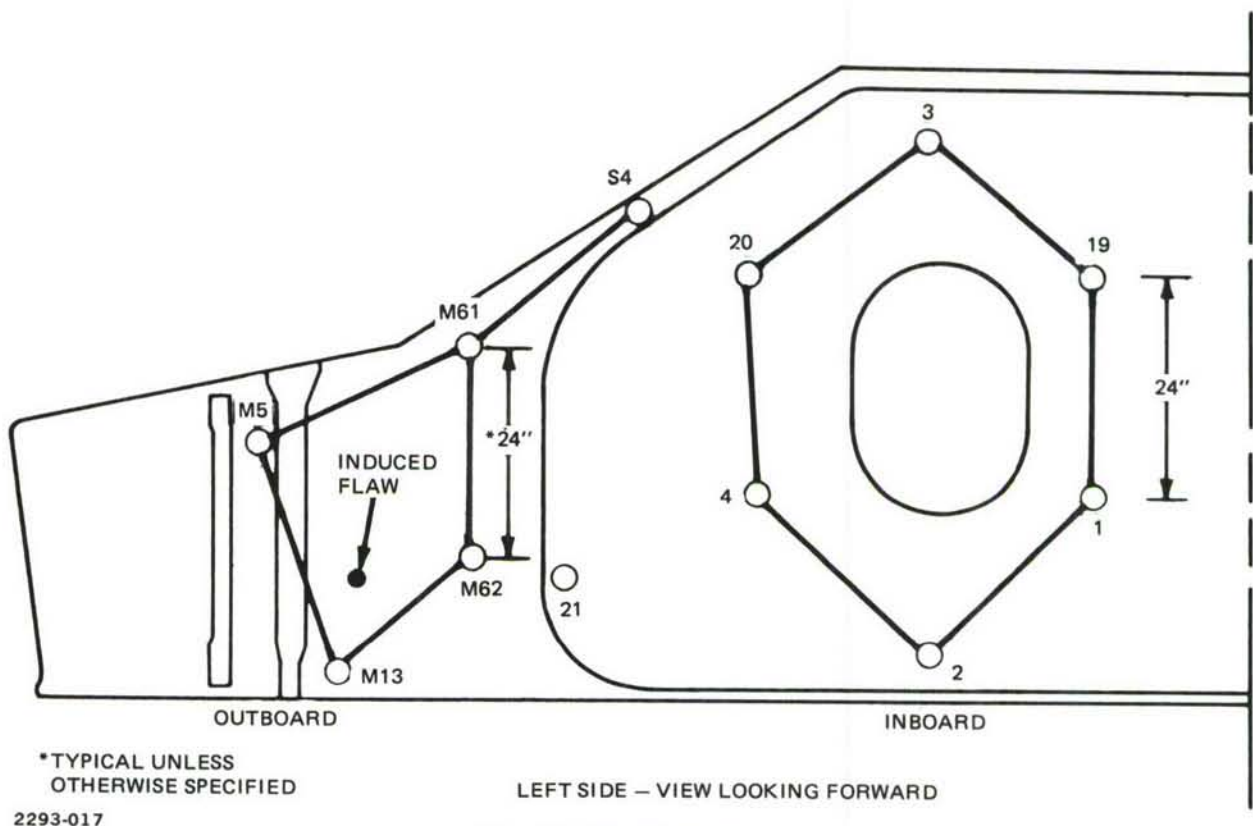


**Fig. 17 FS 992 Bulkhead**

The induced flaw on the FS 932 bulkhead shown in Fig. 18 showed no signs of acoustic emission activity during third life monitoring. Inspection at the end of three lifetimes revealed no induced flaw growth, which correlates with acoustic emission results.

The induced flaw on the FS 992 outboard bulkhead shown in Fig. 17 also showed no signs of acoustic emission activity during the third fatigue life. Inspection at the end of three lives revealed that there was a slight growth of 0.060 inch between flights 784 and 1280. This extremely small growth rate (0.060 inch during 496 flights) demonstrated that the amount of acoustic emission activity generated by an extremely slow-growing crack was not enough to be detected because of the large amount of extraneous noise signals.

The induced flaw on the bottom cover shown in Fig. 15 did show acoustic emission activity during the third fatigue life. Figure 21 shows no significant activity generated on the bottom cover during flights 235 through 250. This graph shows virtually no signal source locations generated for approximately 8 hours of on-line monitoring time. However, Fig. 22 shows a marked increase in AE activity during flights 251 through 264. Signal source locations (based on sensor pair S2 and M41) began to register at a location between hyperbolas (+)3 and (+)6 as shown in Fig. 23. Sensors M3 and M42 were monitored for a short period of

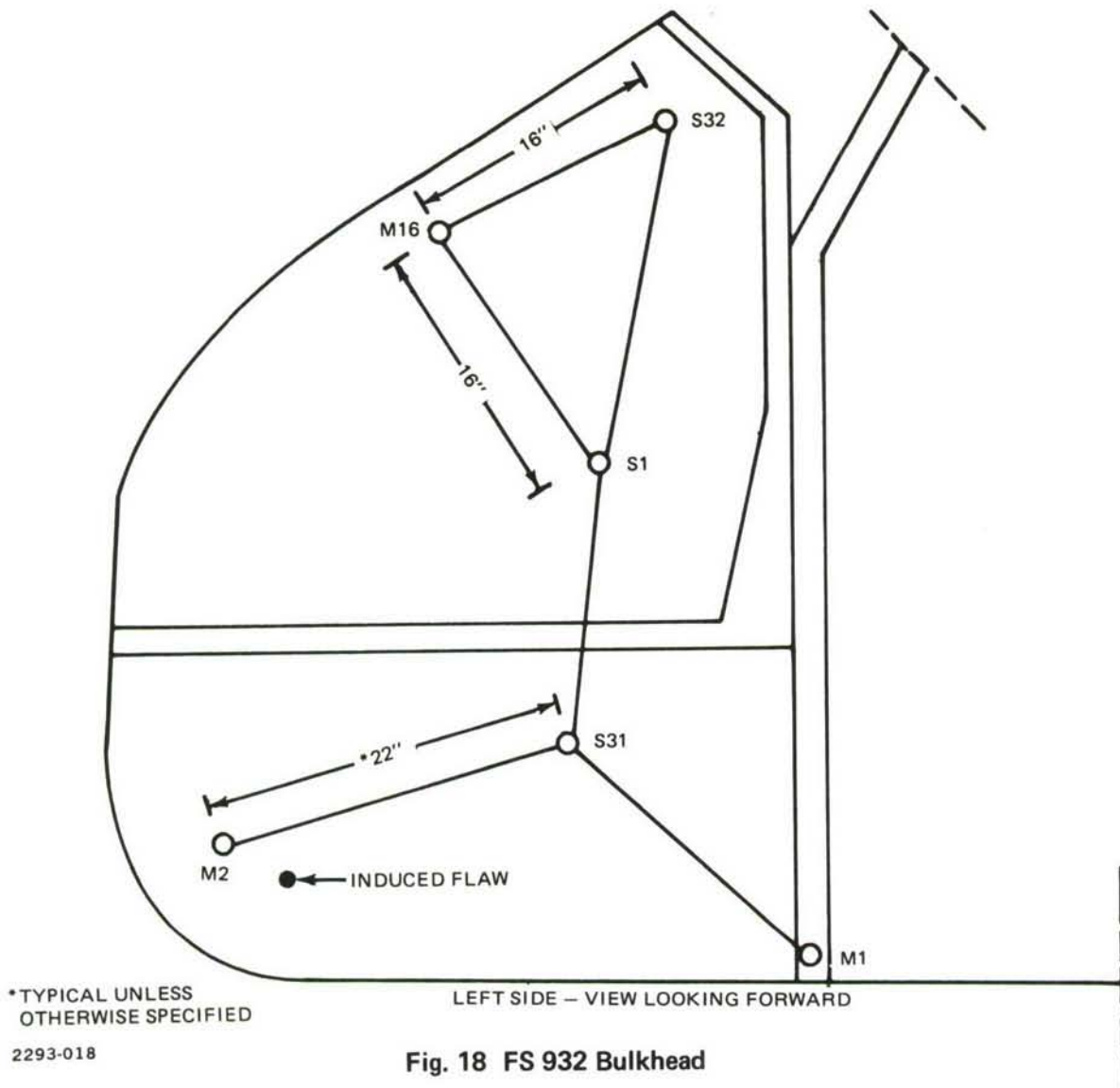
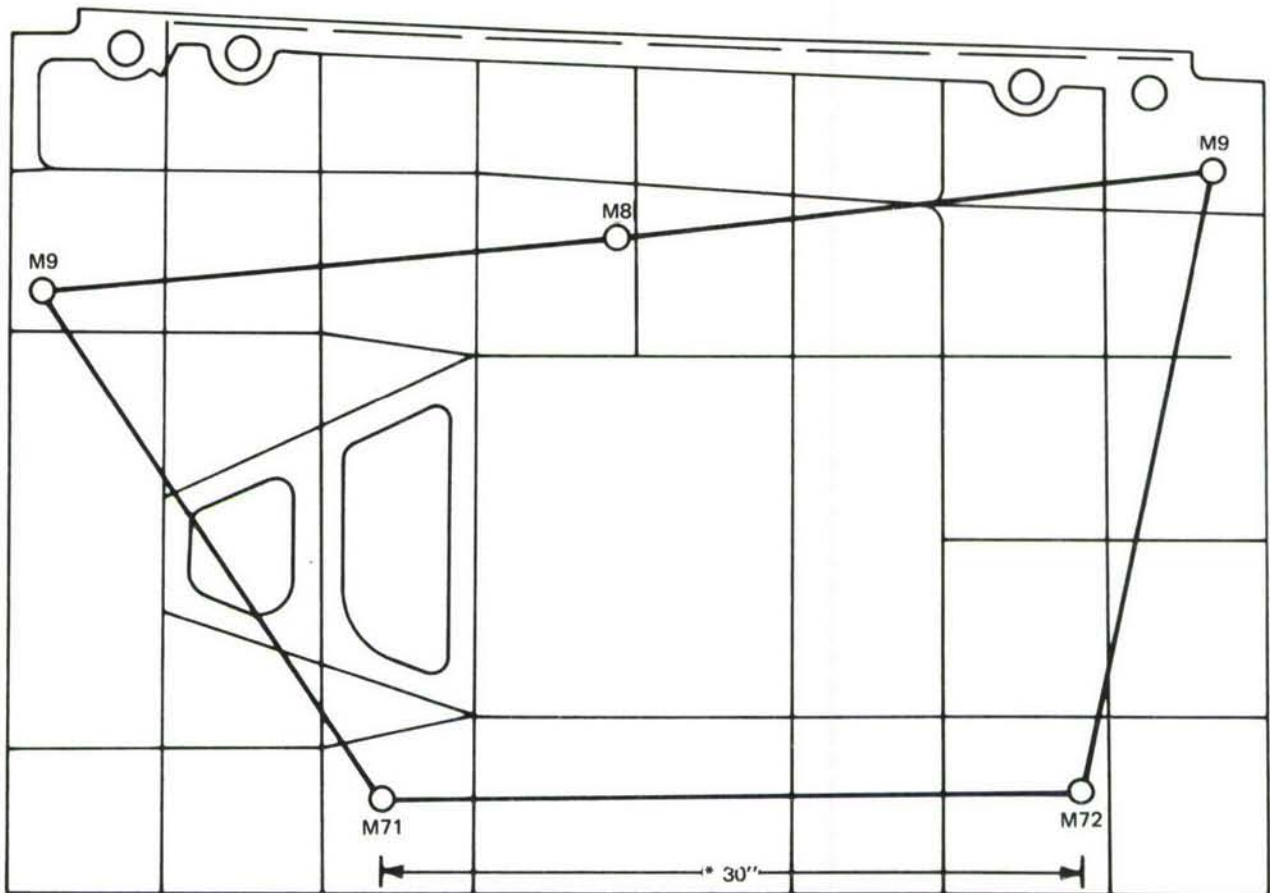


**Fig. 18 FS 932 Bulkhead**

time to verify the induced flaw site. The induced flaw on the bottom cover showed AE crack initiation at that point in the third life test (flights 251-264). Figure 24 shows the same signal source locations generated from the induced flaw location during flights 271 through 279 (approximately 4 hours on-line monitoring time using sensors S2 and M41). Quality Control Inspection revealed an initial crack growth of 0.061 in. from 0.140 in. to 0.201 in. at flight 339. This was the first sign of flaw growth by conventional NDT methods. Signal source locations from the induced flaw were detected approximately 80 flights before detection by conventional NDT methods.

Figure 25 shows an increase in the amount of signal source locations at the induced flaw location. Approximately the same number of signal source locations were detected in two



LEFT SIDE – VIEW LOOKING OUTBOARD

\*TYPICAL UNLESS  
OTHERWISE SPECIFIED  
2293-019

**Fig. 19 XF84 Outboard Intermediate Rib**

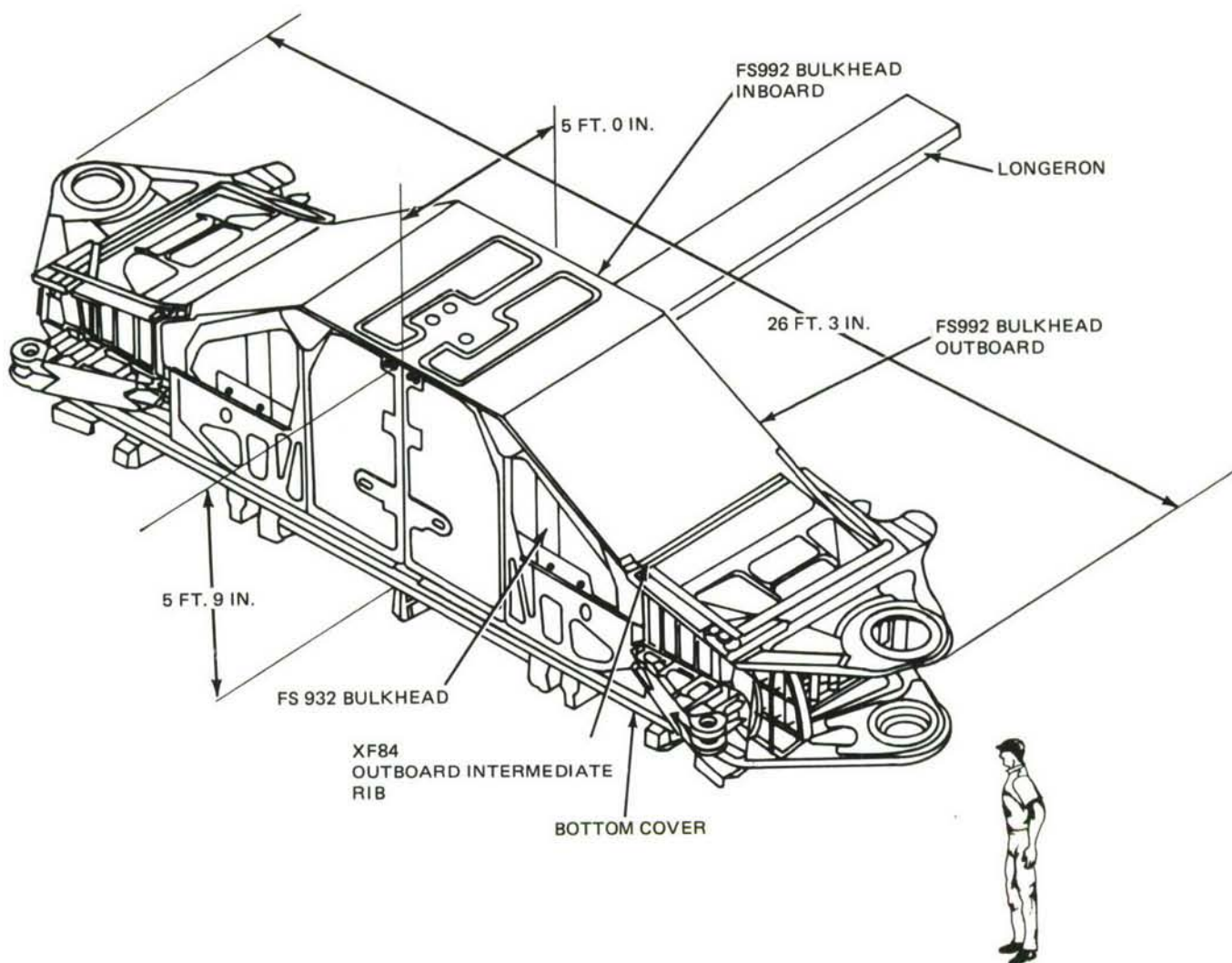
hours (four flights, 362 to 365) as those shown in Fig. 22 during a seven-hour monitoring period.

Figure 26 shows a marked decrease in the number of signal source locations generated from the flaw location during flights 889 to 892. This denotes a general decrease in the crack growth rate.

Quality Control Inspection at the end of the third life revealed a crack growth on the bottom cover of 0.440 in. from 0.140 in. to 0.580 in.

The left upper longeron began to generate multiple signals during flights 262 through 268. Figure 27 shows a histogram of the buildup of these signal source locations between locating sensors 14 and Long.-L during those seven flights.





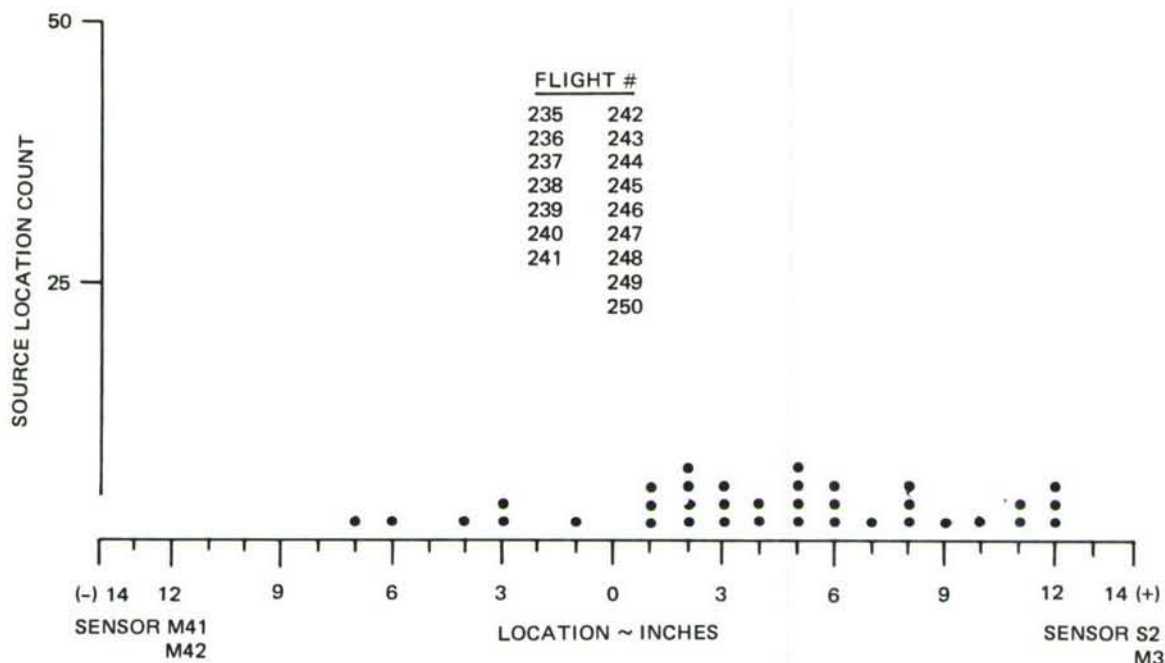
### AMAVS – WCTS

2293-020

**Fig. 20 Areas Monitored (Third Life)**

An inspection several flights later revealed three loose bolts in the area as shown in Fig. 27 between sensors 14 and Long. -L. After the bolts were tightened, the signal source locations at (+)1 to (+)2 inches (Fig. 27) were eliminated. Figure 28 shows the disappearance of these signals from flights 288 through 293. The left upper longeron monitoring indicated no other acoustic emission activity for the remainder of the third life. No cracks were found in the longeron when inspected at the end of three lifetimes.

The FS 992 outboard bulkhead showed no signs of acoustic activity until flight 489. Virtually no AE activity is shown in Fig. 29 for flights 293 through 306 (approximately 7 hours of monitoring time). Multiple signal source locations were detected during flight 491, as shown in Fig. 30.



2293-021W

**Fig. 21 Bottom Cover (Third Life)**

Figure 30 shows the AE activity for 10 minutes of flight 491. The total number of signal source locations for flights 491 and 492 exceeds 1,000. Several visual inspections of the area revealed no cracking or damage.

Figure 31 shows the signal source locations ceased during flights 551 through 562. The multiple signals did not reappear until flight 884. Figure 32 shows the reappearance of the signal source locations between sensors M61 and S4. Another axis was monitored during flight 885 to pinpoint the location of the signal source locations being generated between locating sensors M6(1) and S4. The histogram of the signal source locations being generated between locating sensors M62 and S4 is shown in Fig. 33. The area of indicated source activity is the shaded area of Fig. 34.

Inspection after the third life revealed no cracking or damage on the FS 992 outboard bulkhead. It is important to note, however, that the indicated area is the same in which the 8 to 10-inch crack occurred during the second half of the second life test. As the damaged area was repaired with a bolted cover plate, an effective inspection was not possible.

Figures 35 through 39 illustrate the acoustic emission activity generated from the lower half of the FS 932 bulkhead during monitoring of the third fatigue life. The FS 932 bulkhead had very little acoustic emission activity until flight 643. Figure 35 shows that the activity on the FS 932 bulkhead during flights 565 through 571 is virtually non-existent. During

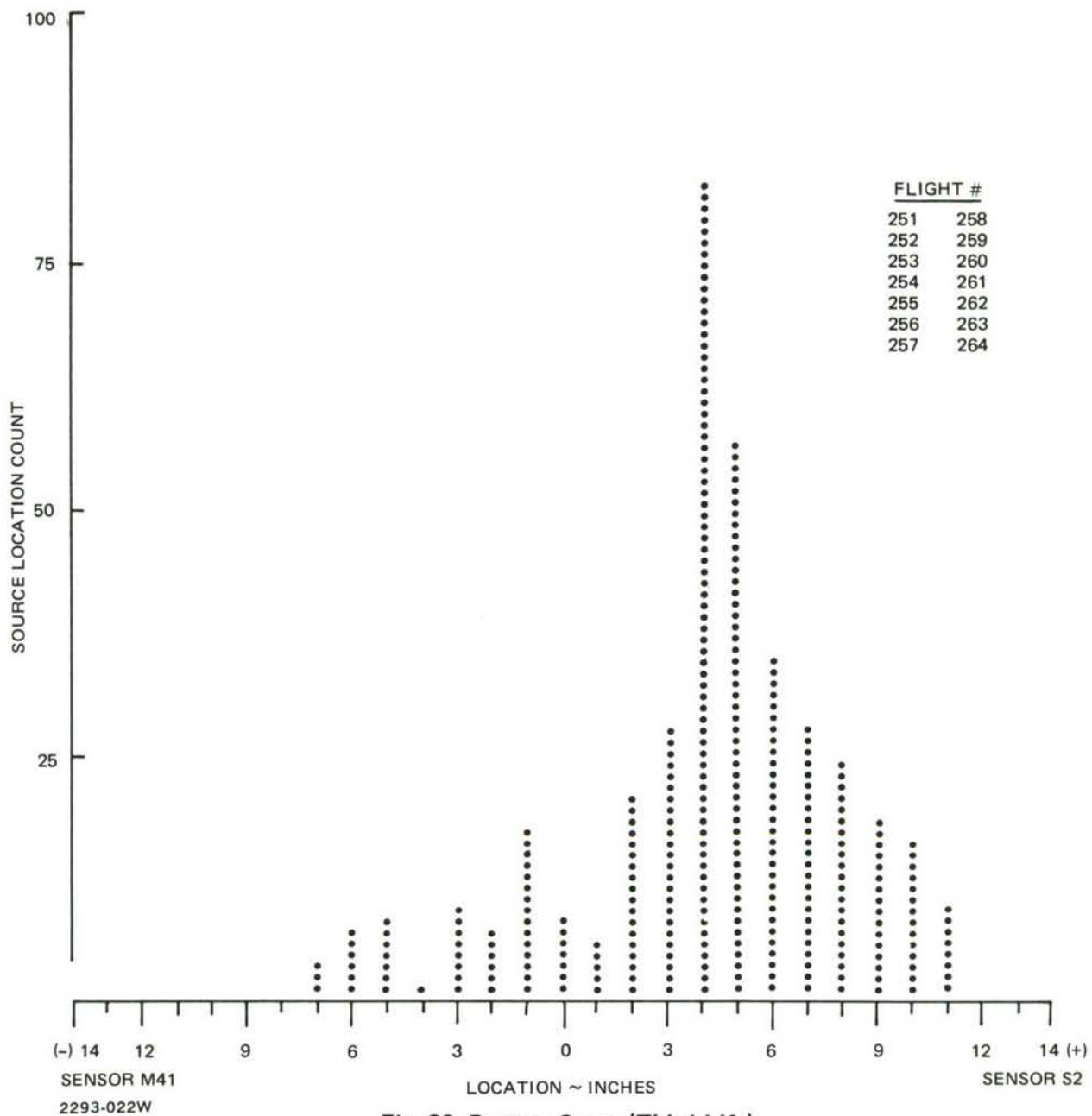
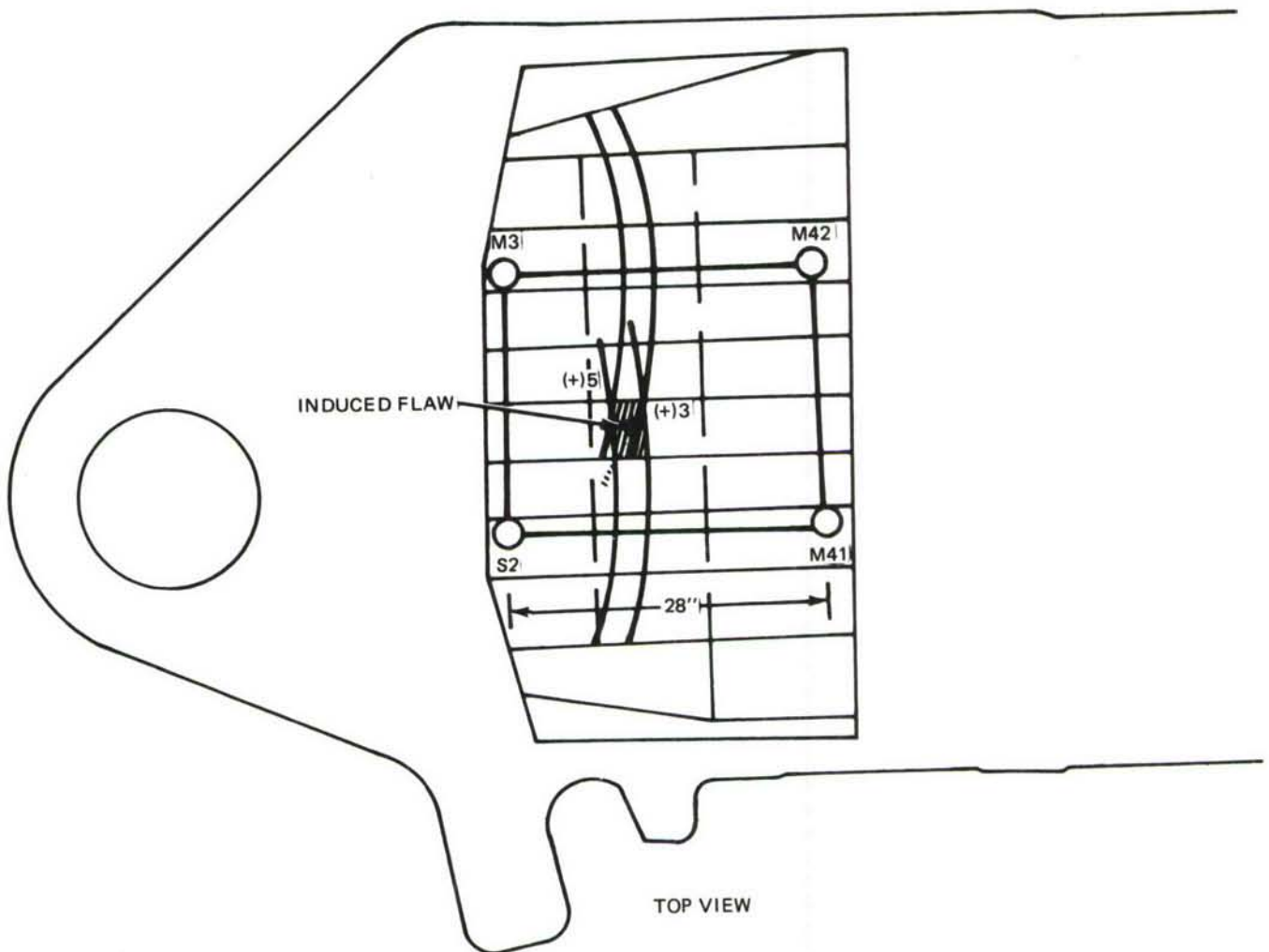


Fig. 22 Bottom Cover (Third Life)

flights 643 through 645, there was an accumulation of signal source locations, as shown in Fig. 36.

An attempt was made to monitor sensors M2 and S31 to determine a location of the activity shown in Fig. 36, by monitoring a different axis. However, signal source locations could not be located by sensors M2 and S31 because of a high background noise level detected by sensor M2. It was determined that the cause of the high background noise level at sensor



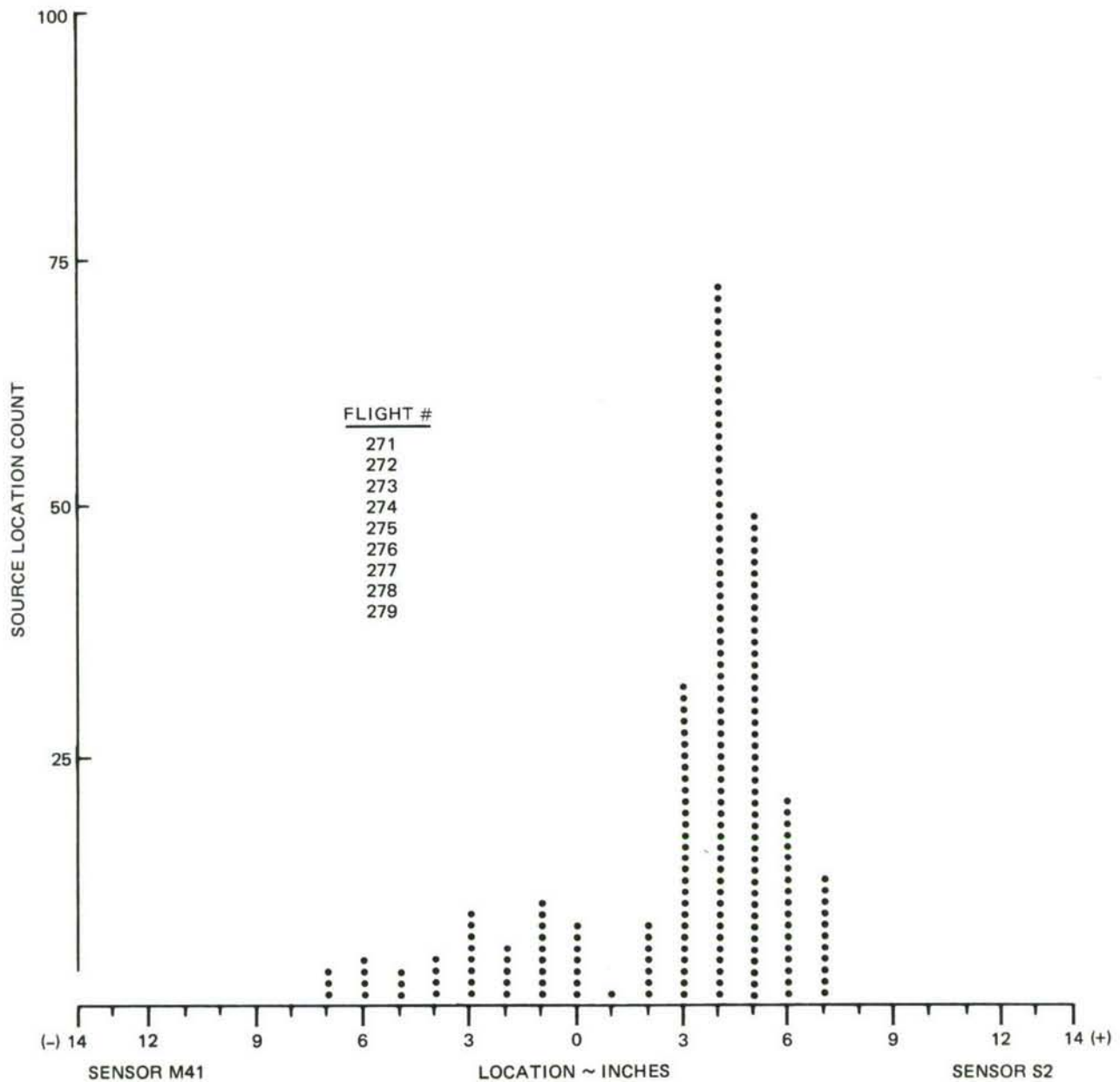


2293-023

Fig. 23 Bottom Cover

M2 was an air leak, shown in the shaded area of Fig. 37. The remainder of the third life test was monitored without the use of sensor M2.

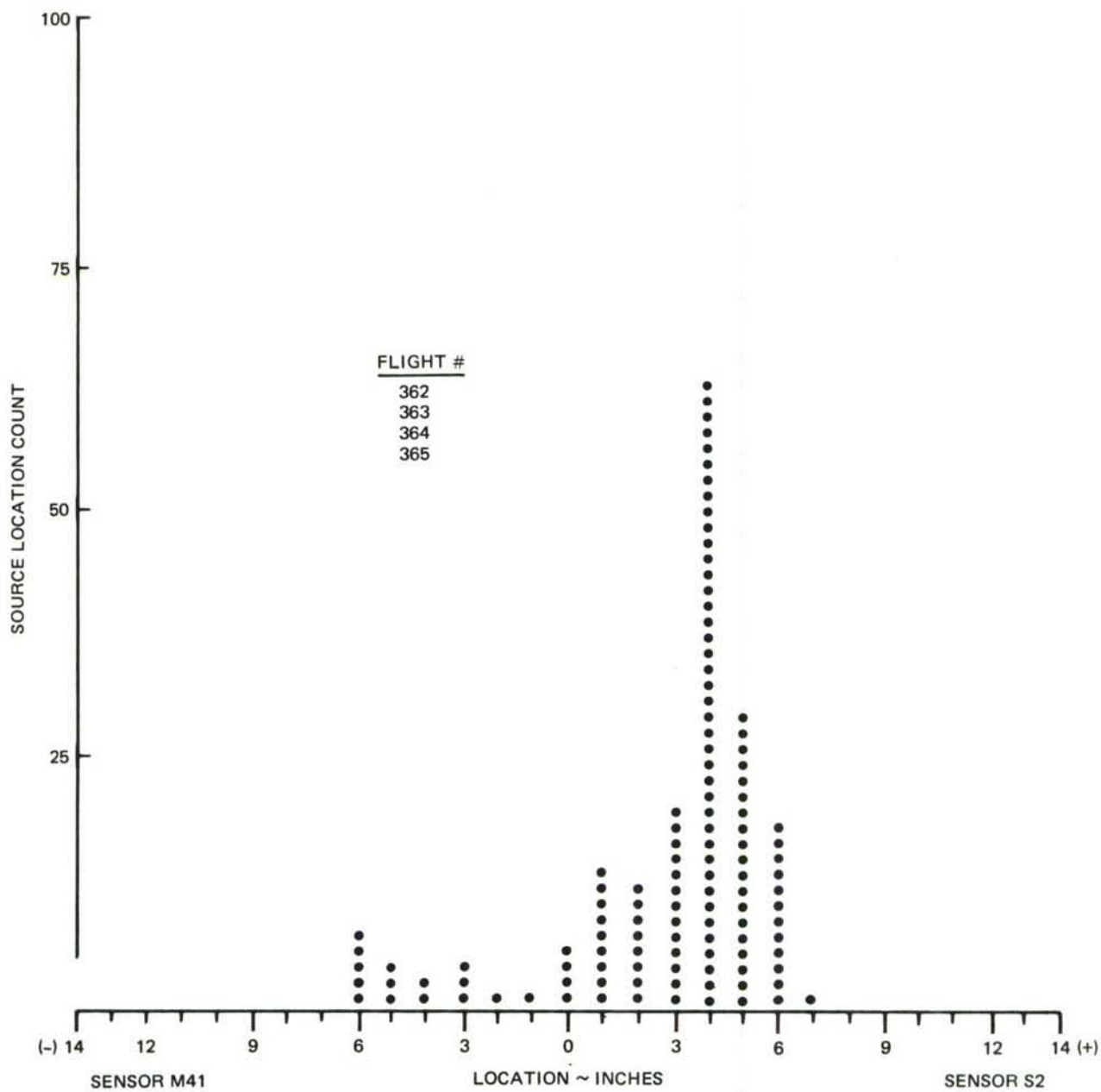
The multiple signal source locations that were generated increased in number as the test continued. Figure 38 shows the increase in signal source locations generated during flights 793 through 796. In Fig. 39 there are signal source locations in two areas between locating sensors  $S3_1$  and  $M_1$ , during flights 889 and 890, indicating the possibility of more than one source of activity, as indicated in the shaded area of Fig. 37. No cracks could be found during the Quality Control inspection at the end of the third life. However, an inspection after flight 500 of the fourth fatigue life revealed four cracks up to 6 inches long emanating from four bolt holes in the shaded area of Fig. 37. The air leak previously detected originated from these cracks.



2293-024W

**Fig. 24 Bottom Cover (Third Life)**

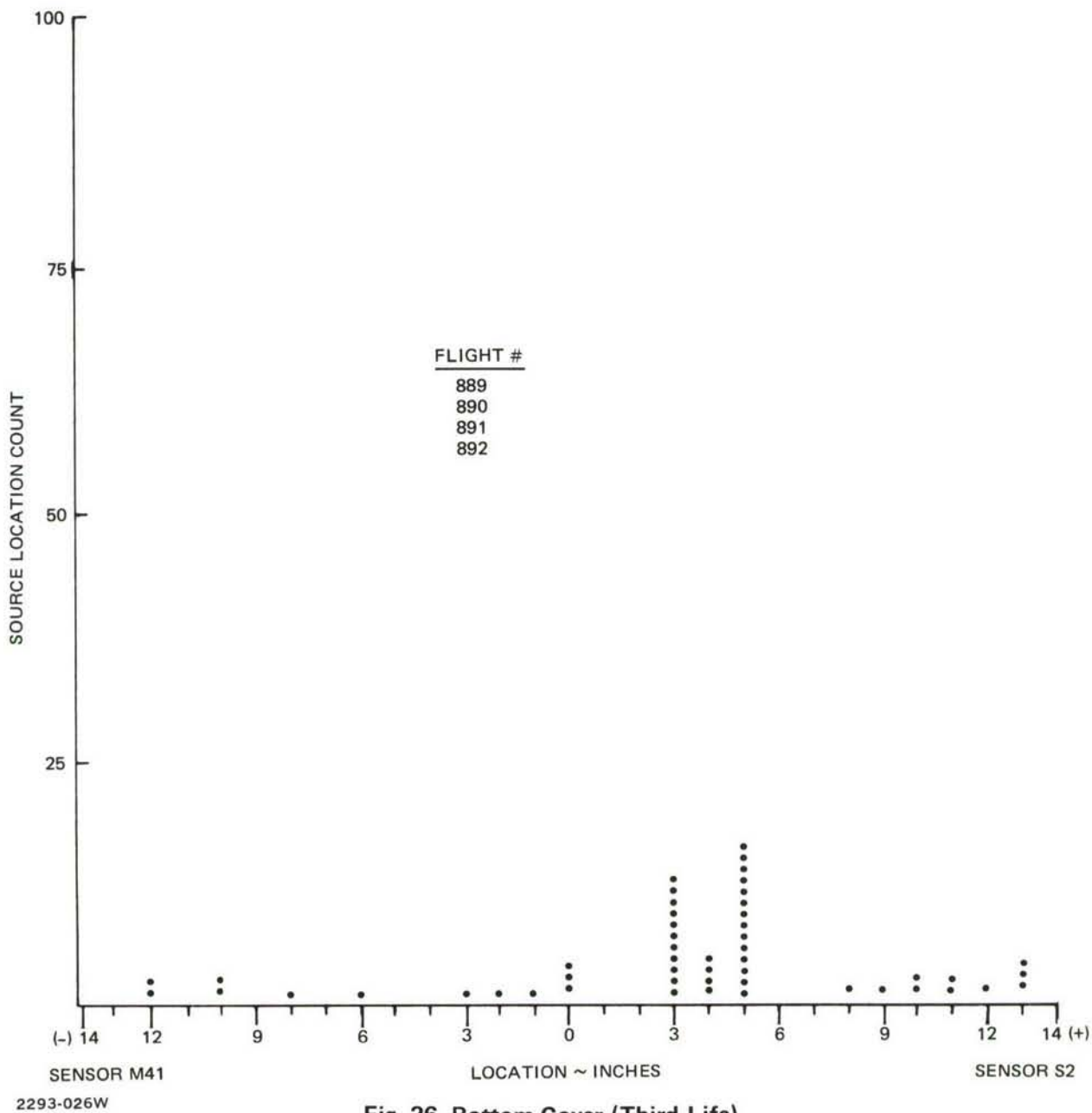
During flight 1159, activity was detected on the upper half of the FS 932 bulkhead, as shown in Fig. 40. Monitoring of this area was discontinued after flight 1164 until an additional locating sensor could be installed to verify the exact origin of the signal source locations on an additional axis. (Sensor M16 was installed at the beginning of the fourth fatigue life.)



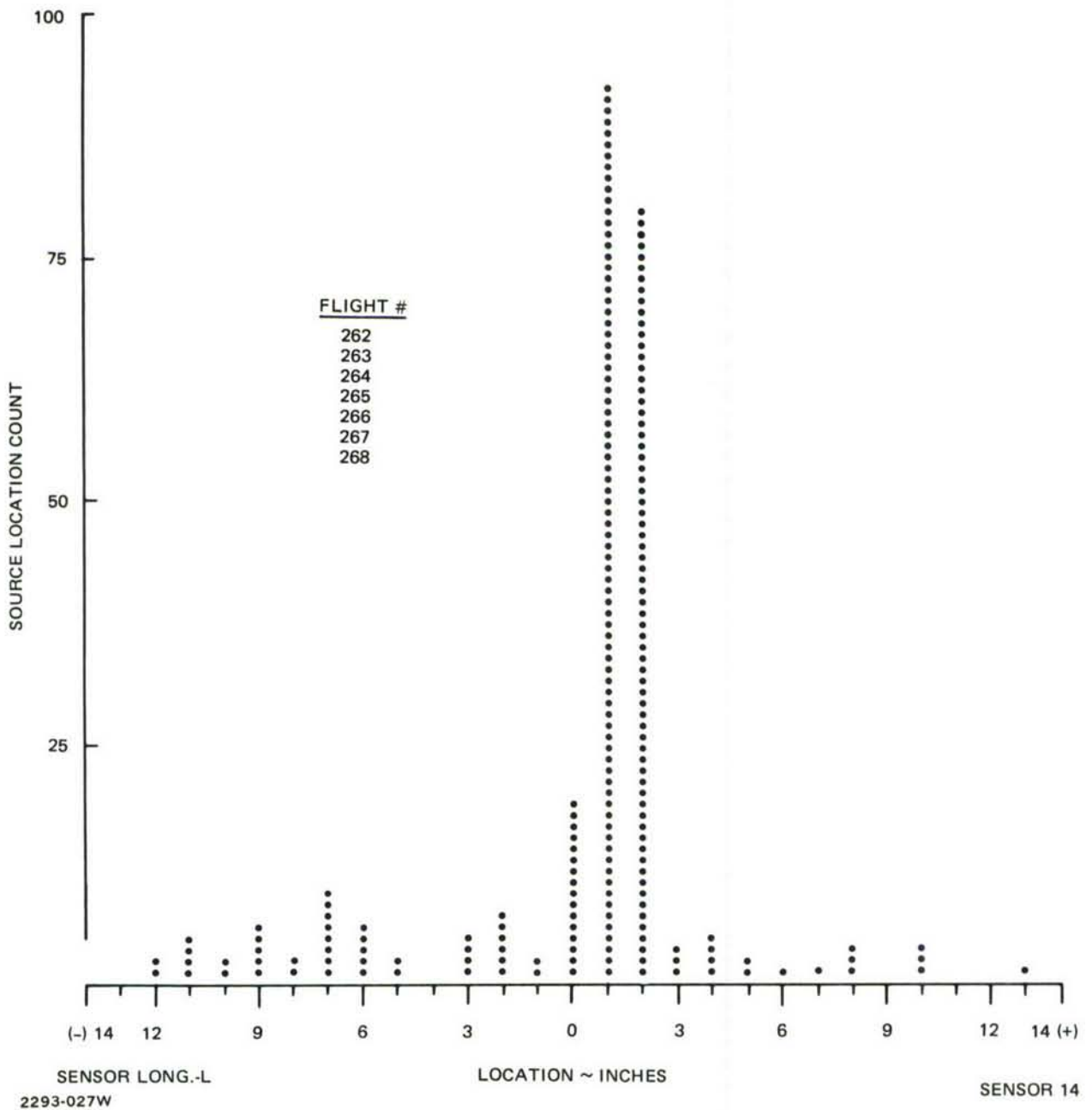
2293-025W

Fig. 25 Bottom Cover (Third Life)





**Fig. 26 Bottom Cover (Third Life)**



**Fig. 27 Left Upper Longeron (Third Life)**

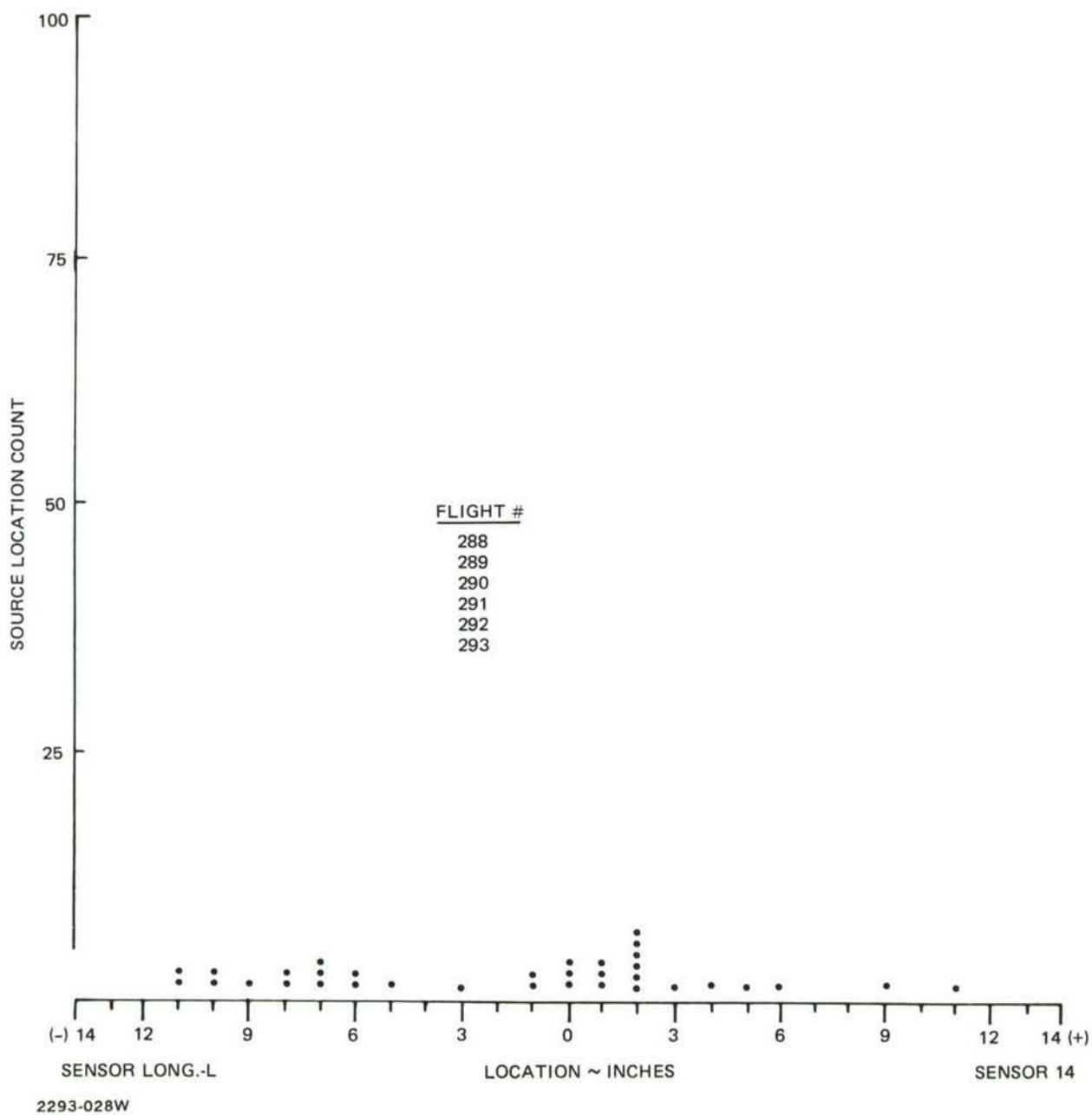


Fig. 28 Left Upper Longeron (Third Life)



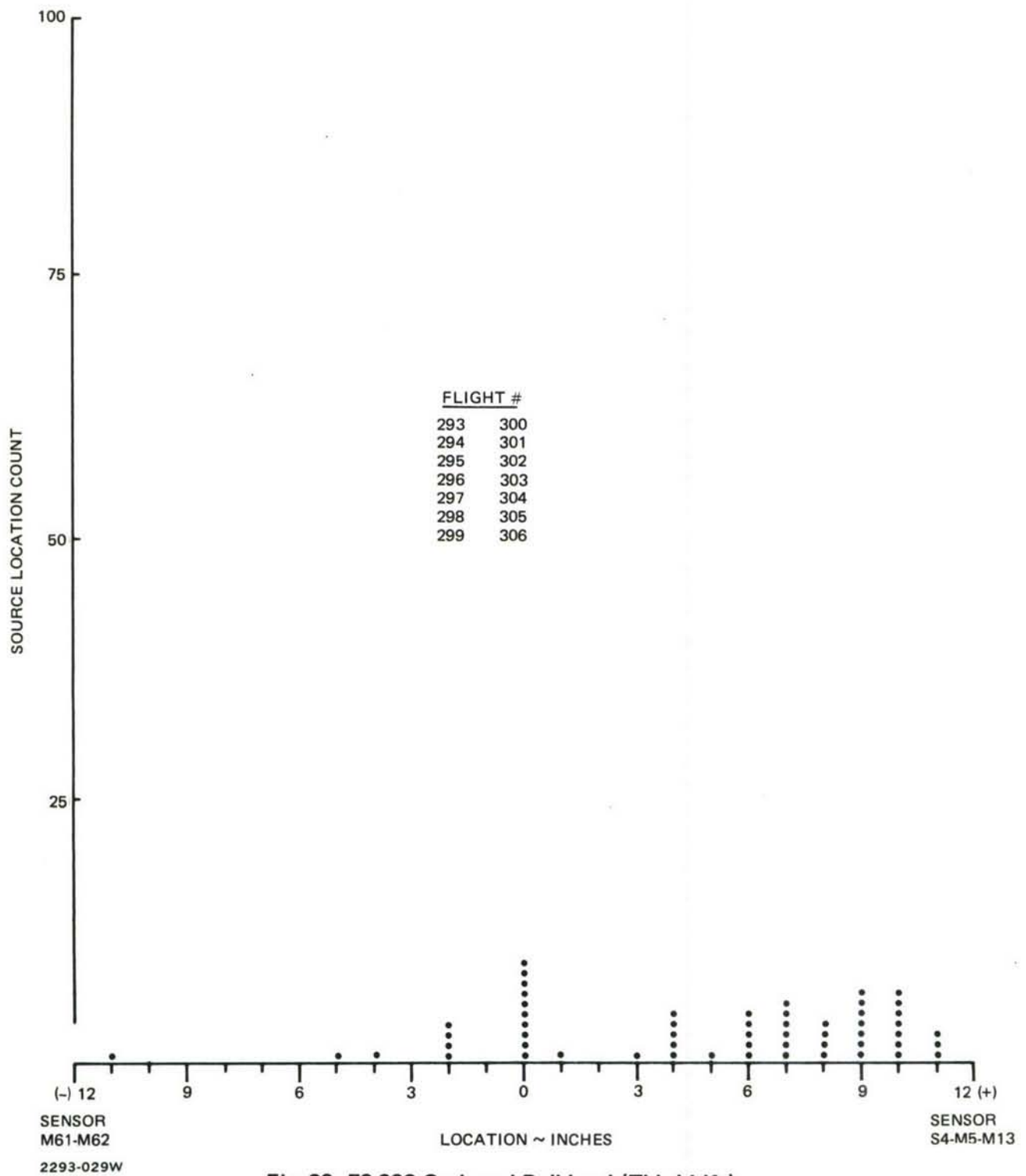
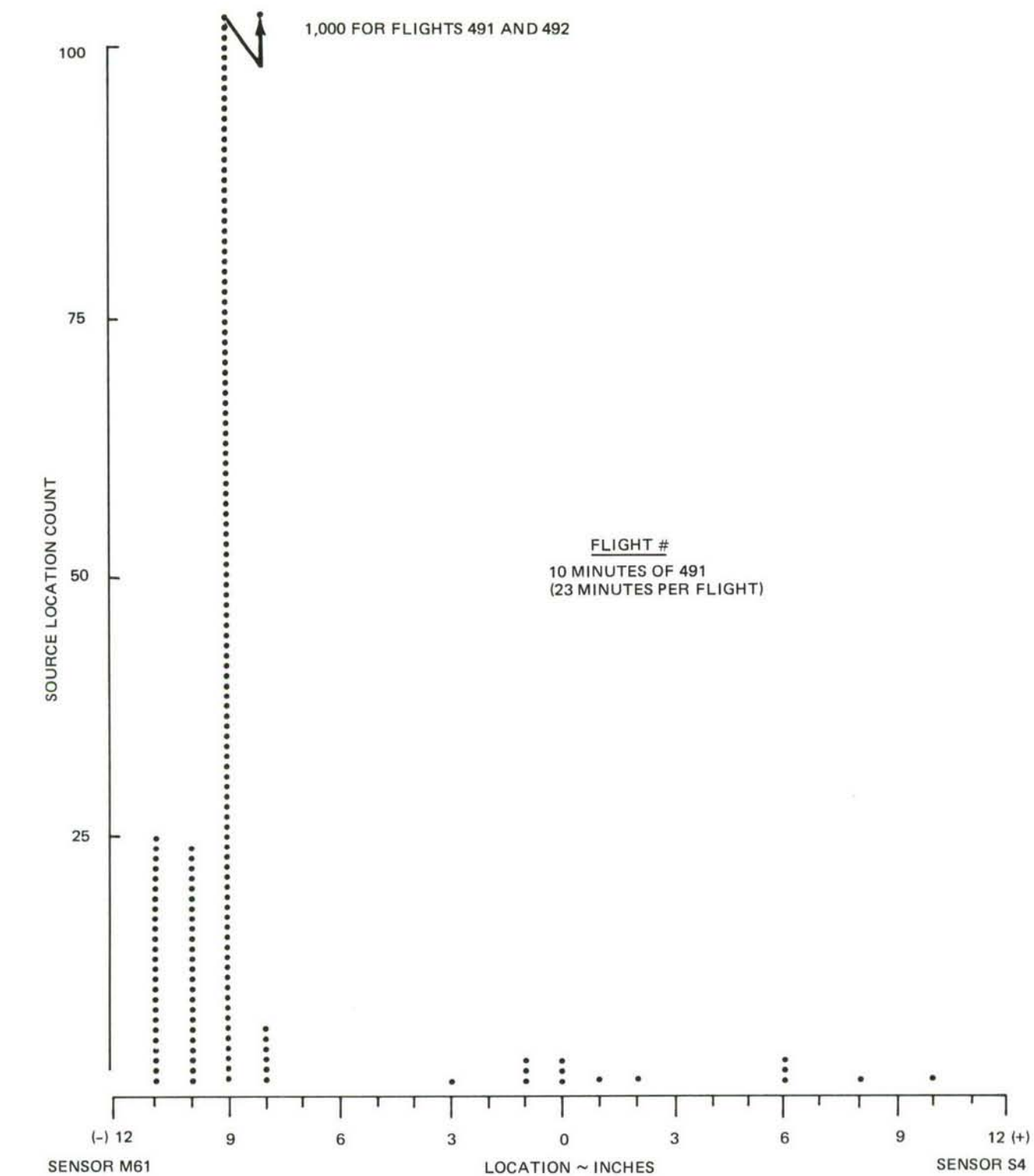
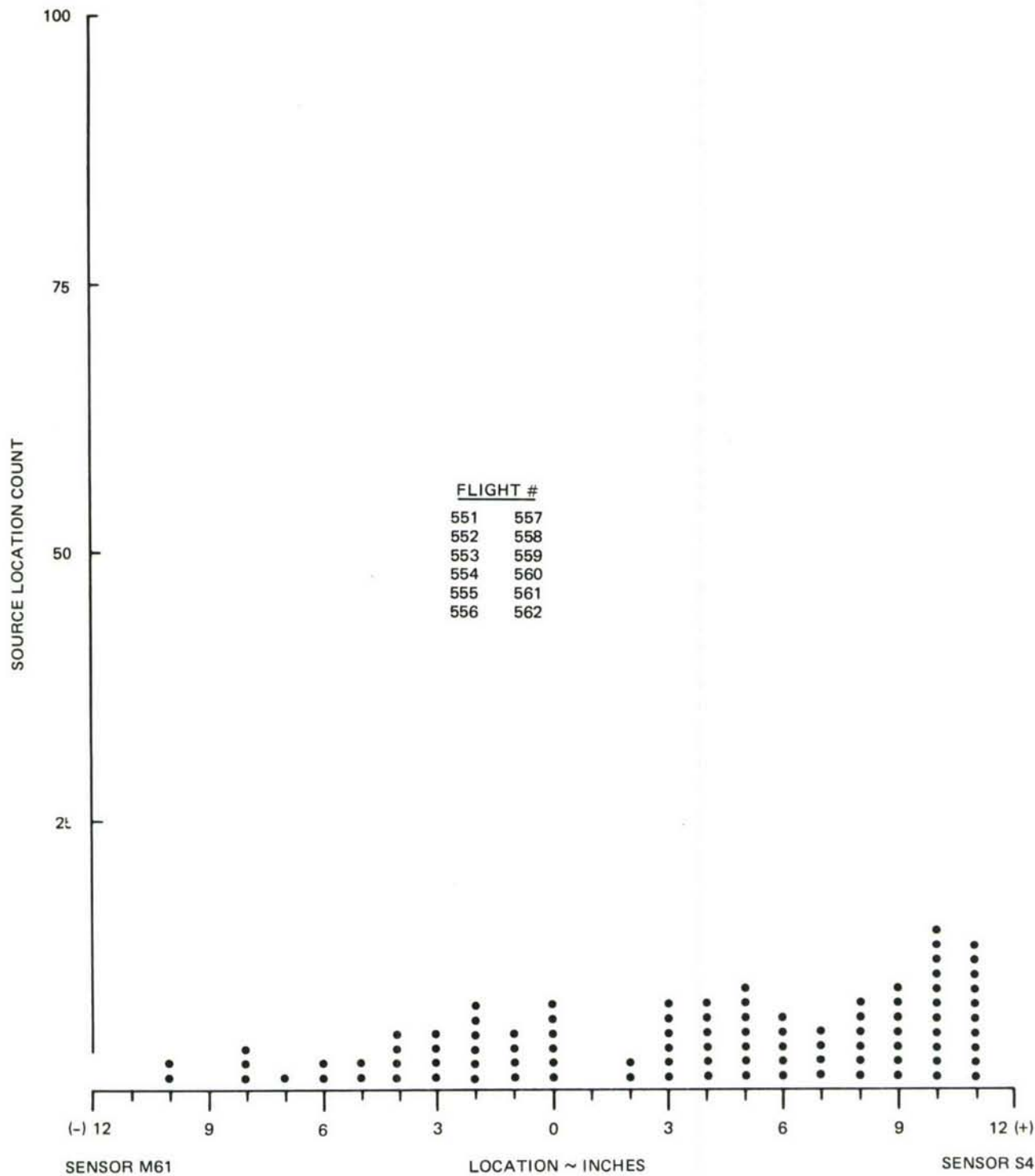


Fig. 29 FS 992 Outboard Bulkhead (Third Life)



2293-030W

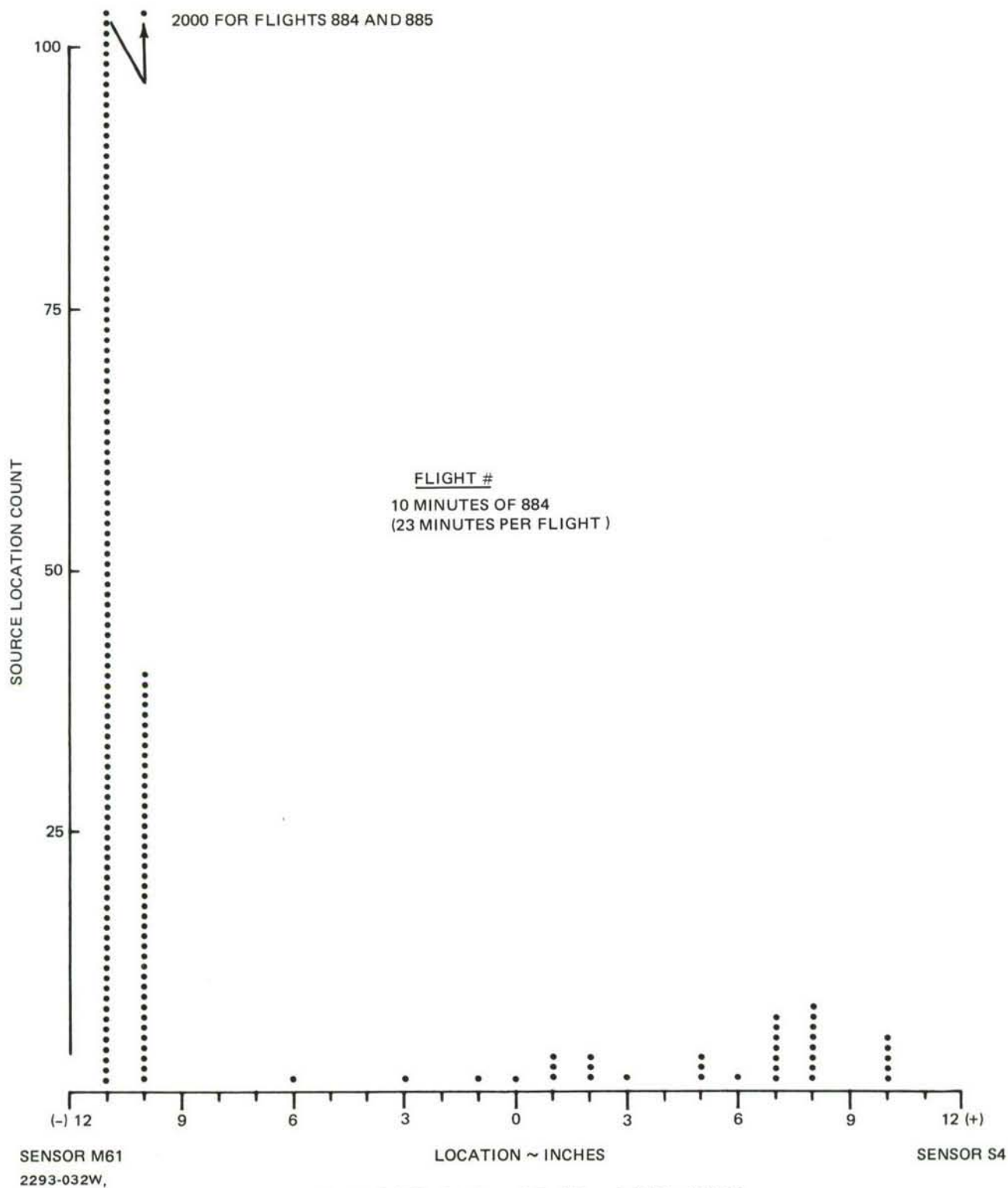
Fig. 30 FS992 Outboard Bulkhead (Third Life)



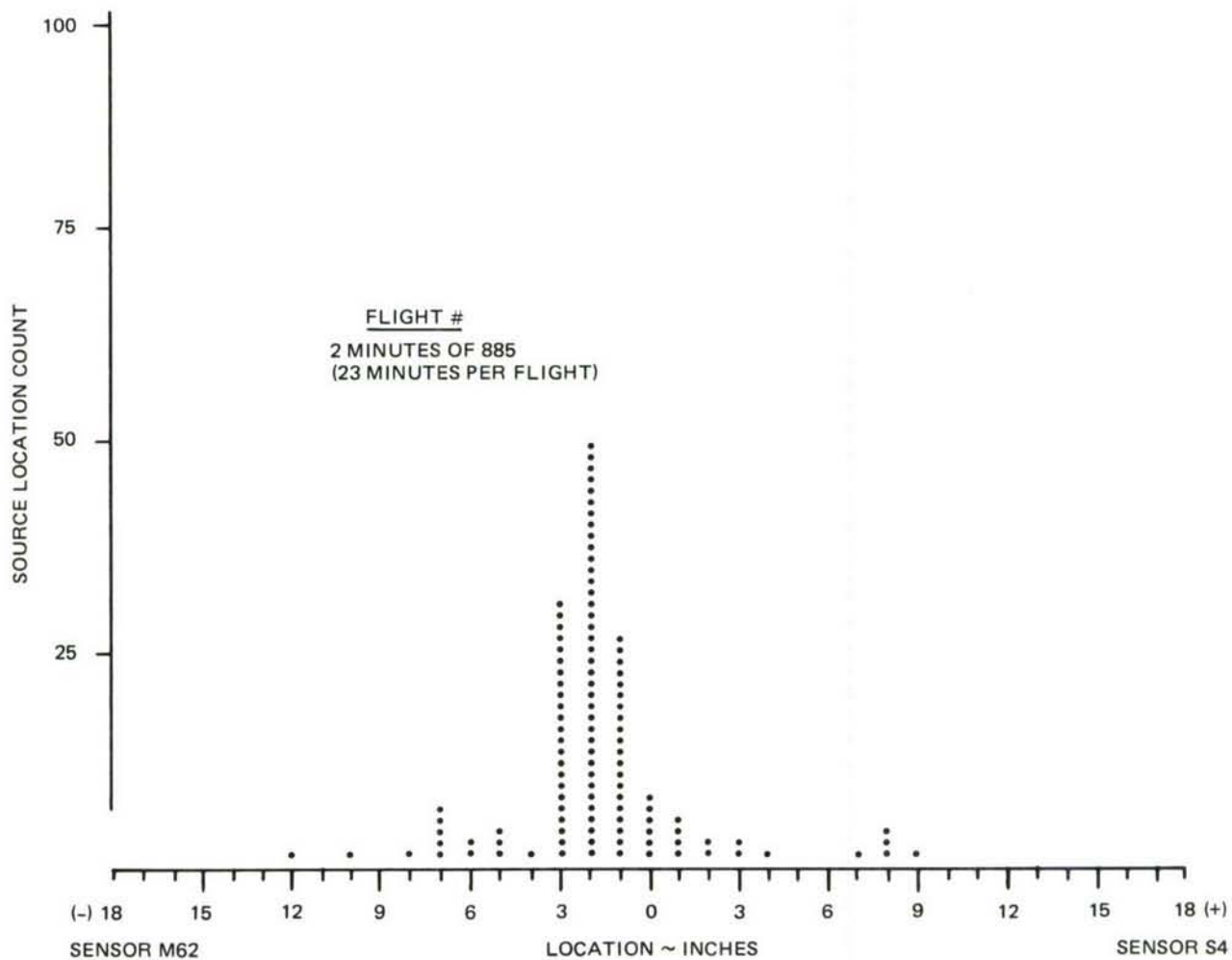
2293-031W

Fig. 31 FS 992 Outboard Bulkhead (Third Life)



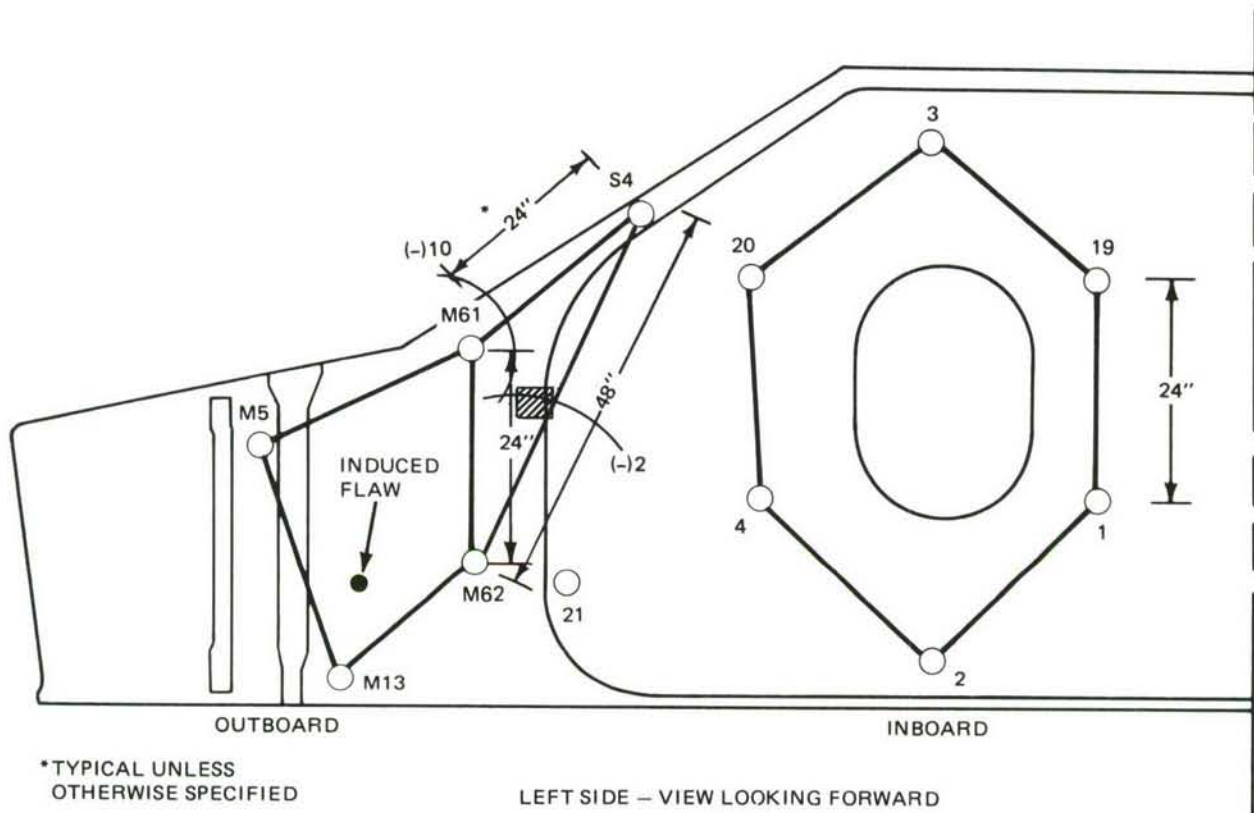


**Fig. 32 FS 992 Outboard Bulkhead (Third Life)**



2293-033W

Fig. 33 FS 992 Outboard Bulkhead (Third Life)



2293-034

**Fig. 34 FS 992 Bulkhead**

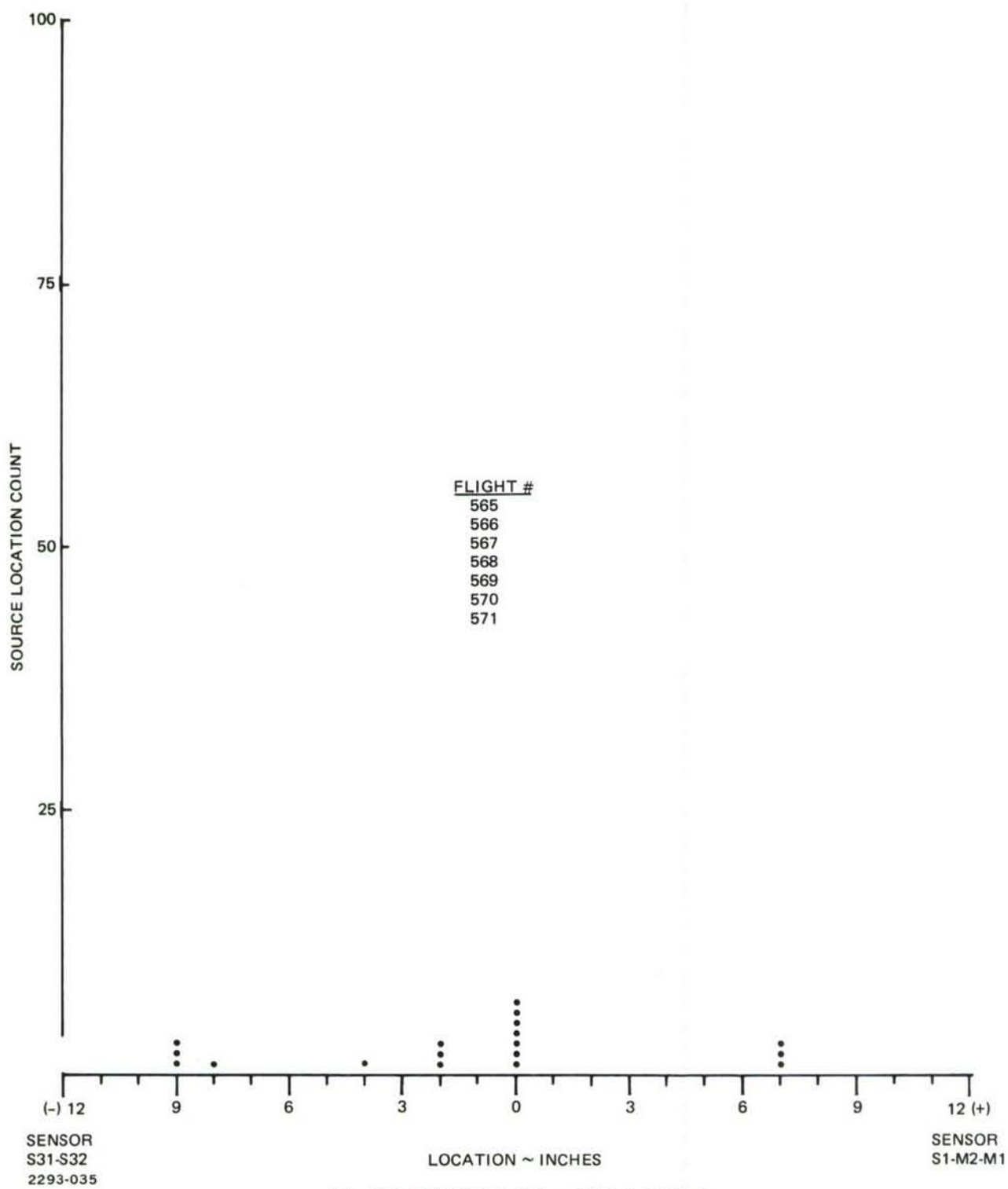


Fig. 35 FS 932 Bulkhead (Third Life)



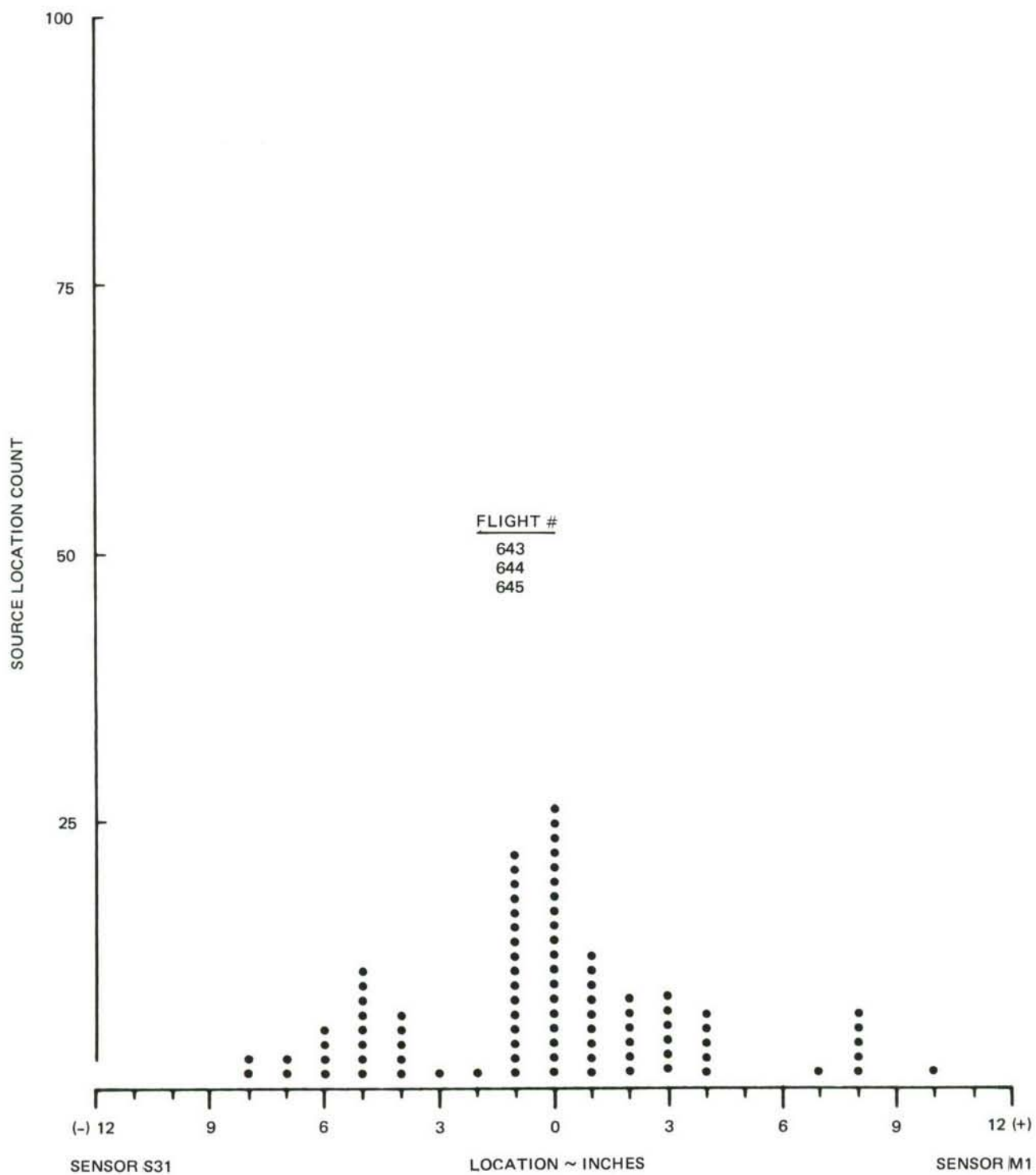
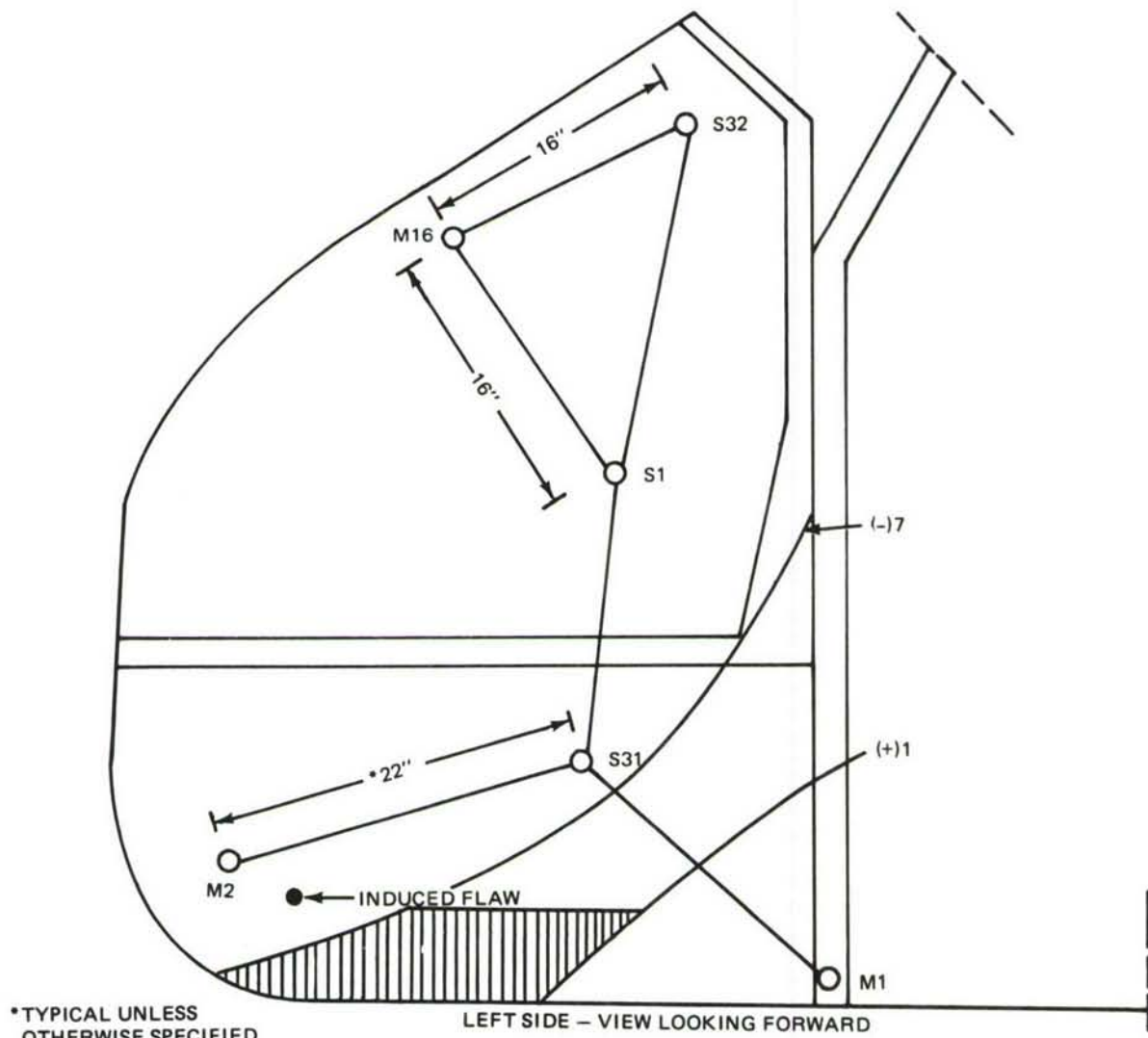
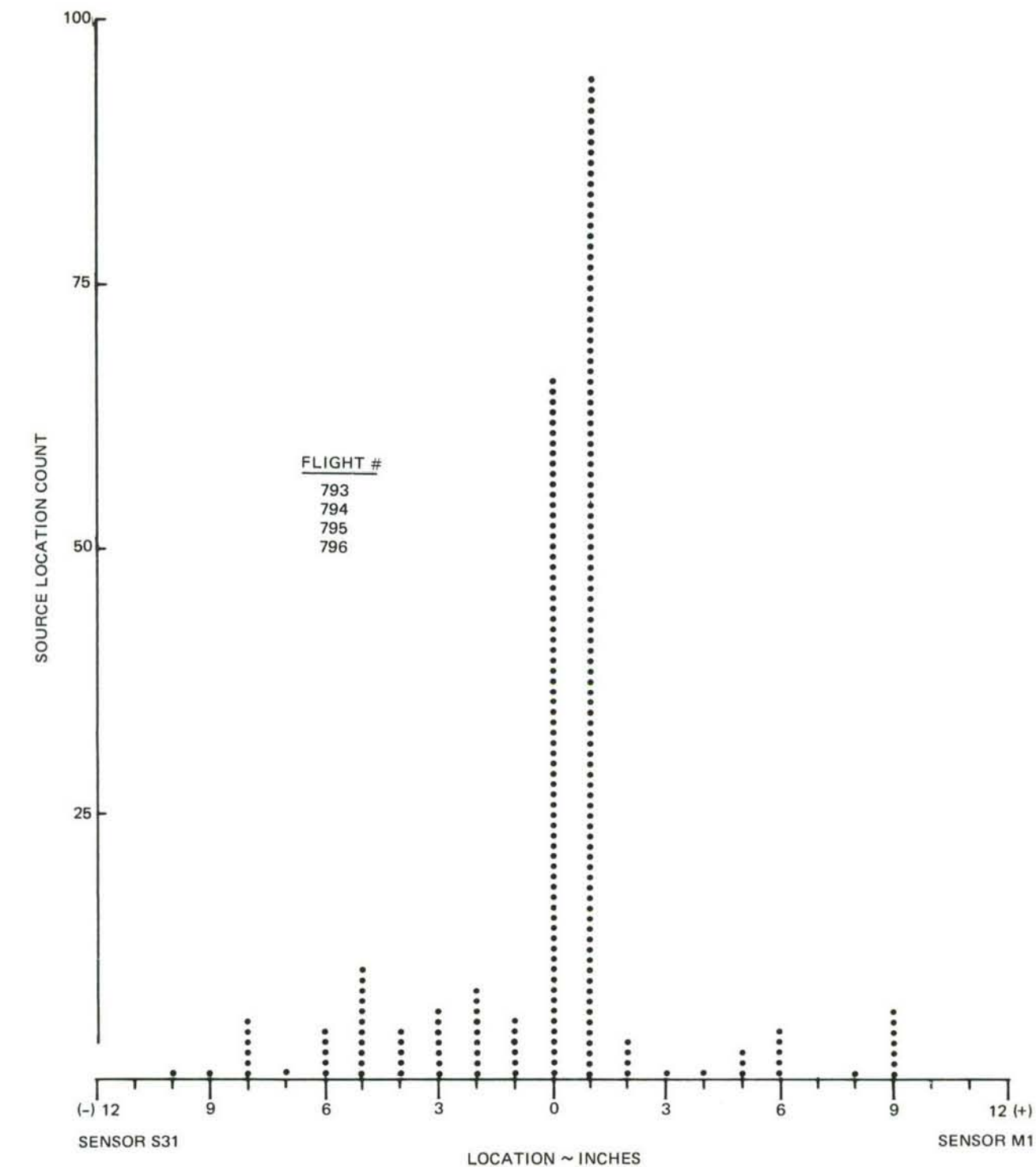


Fig. 36 FS 932 Bulkhead (Third Life)



2293-037

Fig. 37 FS 932 Bulkhead



2293-038W

Fig. 38 FS 932 Bulkhead (Third Life)

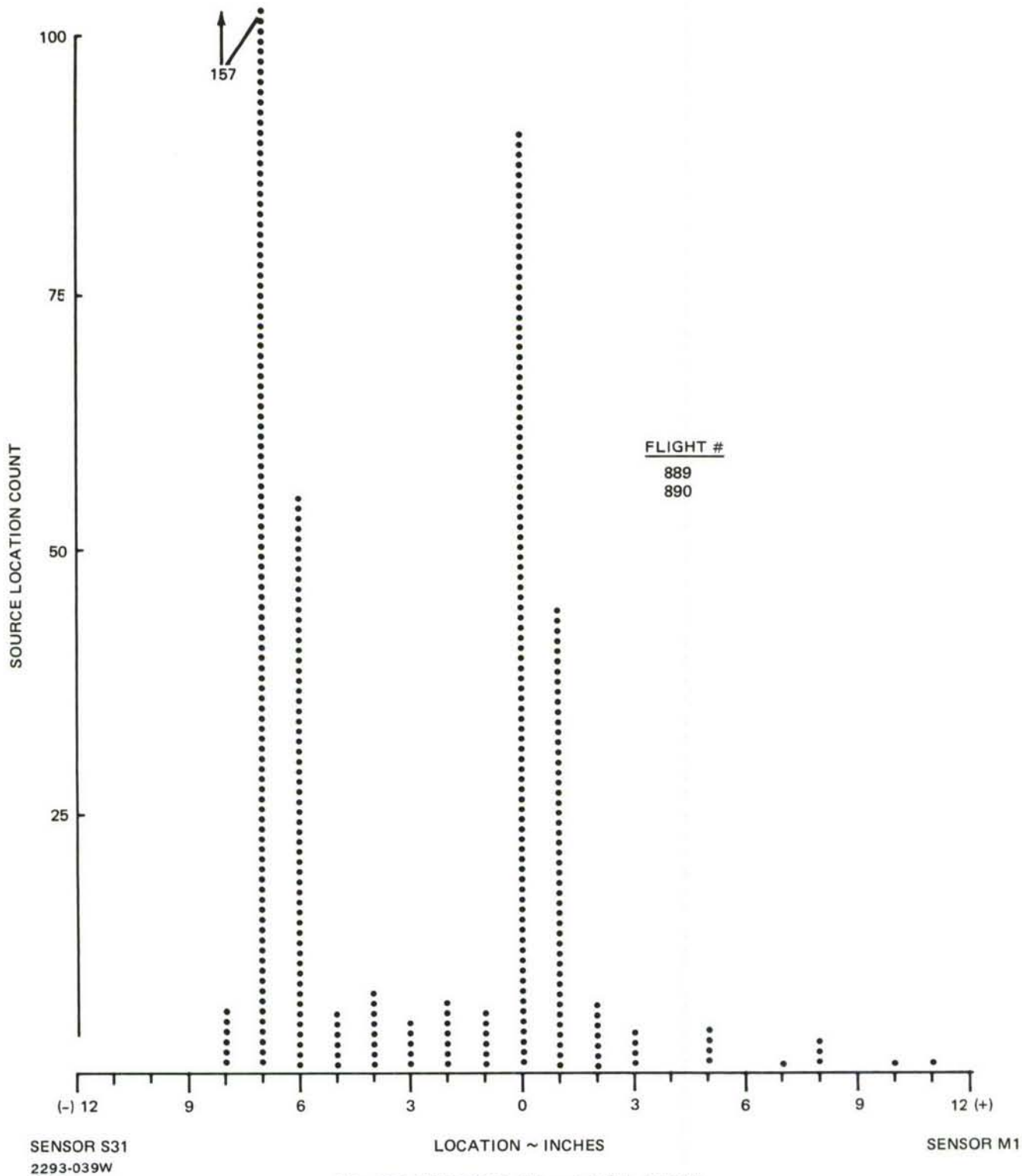


Fig. 39 FS 932 Bulkhead (Third Life)



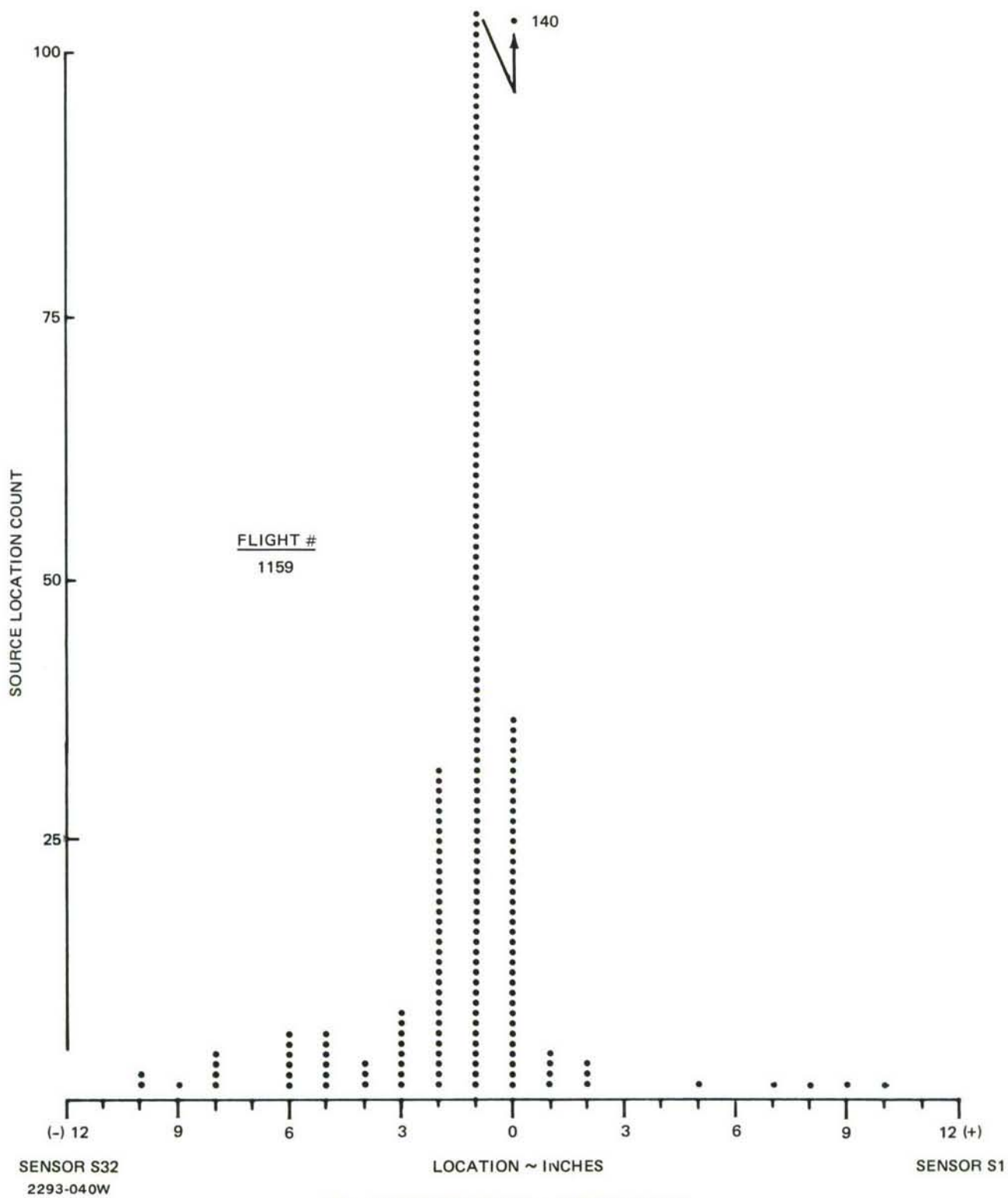


Fig. 40 FS 932 Bulkhead (Third Life)

## Section V

### AMAVS - ACOUSTIC EMISSION MONITORING - FOURTH FATIGUE LIFE

The beginning of the fourth fatigue life was monitored with the same test setup as the third fatigue life, with the exception of locating sensor M16 which was installed on the FS 932 bulkhead, as shown in Fig. 18.

#### TEST RESULTS

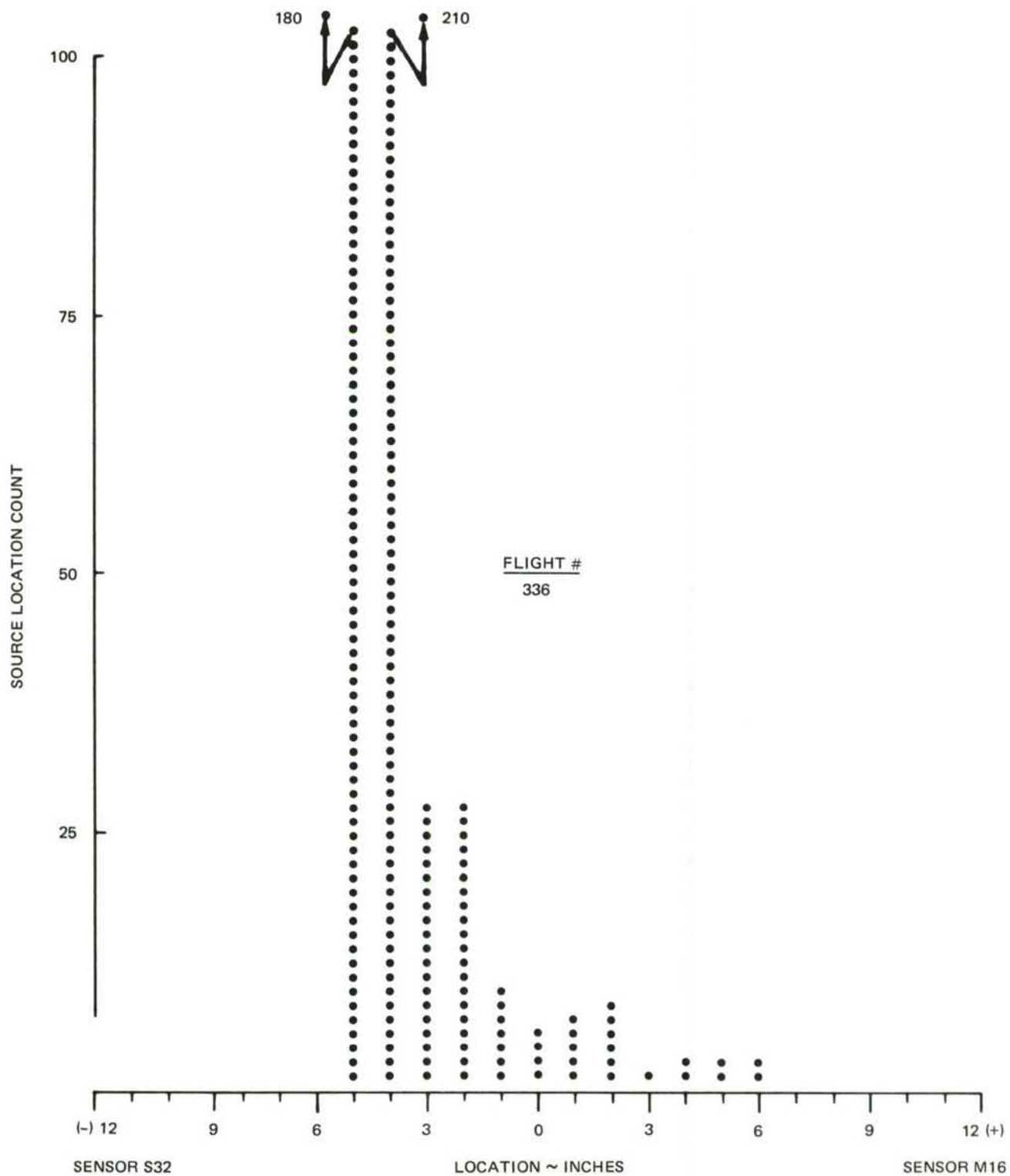
There was no significant acoustic emission activity generated from the FS 992 outboard bulkhead, XF84 Outboard Intermediate Rib, Longerons, or the Bottom Cover during acoustic emission monitoring of the fourth fatigue life. Inspection at the end of four lives revealed no cracking in any of those areas which were visually accessible.

There was significant activity on the upper half of the FS 932 bulkhead during the fourth fatigue life test. Figure 41 shows the presence of the same activity as detected by the signal source locations in Fig. 40 during third-lifetime monitoring.

The signal source locations were detected on two additional axes, as shown in Fig. 42 and 43. The signal source origin of the signals detected on the three axes is shown in the shaded area of Fig. 44. Figure 45 shows the area continued to be active during flights 798 and 799. The shaded area of Fig. 44 was inaccessible and could not be inspected with conventional methods. Verification of the source of the activity detected cannot be determined until the structure is dismantled and the area made accessible for inspection. Locating sensors 17 and 18 were installed on the lower wing pivot which had an induced flaw that was propagating before the area was monitored, as shown in Fig. 46. Signal sources were detected at the locations shown in Fig. 47 and 48 during flights 705 to 708 and 1004 to 1006, which correspond to the flaw location. Acoustic emission monitoring was able to detect crack propagation signals from the time of initial setup on the wing pivot until the end of the fourth life test.

The FS 992 inboard bulkhead showed no signs of any acoustic emission activity during the entire fatigue test until flight 919 of the fourth fatigue life. Figure 49 shows the FS 992 inboard bulkhead with very little activity from flights 424 through 431. An increase in activity on the bulkhead is shown in Fig. 50 between locating sensors 2 and 4. The signal source locations, however, did not accumulate at any one location.

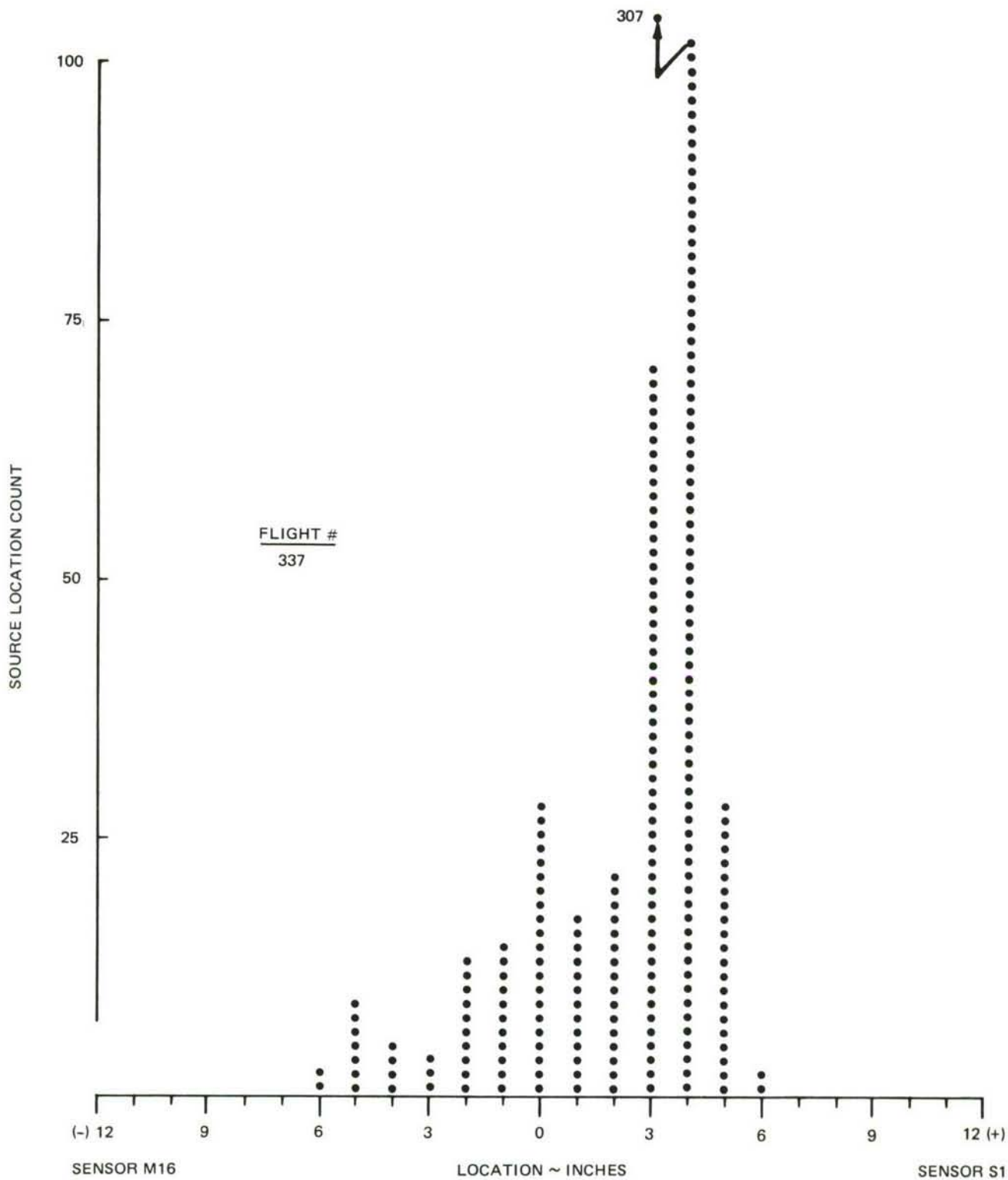




2293-042W

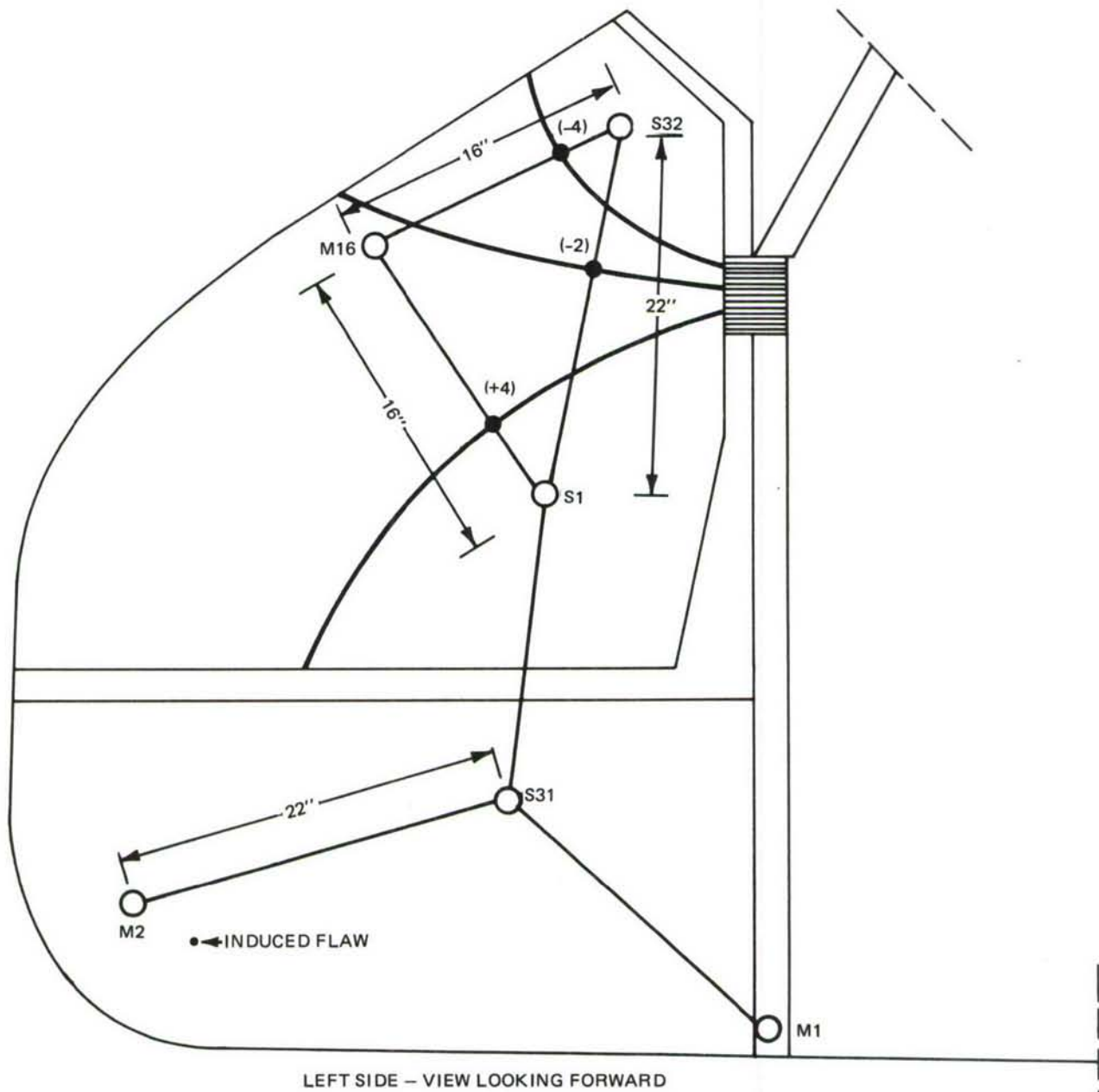
Fig. 42 FS 932 Bulkhead (Fourth Life)





2293-043W

Fig. 43 FS 932 Bulkhead (Fourth Life)



2293-044W

Fig. 44 FS 932 Bulkhead

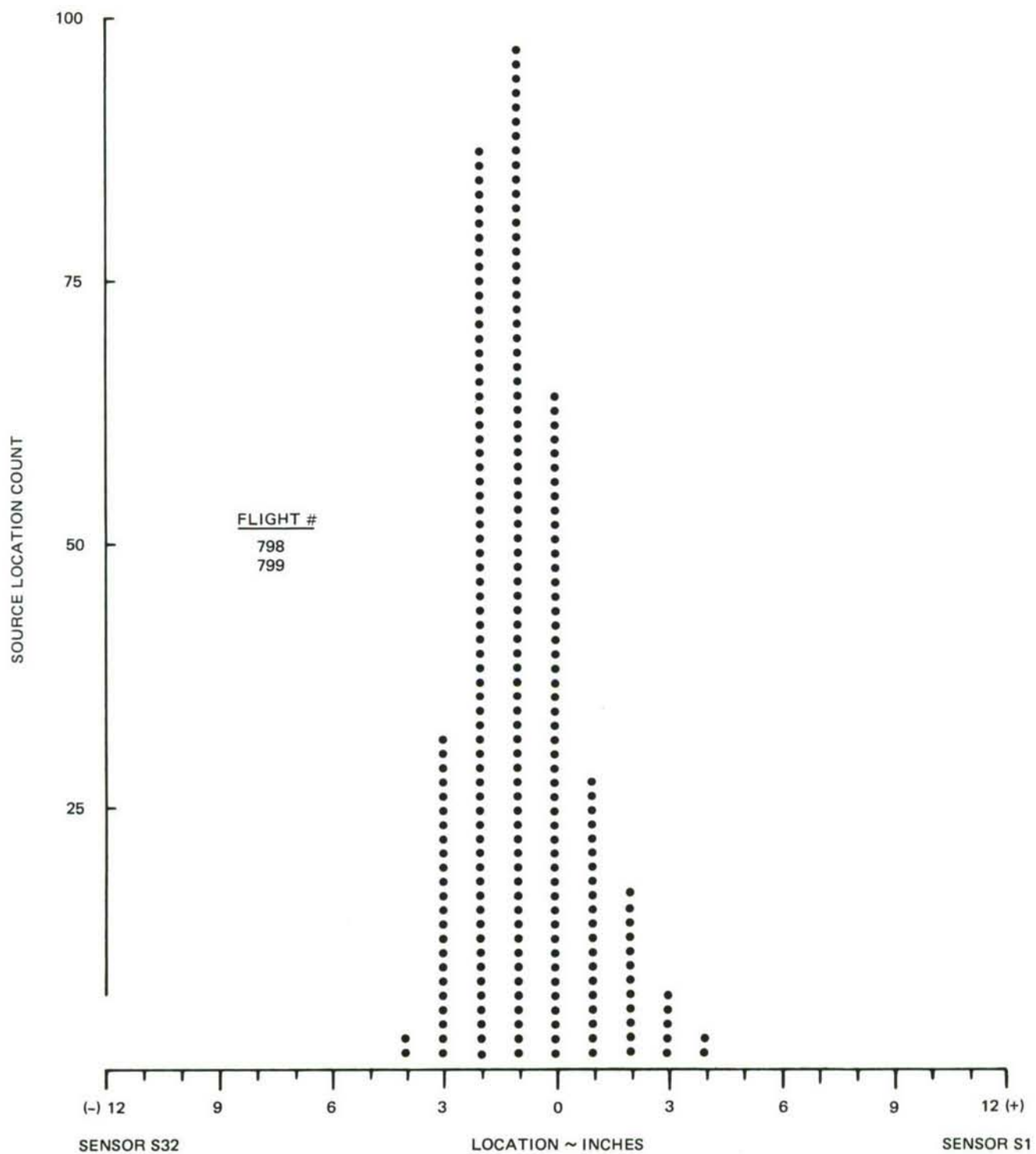


Fig. 45 FS 932 Bulkhead (Fourth Life)

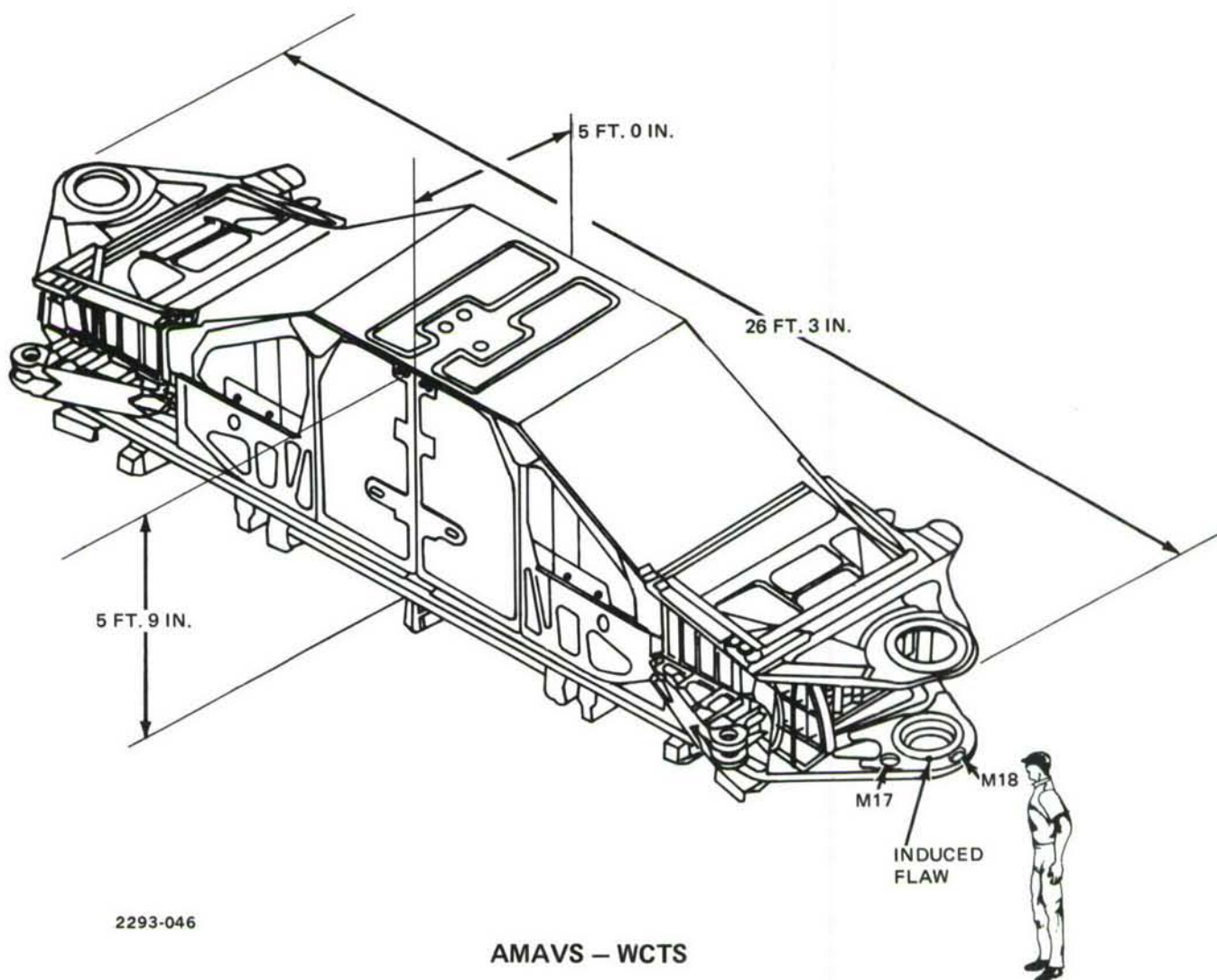


Fig. 46 Areas Monitored – Lower Wing Pivot (Fourth Life)



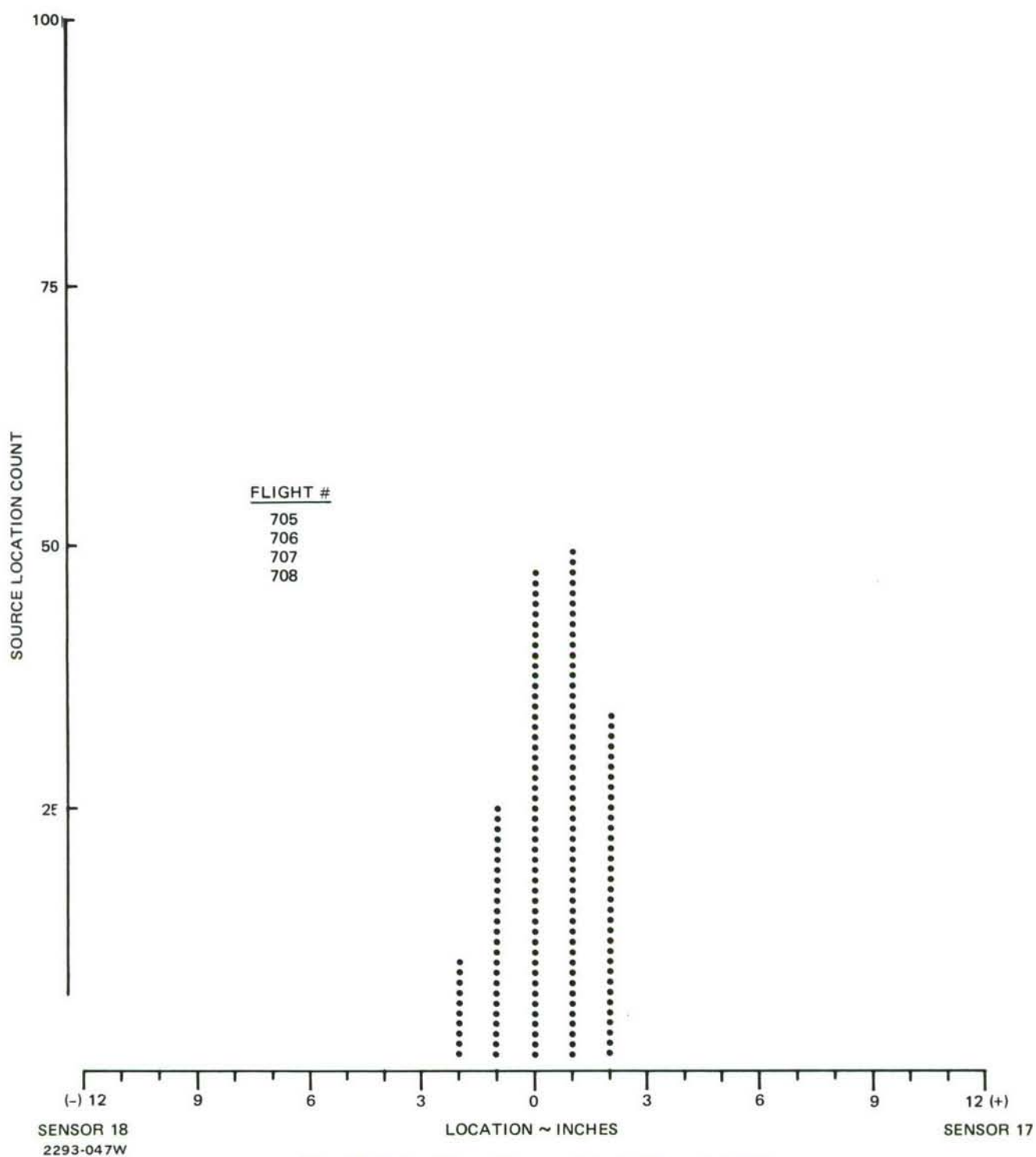


Fig. 47 Wing Pivot (Bottom) Left (Fourth Life)

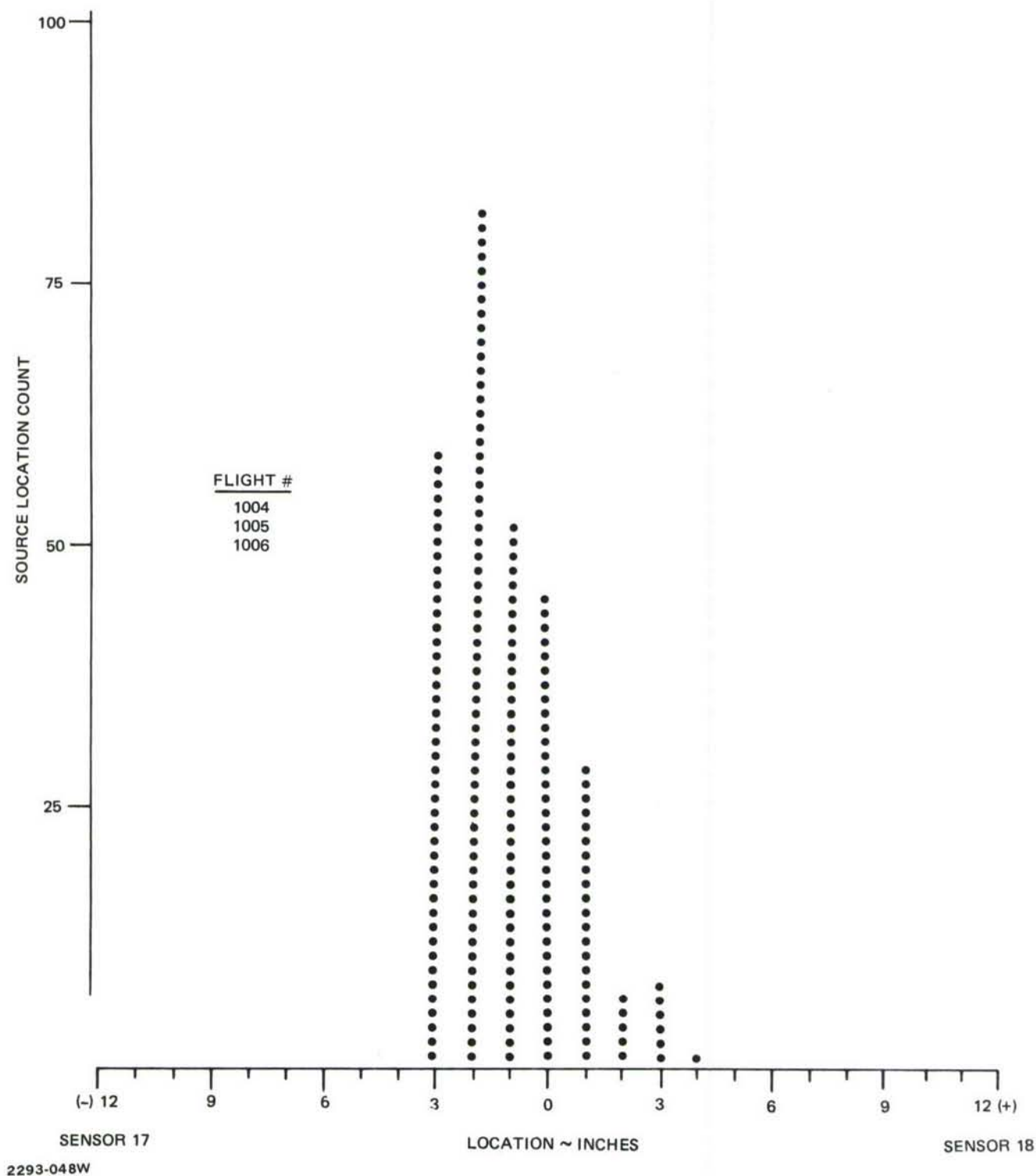
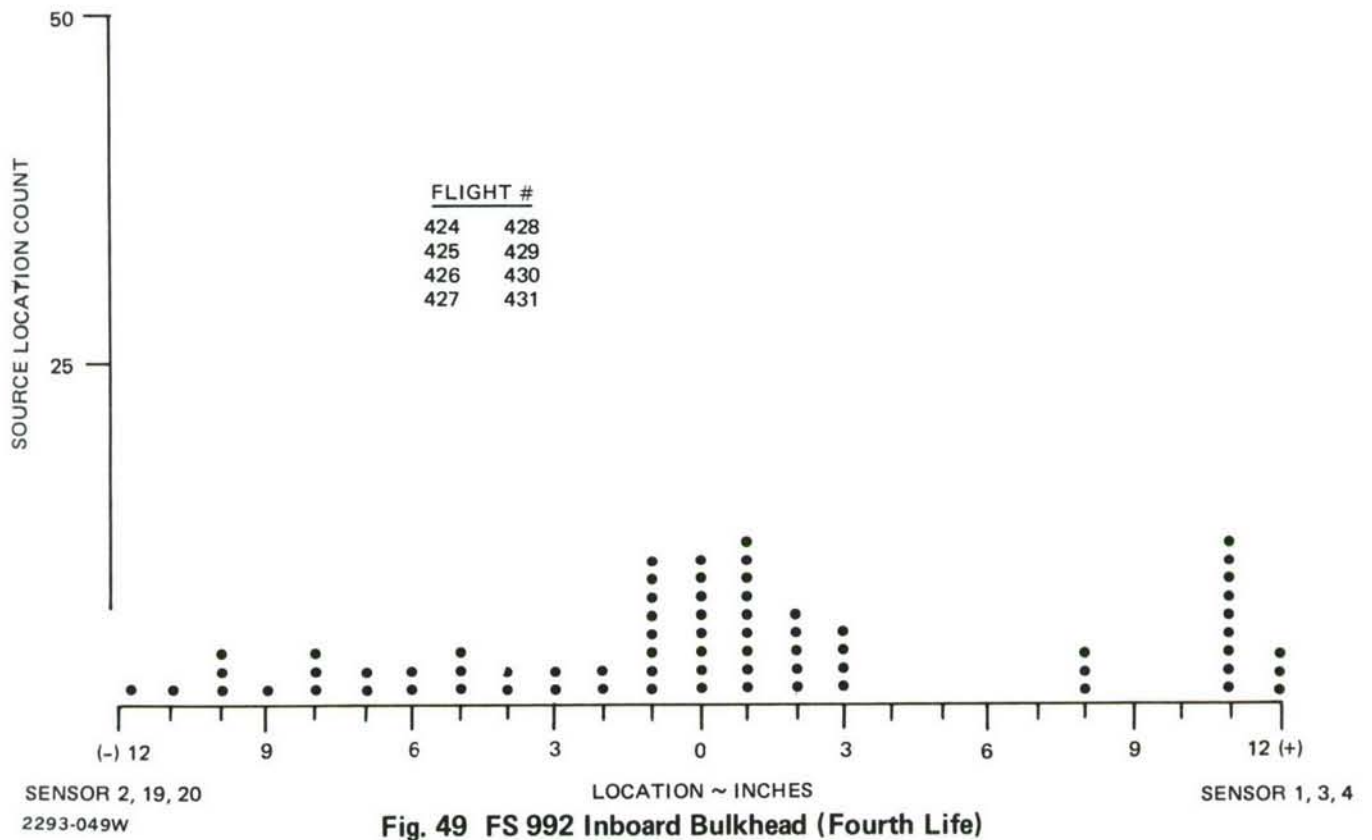
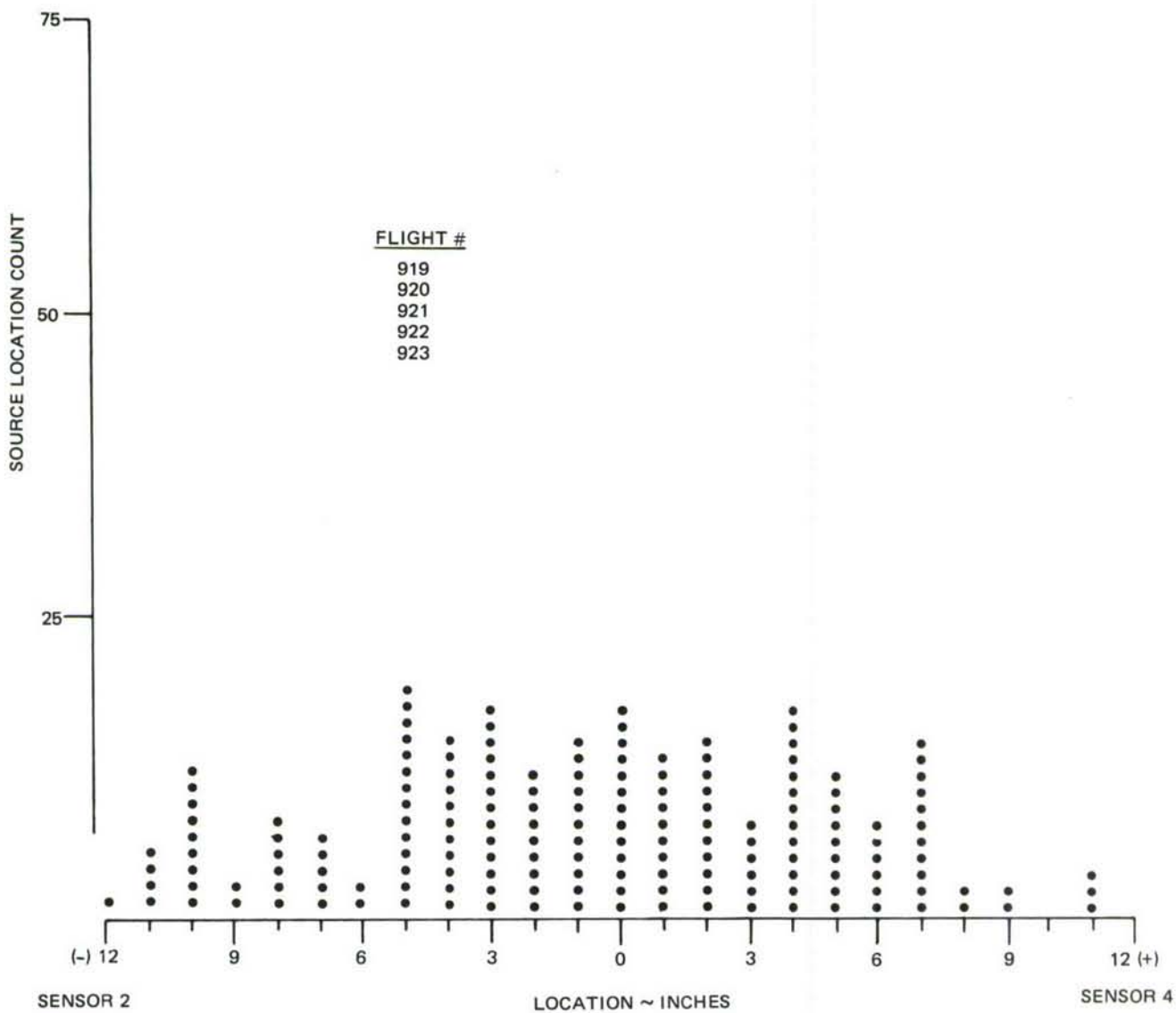


Fig. 48 Wing Pivot (Bottom) Left (Fourth Life)





2293-050W

**Fig. 50 FS 992 Inboard Bulkhead (Fourth Life)**



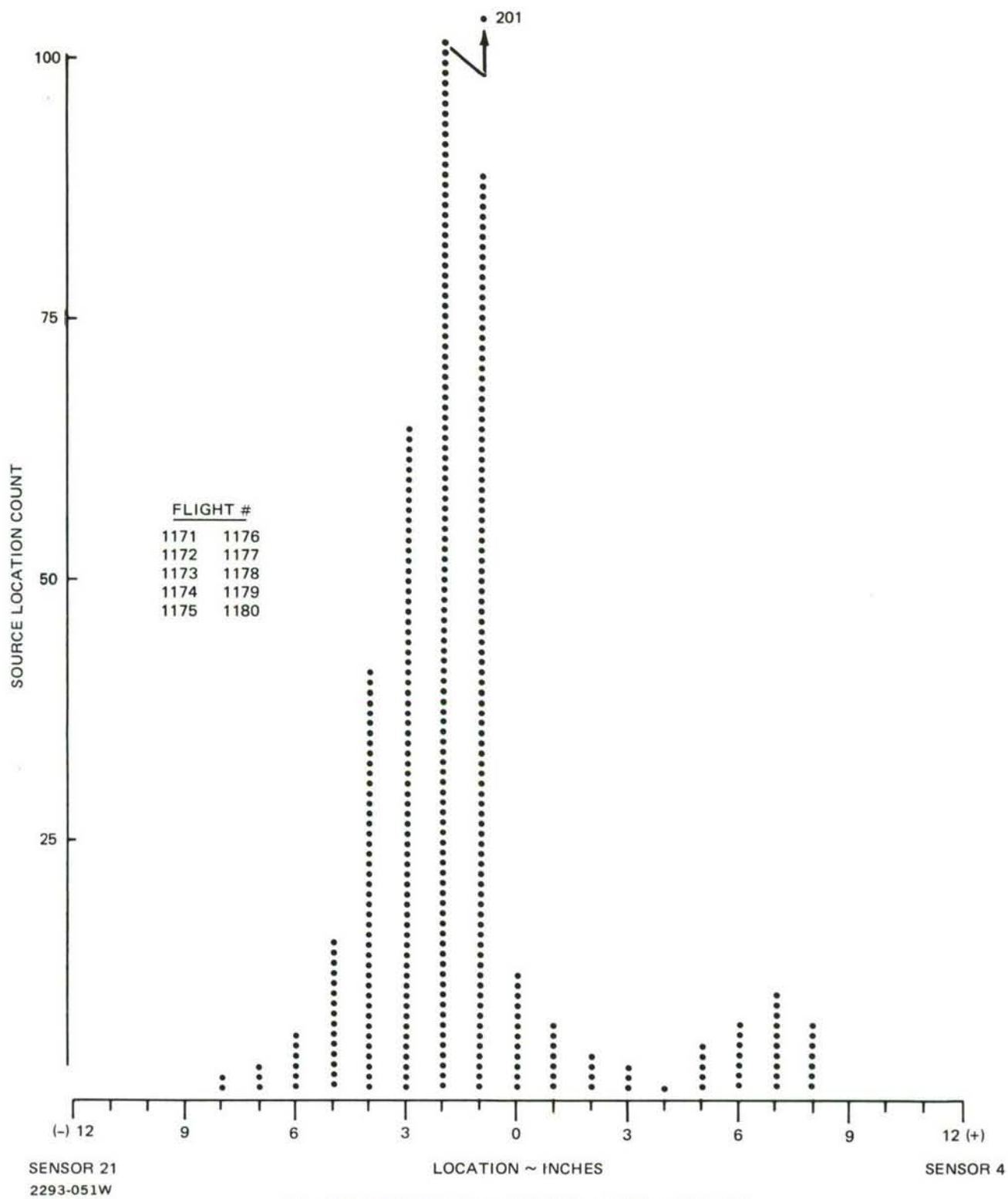
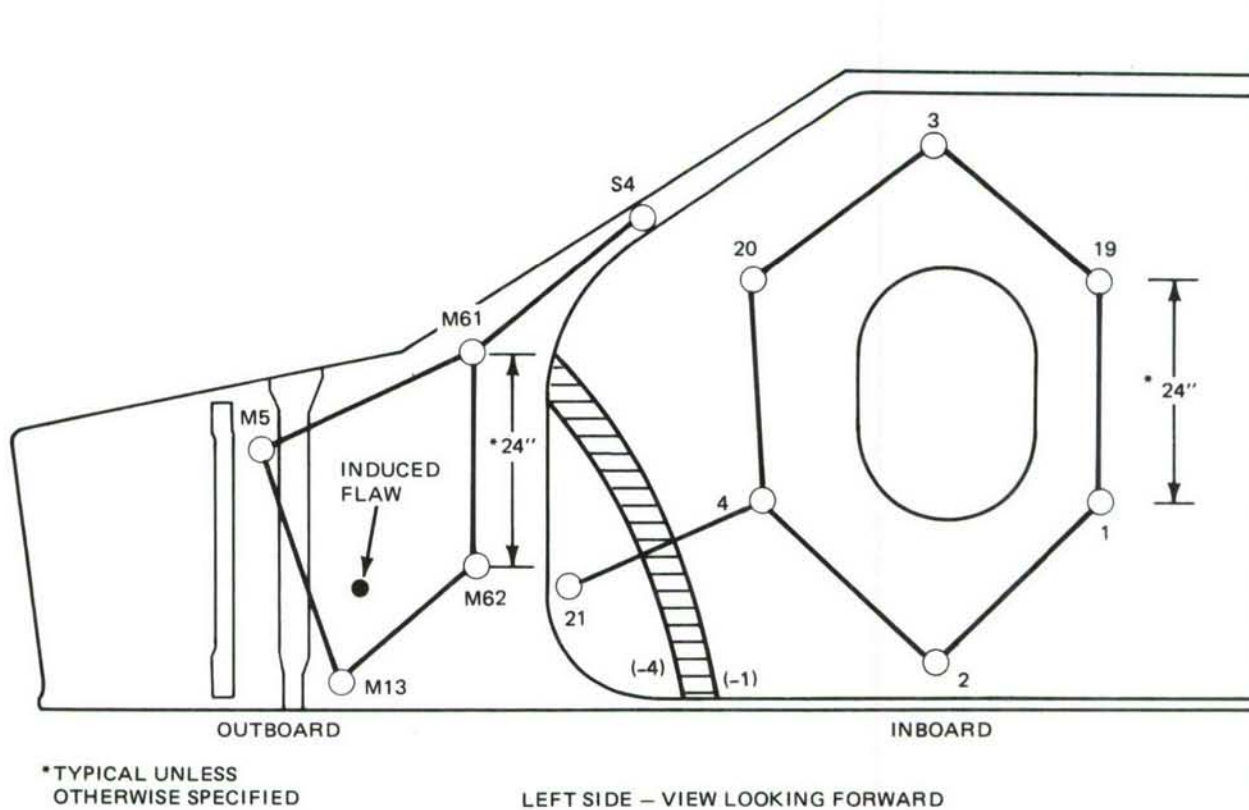


Fig. 51 FS 992 Inboard Bulkhead (Fourth Life)



2293-052

**Fig. 52 FS 992 Bulkhead**

Locating sensors 4 and 20, 3 and 20, 3 and 19, 1 and 19, and 1 and 2 were monitored, but these axes showed no sign of any activity. Based on this result, locating sensor 21 was installed to monitor the lower left area with an additional axis. Figure 51 shows the signal source locations detected by locating sensor axis 4 and 21. This location is shown in the shaded area of Fig. 52. As the fatigue test was near completion, there were not enough cycles left to determine the cause of the signal source location between sensors 2 and 4 or pinpoint the signal source location in the lower left hand corner after detection by sensors 4 and 21. A visual inspection of the area by AE personnel revealed no signs of cracking or damage. However, a thorough inspection after disassembly of all the surfaces in the area is required to determine the existence of an AE signal source.

No acoustic emission activity was detected from the induced flaws in the bottom cover, FS 992 outboard bulkhead, or the FS 932 bulkhead during the fourth life test. The flaw in the bottom cover propagated 0.35 inch between the end of the third and fourth lives. The induced flaws in the FS 992 and FS 932 bulkheads propagated 0.13 and 0.30 inch, respectively. This small amount of crack propagation was not detectable because of the multitude of extraneous noise signals encountered during the fatigue test.

## Section VI

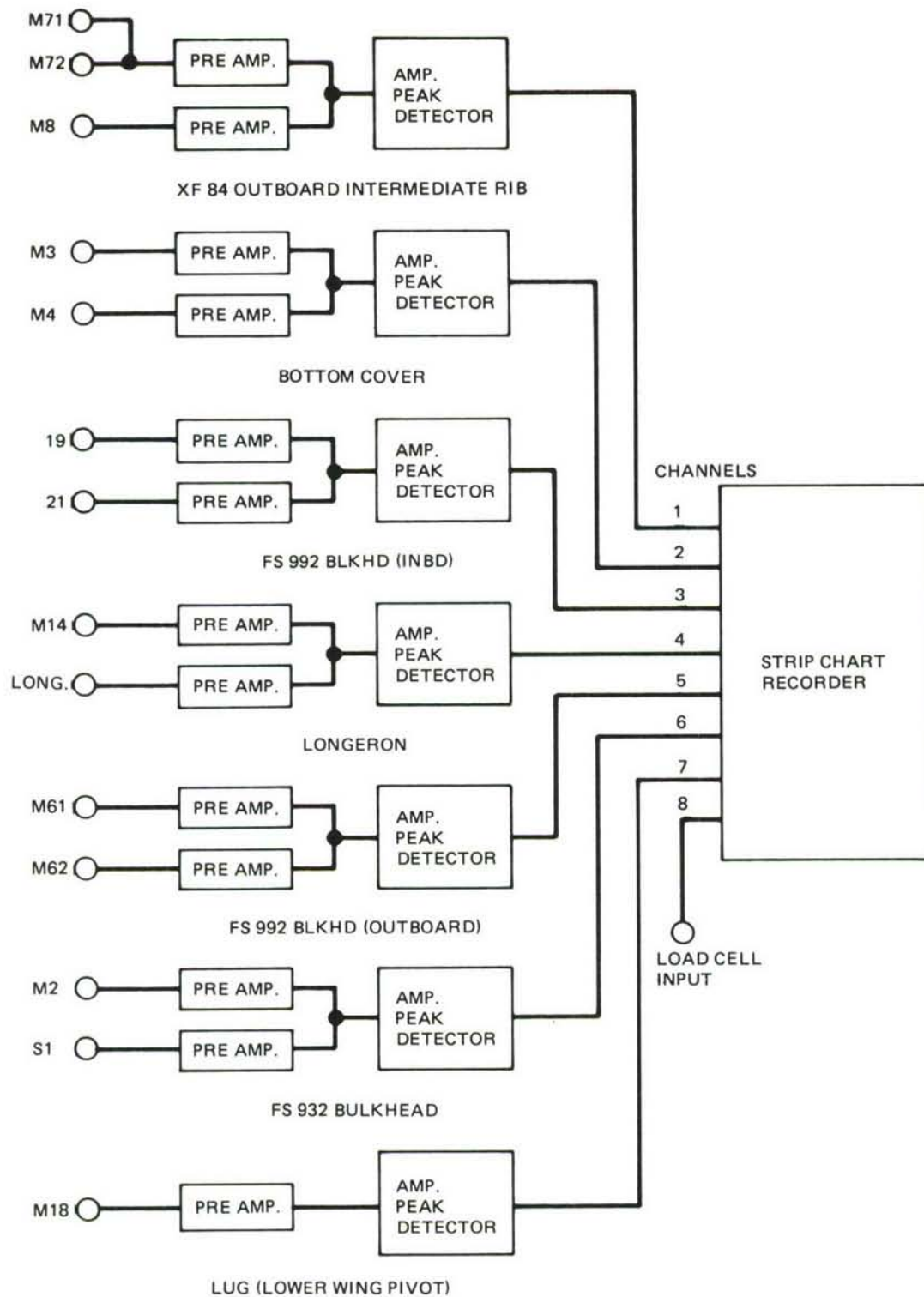
### AMAVS - STATIC TEST

The seven areas monitored during the fourth fatigue life were also monitored during the static tests to failure. All seven areas were simultaneously monitored for relative activity without extraneous noise discrimination. The relative activity was recorded on seven channels of a strip chart recorder.  $\Delta T$ , signal source location data was not obtained during these tests. The sensors used in each area and the block diagram of the monitoring system is shown in Fig. 53.

The purpose of monitoring the static failure test was to determine if there was a detectable difference between the extraneous noise signals caused by the loading and the AE signals generated during structural failure. This information would indicate the possibility of locating the failure area prior to or during failure by comparison of sensor activity.

Figures 54 and 55 show the strip chart recordings of the detected activity during the aft sweep static loading increments. The maximum peak output of the amplifiers was 5 volts and is shown as the full voltage scale for each recording channel. A high degree of activity is denoted by the recording pen remaining at the maximum level as compared to pen excursions between zero and 5 volts. With reference to Fig. 54, it can be seen that the Lower/Left Wing Pivot (Lug), Bottom Cover, and XF84 Outboard Intermediate Rib (circled areas) have a higher degree of activity than any of the other areas during the 100% loading. During the structural failure which occurred at 128% of limit load, as may be seen in Fig. 55, high activity was detected on the Lower Wing Pivot (Lug) and the Bottom Cover (circled areas). The failed structural member (lower forward outboard longeron), was located between these two areas. A high degree of activity was also detected on the XF84 Outboard Intermediate Rib which was adjacent to the Bottom Cover area.





2293-053

**Fig. 53 AMAVS Static Test System Block Diagram**

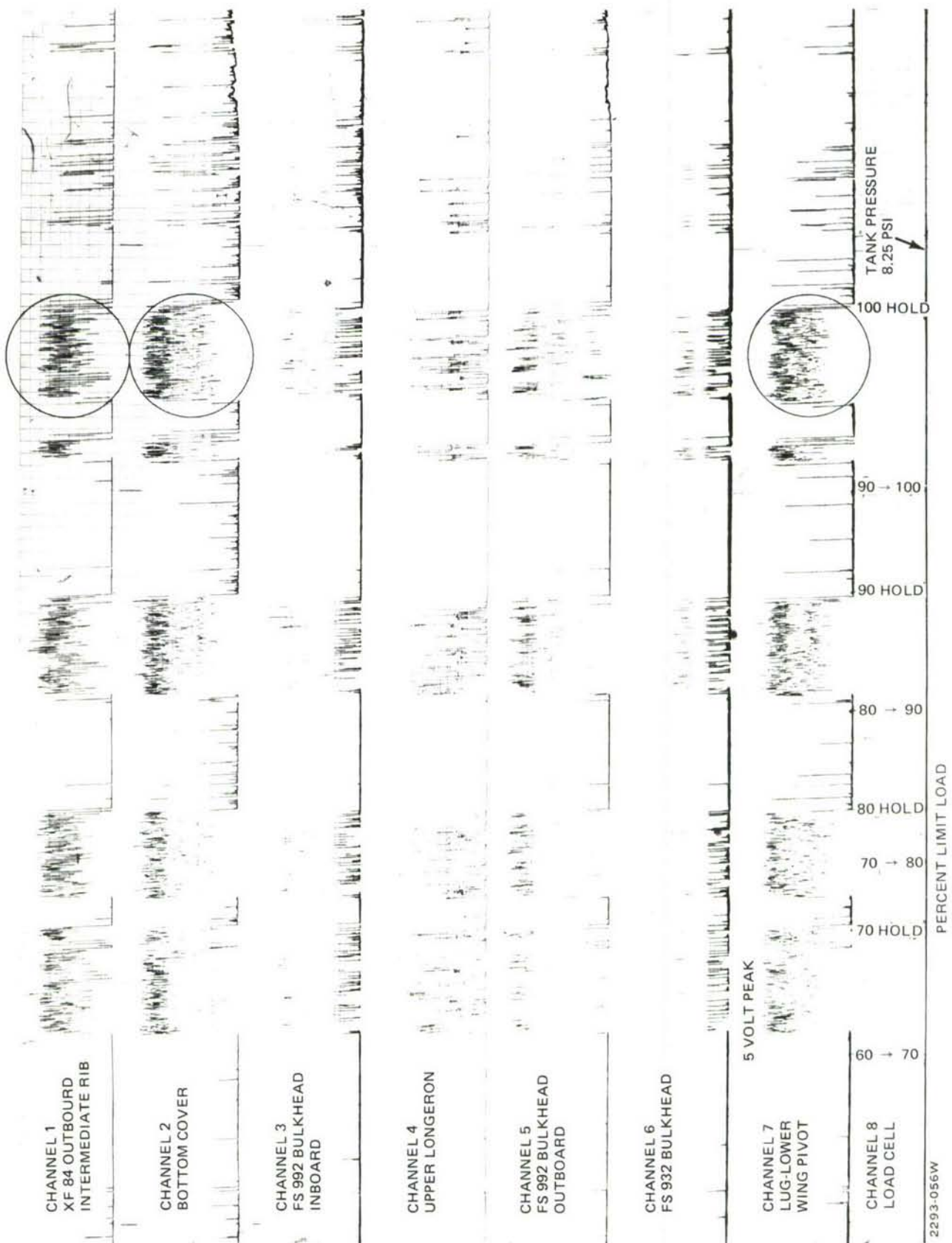


Fig. 54 AMAVS Static Test

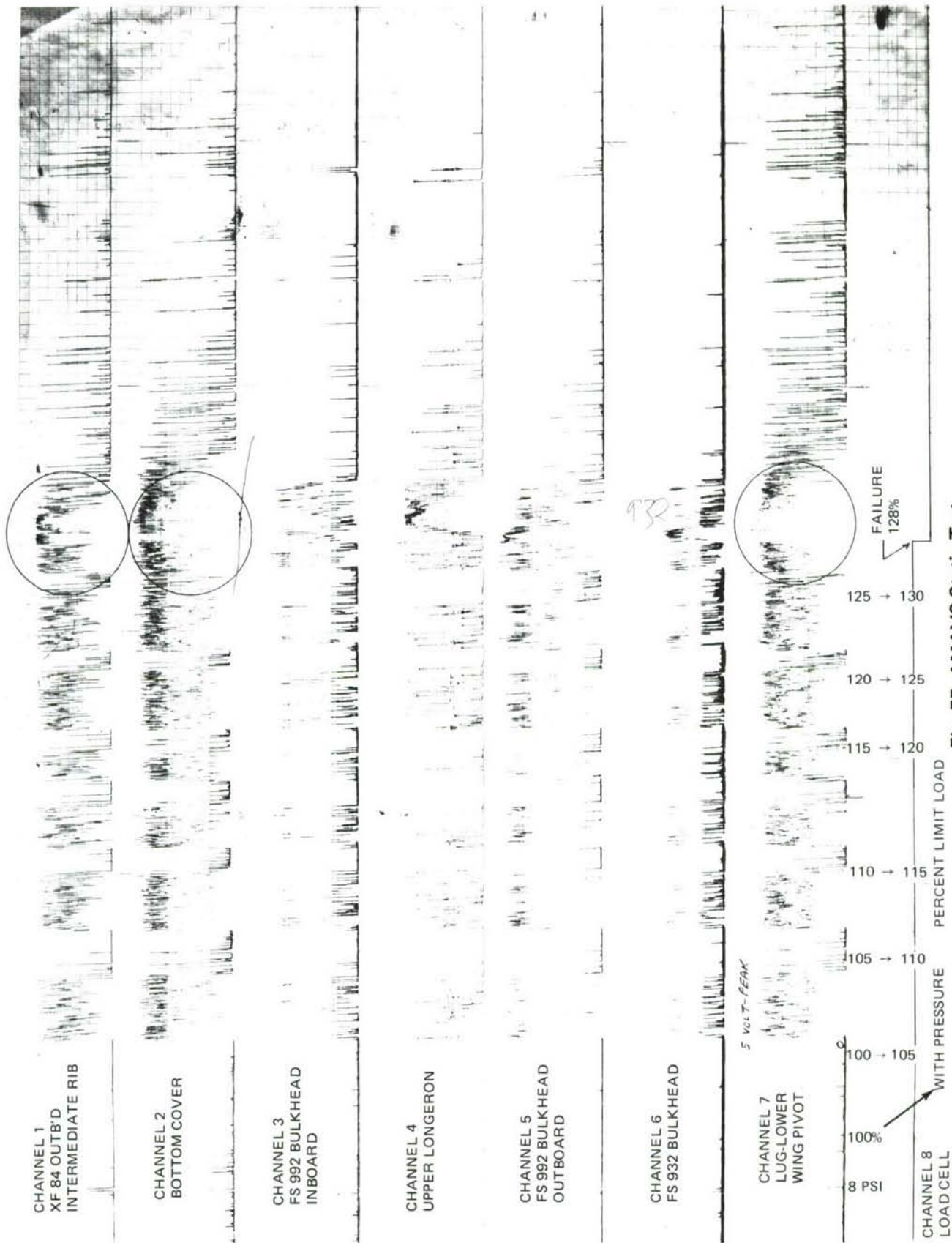


Fig. 55 AMAVS Static Test

2293-057W



## Section VII

### CONCLUSIONS

The feasibility of real-time AE monitoring of a full-scale complex structure during fatigue testing was demonstrated. The Grumman-developed AE System detected and located crack propagation in the Bottom Cover (induced flaw) and the FS 932 bulkhead prior to detection by any other means.

Extraneous noise signal interference caused by load application must be identified and eliminated for successful AE monitoring during structural fatigue tests. Spatial discrimination alone is not sufficient for the reduction of the extraneous noise signal interference required for monitoring complex structures. A means of discrimination, such as Grumman's "Wave Form," must be provided to distinguish extraneous noise signal sources from AE events within the area being monitored. Complex structures with rubbing surfaces, bolts, fasteners, and cover plates create extraneous noise signal sources which cannot be eliminated with spatial discrimination.

Monitoring two of six independent areas simultaneously on a manual time-sharing basis was sufficient to detect crack propagation. The simultaneous monitoring of areas with different metallic construction requires independent AE processing systems because of sound velocity differences.

The initial propagation of the induced flaw in the Bottom Cover during the third fatigue life (0.061 inch during 80 flights) was detected and located by AE monitoring. However, the AE activity generated by the extremely slow propagation of the induced flaws (0.130, 0.30, and 0.35 inch) during the fourth fatigue life (1280 flights) was not sufficient to be detected in the severe background of extraneous noise signals. The detection of slow crack growth and determination of a minimum detectable crack length is a function of the severity of the extraneous noise signal background, and cannot be discussed in a quantitative manner. Extraneous noise signals are not constant during fatigue cycling and AE event signals do not occur at the same point during load application. Therefore, it is not possible to determine how many AE events per cycle are detected of the total number generated during crack propagation.

During the static test the two monitored areas in proximity to the structural failure detected much more activity during the failure load than the other areas. There was apparently a detectable difference between the AE event signals and the loading extraneous noise signals during the failure load. As the failure area was not monitored for AE, the location was approximated between the monitored areas of greatest activity. More useful information relating to the failure load at crack initiation and propagation could be obtained by eliminating the extraneous noise signals from the output recording device.



## Section VIII

### RECOMMENDATIONS

The areas where activity was detected with AE monitoring which are inaccessible for inspection should be examined when the AMAVS is dismantled. These areas are the FS 992 Outboard Bulkhead (Fig. 34), the FS 932 Bulkhead (Fig. 44), and the FS 992 Inboard Bulkhead (Fig. 52).

Based on the results of monitoring the AMAVS structure with two AE monitoring systems for six areas, AE detection of damage on large complex structures can be accomplished by monitoring areas on a time-sharing basis.

Several flights of fatigue loading (one to two hours) should be sufficient to determine the presence of crack propagation if an effective means of extraneous noise discrimination is utilized.

Time should be allowed on future tests, during the initial fatigue loading flights, for AE personnel to halt the test and optimize extraneous noise discrimination functions. This would involve moving or adding sensors to eliminate interference from extraneous noise signal sources generated with fatigue load application.

A proposed AE system which is recommended for complete area monitoring is shown in Fig. 57. It is referenced to the left half of the AMAVS with the areas designated in Fig. 56. The area monitoring concept is based on the use of multiple single axes as described in "System Operation", Section II of this report. Six independent areas can be monitored simultaneously on a time-share basis with the other ten areas. All the individual preamplifier channels are connected to a switch control unit for selection of multiple or single axis monitoring in each area. A total of six non-computerized independent AE monitoring control units are required. A single 19-inch rack and cabinet can accommodate the modules and amplifiers for two systems, as shown in Fig. 57. The processing modules must include an effective means of extraneous noise discrimination such as Slave Sensor, Coincidence, and Wave Form, or the equivalent. The output device for each system is linear locator with a graphic display format, as used to present the

data in this report. The hard copy unit is used to provide a record of detected AE signal source locations.

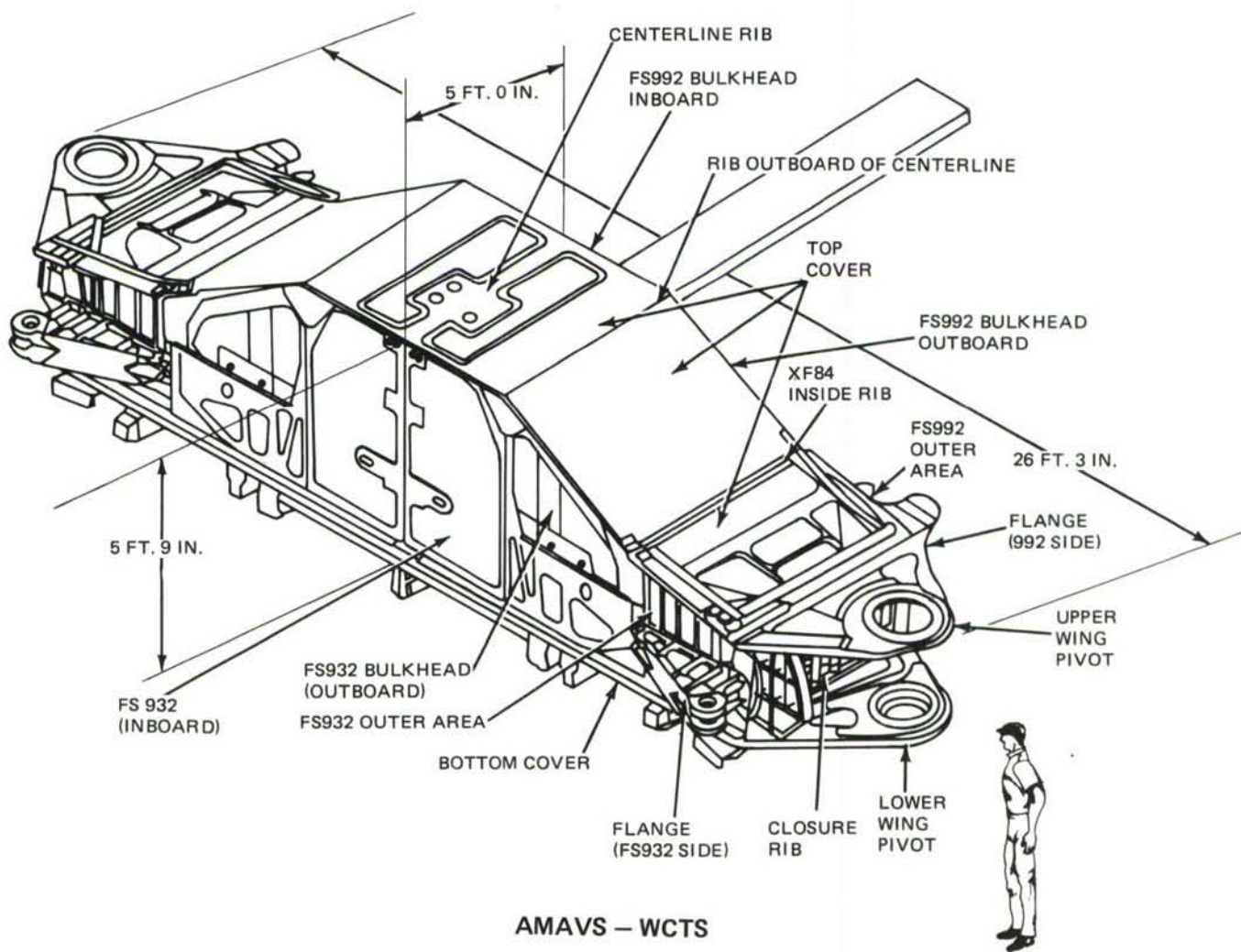
The advantages of the AE System monitoring concept shown in Fig. 57 are:

Individual filter-amplifier and processing channels are not required for each sensor-preamplifier channel used

The preamp switch control unit provides a means to remotely verify the detection of an AE event source location by singly monitoring several axes in one area

Computerized AE source location systems are not required for multiple large area monitoring.

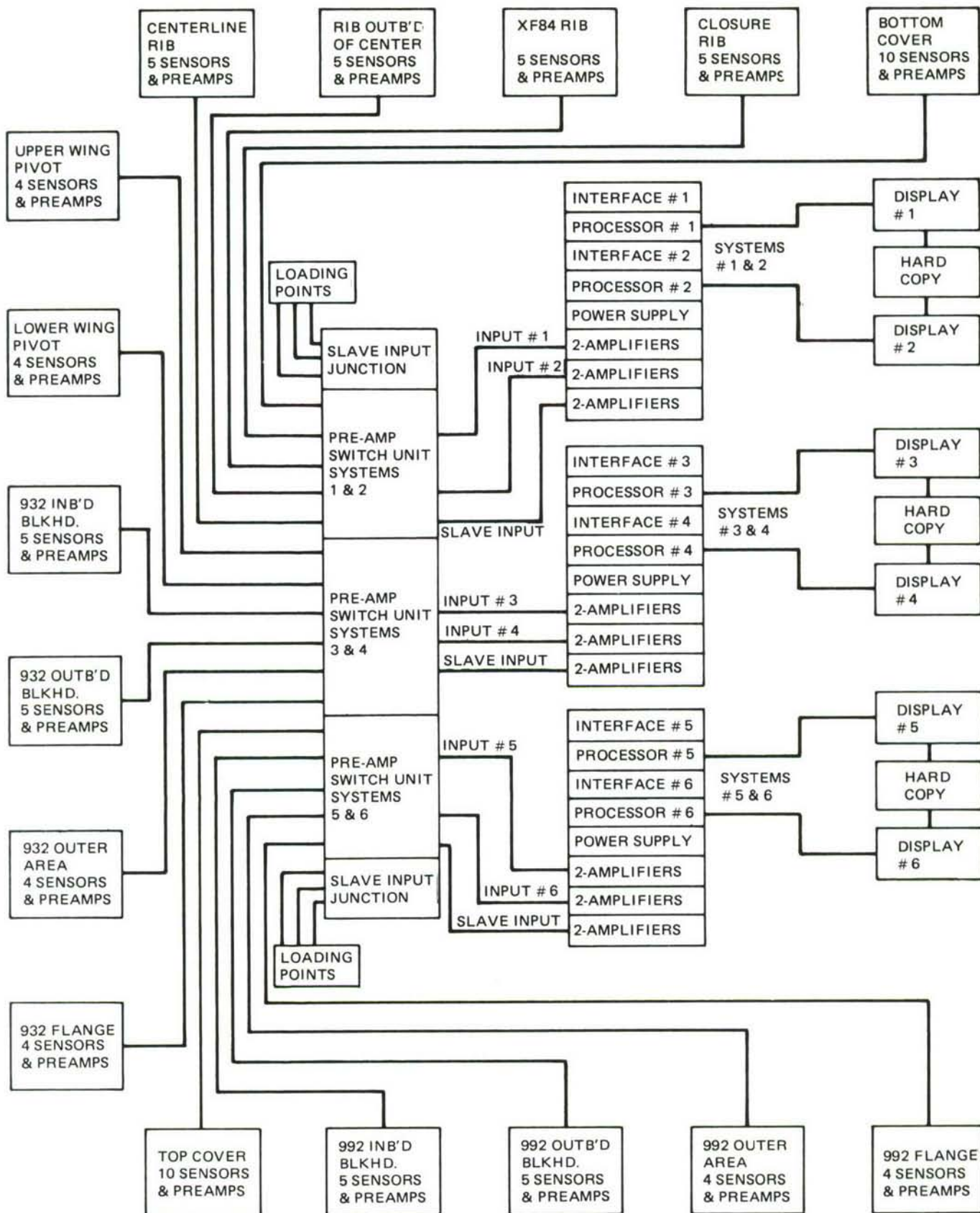
In full-scale static testing, an AE Monitoring System which detects relative activity in an area would be more effective in determining load failure initiation if extraneous noise discrimination methods were utilized.



2293-056

Fig. 56 Area Designation for Proposed AE Monitoring System





2293-057

Fig. 57 Proposed AE Monitoring System

## GLOSSARY OF TERMS

Acoustic Emission - AE

AE Event Signal - Individual bursts of stress waves or sonic energy generated by crack initiation and propagation.

Background Noise Level - Peak voltage level at amplifier channel output, inherent to the system, affected by test operating environment.

Threshold Detection Level - Variable DC voltage level adjusted above the background noise level which must be exceeded by an AE event signal for detection.

Extraneous Noise Signal - An unwanted event signal, transient in nature, caused by anything other than a valid AE event signal (i.e., vibration, rubbing, or rattling, noise generated by fatigue load application).

$\Delta T$  (Delta-Time) Data - Source location data in terms of the time difference in arrival (microseconds) of an AE event or extraneous noise signal at two locating sensors.

Locating Sensors - Sensors placed within the area of surveillance connected to channels which generate  $\Delta T$  data.

Extraneous Noise Discrimination - AE system capability of identifying and rejecting erroneous  $\Delta T$  data caused by extraneous noise signals.

Signal Source Location - The source origin of an event signal referenced to the two locating sensors at which it was received.

Signal Range Time - An adjustable amount of time allowed (100-500 microseconds) to acquire and identify  $\Delta T$  data which is accepted or rejected at the end of this time period.

Spatial Discrimination - Capability of identifying signals originating from outside a predetermined area and rejecting the erroneous  $\Delta T$  data resulting from such signals.

Slave Sensors - Sensors placed outside the area of surveillance, such that they will detect extraneous noise signals prior to detection by the locating sensors and provide an input signal for spatial discrimination.



Coincidence Time - A form of spatial discrimination, utilizing a preset time limit (1-999 microseconds) for signal detection at two locating sensors, which effectively restricts the area of surveillance.

Wave Form Discrimination (WFD) - Rejection of extraneous noise signals, regardless of source origin, by imposing preset requirements on the locating signal wave form which distinguish most extraneous noise signals from AE events.

Multiple Signals - Signal source locations at the output device generated in groups of three or more per second.

Location Count - The number of times the same signal source location is indicated during a specified time interval.

Real-Time - Detection and location of signal events as they occur.